PHLOEM FUNCTIONS REVEALED BY THE *nakr1-1* MUTANT

A DISSERTATION
SUBMITTED TO THE FACULTY OF THE GRADUATE SCHOOL
OF THE UNIVERSITY OF MINNESOTA
BY
Hui Tian

IN PARTIAL FULFILLMENT OF THE REQUIREMENTS
FOR THE DEGREE OF
DOCTOR OF PHILOSOPHY

Adviser: Dr. John M. Ward

December 2010

i. Acknowledgements

I would like to acknowledge Plant Biological Science Program for all the support I received during my PhD studies. I thank my committee, especially my advisor John Ward for the guidance during my study and research. John gives me a lot of freedom to explore science and helps me find my own way to be an academic. Whenever I am in hard times he is always with me, nice and patient. I also appreciate the help from the rest of my committee, Neil Olszewski, Steve Gantt, Bill Gray and Nevin Young. Their suggestions have been invaluable treasure that will company and guide me through my whole career life.

I would also like to thank my current and previous labmates, Anke Reinders, Ye Sun, Ali Sivitz, Chirs Wilson and Ravi Vyzasatya, especially Anke as a great resource in both science and real life. Anke helped me with the ^{14}C-sucrose loading experiment. My project is collaborated with Dr. David E. Salt's lab in Purdue University. I had the opportunity to visit Salt lab twice during my graduate studies, and had great communication with people in his lab. All elemental analyses were done in Salt lab by Brett Lahner. DNA chip analyses for identifying *AtNaKR1* were performed by Ivan Baxter. Elena Yakubova contributed in growing plants and preparing samples for elemental analysis. I feel extremely fortunate to have such a reliable and excellent group to help me in my research. Also I would like to thank Manjula Gopalraj in Neil Olszewski lab for being always warm and encouraging. Her company helped me go through a lot of stressful days.

Finally I would like to thank my dear family- especially my parents, all my relatives and friends in China for being supportive all these years! Without their faith and unfailing love for me, I might have never come to this step!

ii. Abstract

Na^+ is a non- essential element for plant growth. Na^+ accumulation within plants, especially the shoot tissue causes osmotic stress and Na^+-specific toxicity that threatens plant survival and reduces crop yield. The control of Na^+ accumulation in the shoot is mainly at the root level, by regulating net Na^+ uptake into roots and Na^+ transport from root to the shoot. My thesis work is mainly on the characterization of a fast neutron mutagenized Arabidopsis mutant, *nakr1-1*, that accumulates Na^+ and K^+ in the shoot tissue and has pleiotrophic developmental phenotypes (including short roots, late flowering and loss of apical dominance). Using traditional mapping together with DNA- chip based mapping, a 7-bp deletion was identified that caused loss- of- function mutation of a gene encoding a putative heavy-metal-binding protein. The metal-binding feature of the protein was confirmed by elemental analysis of maltose binding protein (MBP)- tagged NaKR1 expressed and purified from *Escherichia coli*. *AtNaKR1* was specifically expressed in the phloem companion cells. NaKR1 protein was phloem mobile and unloaded at the phloem terminal into the proximal root meristem region. *nakr1-1* mutation caused severe phloem function defects as demonstrated by less efficient ^{14}C- sucrose loading and starch accumulation in rosette leaves. Phloem function defects were also responsible for the Na^+/K^+ accumulation in the shoot tissue based on the reciprocal grafting results together with ICP- MS analyses. Moreover elemental analysis of xylem sap indicated Na^+ and K^+ accumulation phenotypes were not caused by increased root- to- shoot transport of Na^+ and K^+. *nakr1-1* mutation

affects root meristem maintenance after germination as revealed by study of root meristem size, cell pattern and starch accumulation in root columella cells and quiescent center activity. My work provided evidence that phloem recirculation plays more important roles than had been suggested by previous literature in controlling shoot Na^+ accumulation. Understanding how Na^+ and K^+ redistribution is regulated might have potential application in improving salinity tolerance of crop plants and the improvement of seed quality.

iii. Table of Contents

iv. List of Tables

v. List of Figures

1. INTRODUCTION: Literature Review

Part I. Control of Na^+ accumulation in higher plants

Salinity has been a major constraint for crop production. It has been estimated that 20% of the irrigated soil is salt affected. Irrigated land produces one third of the world's food (Munns, 2002; 2005). Saline soil contains high levels of Na^+, which is the main cause of ionic damage to most species (Tester and Davenport, 2003).

Osmotic and salt specific effects on plant growth

High concentrations of Na^+ affect plant growth by two mechanisms: the osmotic and ionic stresses. When salt- sensitive plants are exposed to salt stress for hours, their shoot growth and to a less extent root growth is permanently reduced. This effect is more due to osmotic than Na^+- specific damage (Munns, 2002). Part of the osmotic problem is caused by the negative water potential of the soil solution. Plants need to maintain lower internal water potential than that of the soil to maintain turgor and water uptake. This requires either uptake of solutes from the soil or the synthesis of metabolically compatible solutes that are energetically expensive (Tester and Davenport, 2003). Osmotic damage also occurs when high concentrations of Na^+ build up in leaf apoplast since Na^+ enters leaf through xylem sap and is left behind when water evaporates (Öertli, 1968; Flowers et al., 1991). With high concentrations of Na^+ in the leaf apoplast, plants have difficulty maintaining low Na^+ level in the cytosol, especially low Na^+:K^+ ratios

(Gorham et al., 1990; Dubcovsky et al., 1996; Maathuis and Amtmann, 1999). Na^+ specific toxicity is largely caused by its competing with K^+ over its essential cellular functions. A high Na^+: K^+ ratio in the cytosol interferes with the activity of multiple enzymes that require K^+ as cofactors (Bhandal and Malik, 1988). Moreover high concentration of Na^+ in the cytosol also affects protein synthesis by interfereing with ribosome function (Blaha et al., 2000). The other Na^+ related toxicity includes affecting plasma membrane permeability, the production of reactive oxygen species explicit. Na^+ accumulation causes soil decay and thus affects water and nutrient uptake into roots. Na related stress always interact with other environmental factors, such as drought (Tester and Davenport, 2003).

Leaves are more vulnerable than roots to Na^+ related damage. Upon exposure to a saline environment, roots maintain Na^+ at a relatively constant level (10-30 mM, (Tester & Davenport, 2003). Na^+ accumulation in the shoot however increases over time due to transpiration. A plant transpires 50 times more water than it retains in the leaf tissue, as a result Na^+ builds up within leaves over time (Munns, 2005). The most severe damage is to the leaf tissue, including leaf necrosis, reduced photosynthesis and reduced stomata conductivity. As Na^+ mainly accumulate in old leaves, the rate of leaf death is crucial for plants to survive in saline soil. Only when new leaves are produced at a rate greater than the rate at which old leaves dies will there be enough photosynthesizing leaves for plants to make flowers and seeds (Munns,

2005). One way for reducing Na^+ accumulation in the shoot is to redistribute it through the phloem translocation stream. Till now there is limited evidence of significant Na^+ recirculation from shoot to root and Na^+ transport from root to shoot is considered to be largely unidirectional. Control of Na^+ accumulation in shoot is thus of major importance for most species to survive salt stress. Most salt sensitive species have poor ability to sequester Na^+ to the vacuoles and have to rely on other mechanisms to deal with Na^+ accumulation.

Mechanisms for Na^+ tolerance

Na^+ transport processes have major roles in salinity processes. There are two distinct mechanisms for Na^+ tolerance: (1) the sequestration of Na^+ into intracellular compartment to prevent Na^+ accumulation in the cytosol and the apoplast, and the signaling process to prevent Na^+ related damage to the cell. (2) the partitioning of Na^+ at the whole plant level to avoid Na^+ overaccumulation in fast growing tissues. This includes several processes: 1. Regulation of Na^+ delivery to the shoot; 2. Regulation of Na^+ recirculation out of the shoot; 3. Allocation of Na^+ to specific parts of the plants, such as the stem, leaf petiole or leaf margin. There are other mechanisms that are involved in improving tolerance to saline stress, such as water- use efficiency, osmotic adjustment, secretion of Na^+ to the leaf surface and advance of flowering time etc., not included in this introduction. More detailed information can be obtained from the reviews by Tester and Davenport (2003) and Munns, (2005).

NHX mediated Na^+ sequestration and salt tolerance

An important strategy used by many plants to survive salt stress is to sequester Na^+ into the vacuole. Na^+ accumulation in vacuoles will decrease the toxic Na^+ level in the cytoplasm, and provide osmotic potential in the vacuole to maintain turgor pressure essential for cell expansion under salt stress. This process is mediated by vacuolar membrane localized Na^+/H^+ antiporter. AtNHX1 was the first vacuolar localized Na^+/H^+ antiporter identified in plants, based on its sequence similarity to human NHE and yeast scNHX1 transporter (Gaxiola et al., 1999). The Arabidopsis genome has six *NHX* genes (*AtNHX1-6*). AtNHX1 and AtNHX2 are the predominant isoforms. When expressed in yeast, AtNHX1,2 and 6 complemented the salt sensitivity of *nhx1* mutant and led to increased Na^+/K^+ accumulation in yeast (Gaxiola et al., 1999; Yokoi et al., 2002). AtNHX1 and AtNHX2 are induced by salt, osmotic stress and ABA treatment; AtNHX5 however is only induced by salt stress in an ABA independent manner. The functional overlap and differential expression of AtNHXs genes suggest they play important roles in plants and different tissues have different requirements for their expression (Yokoi et al., 2002). The transport of Na^+ into vacuoles is an energy- dependent process relying on the proton motive force established by the vacuolar membrane localized H^+- pumping ATPase and pyrophosphatase proteins (Blumwald et al., 2000). Salt treatment also induced the activity of both vacuolar proton pumps, although in both salt- tolerant and salt- sensitive species (Hasegawa

et al., 2000; Maeshima, 2000). The importance of NHX antiporters in salt tolerance has been revealed by overexpression or silencing experiments. Overexpression of *AtNHX1* or its isoforms in various plant species show significantly increased salt tolerance (Apse et al., 1999; Zhang and Blumwald, 2001; Zhang et al., 2001). On the other hand, Arabidopsis null mutants of AtNHX1 and tomato plants with LeNHX2 silenced are more sensitive to salt stress than control plants (Apse et al., 2003; Rodríguez- Rosales et al., 2008). Interestingly, overexpression of vacuolar localized pyrophosphatase (AVP1) also enhanced the salt tolerance of transgenic plants (Gaxiola et al., 2001).

The exact mechanism for NHX overexpression mediated salt tolerance remains unclear, since the increased salt tolerance is not always accompanied with increased vacuolar Na^+ accumulation (Rodríguez-Rosales et al., 2008; Zhang et al., 2008). NHX has been identified with K^+/H^+ exchanger activities. LeNHX2 from tomato plants when expressed in yeast affects the accumulation of K^+ but not Na^+ in intracellular compartment (Venema et al., 2003). Similarly, disruption of *ScNHX* in yeast has more effect on internal K^+ than Na^+ accumulation (Quintero et al., 2000; Venema et al., 2003). Overexpression of H^+- pyrophophatase in yeast increased the vacuolar pH gradient, and resulted enhanced salt tolerance, increased K^+ levels and reduced Na^+ levels in the presence of ScNHX1 (Gaxiola et al., 1999). Therefore over-expressing *NHX* genes induced salt tolerance might be partially due to the increased K^+ accumulation. *NHX* genes are also

involved in vacuolar pH regulation (Fukada- Tanaka et al., 2000; Brett et al., 2005) and vesicle trafficking (Mukerjee et al., 2006). These also present an alternative explanation for NHX protein mediated salt-tolerance. Consistently, overexpressing vesicle trafficking protein AtRab7 (Mazel et al., 2004) and suppression of vesicle- SNARE (Leshem et al., 2006) in Arabidopsis also increased tolerance to salt and osmotic stress and increased Na+ sequestration into the vacuoles.

Salt stress induced signaling

Salt stress induced signal perception mechanism remains unknown. It might involve proteins such as stretch- activated channels and ion specific receptors (Tester and Davenport, 2003). An early response to the sudden increase in extracellular Na^+ is a transient rise in cytosolic Ca^{2+} (Knight et al., 1997). Saline induced Ca^{2+} transporter/channel activities (Allen and Sanders, 1994, Wimmers et al., 1992) and components of Ca^{2+} related signaling pathways (Hirayama et al., 1995; Ishitani et al., 2000) also suggest Ca^{2+} signaling plays important roles in plant salinity response. Protein phosphorylation / dephosphorylation also plays important roles in plant responses to salt stress. Overexpression of GSK1/shaggy- like protein kinase in Arabidopsis resulted in plants exhibiting stress- response phenotypes accompanied by enhanced salt tolerance and increased Na+ accumulation in the shoot tissue of transgenic plants (Piao et al., 2001). It's possible the increased kinase activity activated Na^+ pump activity directly or indirectly.

Multiple myriad kinases and phosphatases have been found involved in salinity response, including metabolic phosphatases (HAL2, Gil-Mascarell et al., 1999), Ca^{2+}- dependent protein kinases (CDPKs) (SOS2, Halfter et al., 2000), mitogen- activated protein kinase (MAPK) cascades (Kovtun et al., 2000; Tena et al., 2001), Ca^{2+}/ calmodulin- activated serine/threonine-specific protein phosphatases (Pardo et al., 1998; Kudla et al., 1999) etc.

Much evidence indicated that hormonal signals play predominant roles in plant growth under saline conditions (Munns et al., 2002). Signals derived from root are translocated through the xylem sap to the shoot to reduce leaf growth and change leaf architecture. Root growth itself is also under the control of this signal (James et al., 2002). Abscisic acid is a likely candidate for this signal since it's translocated to the shoot through the xylem transpiraton stream and retranslocated via the phloem sap (Munns & Cramer, 1996). However, it is still unclear if ABA is the only signal in this long distance signaling.

SOS (*Salt Overly Sensitive*) signaling is the most well studied signaling pathway for plant salt stress response (Mahajan et al., 2008). *sos* mutants (*sos1, sos2* and *sos3*) were screened using root bending assay in Arabidopsis T-DNA and fast neutron induced plants (Wu et al., 1996; Zhu et al., 1998). These mutants show similar phenotypes as being hypersensitive to high amounts of external Na^+/Li^+ and unable to grow in K^+ deficiency conditions. The fact that double mutants do not show any additive

phenotypes suggests that they are involved in the same pathway. SOS3 encodes a myristoylated calcium- binding protein (Ishitani et al., 2000). Salt stress induced Ca^{2+} elevation is sensed by SOS3 which interacts with SOS2 protein kinase and the SOS2-SOS3 complex phosphorylates the plasma membrane localized Na^+/H^+ antiporter SOS1 and activates Na^+ efflux process (Shi et al., 2000; Halfter et al., 2000). SOS1 contains a N-terminal region of transmembrane domains with substantial similarity to Na^+/H^+ antiporters of animals and microorganisms, and a unique regulatory region at the C terminal. A recent study discovered the direct interaction between the C-terminal region of SOS1 with RCD1 (Radical- induced Cell Death), an important transcriptional regulator of oxidative- stress response in plants, suggesting SOS1 is also involved in detoxification of ROS (Katiyar-Agarwal et al., 2006). *sos2* mutant has the most severe phenotype compared with *sos1* and *sos3* under salt stress conditions. It has been found that SOS2 protein kinase has targets in addition to SOS1. SOS2 activates Arabidopsis Ca^{2+} transporter CAX1 to integrate Ca^{2+} transport and salt tolerance (Cheng et al., 2004). SOS2 interacts with subunits of vacuolar H^+-ATPase to promoter Na^+ sequestration into vacuoles (Batelli et al., 2007). A close homolog of *SOS3*, *AtCBL10/ScaBP8* was recently found to be involved in salts- stress regulation by directly interacting with SOS2 and function in Na^+ exclusion from plasma membrane and sequestration into vacuole (Kim et al., 2007; Quan et al., 2007). Compared with the root phenotype of *sos3*,

scabp8/cbl10 phenotypes were stronger in the shoot than the root. Direct interaction of SOS2 with a protein phosphatase ABI2 was also detected. ABI2 might play antagonistic roles as SOS2 in salt stress responses by dephosphorylating proteins that are phosphorylated by SOS2 (Ohta et al., 2003). The root defect phenotypes in *sos* mutants are more related to K^+ deficiency than Na^+ toxicity. Yeast experiments indicated that SOS1 does not transport K^+ (Quintero et al., 2002). The Na^+/H^+ antiporter activity of SOS1 however, is necessary for maintaining plant K^+ homeostasis in salt stress conditions, possibly by affecting a plasma membrane depolarization-activated outward rectifying K^+ channel as well as by affecting H^+ pump activities (Shabala et al., 2005; Qi and Spalding, 2004).

Na^+ entry and efflux from the roots

Na^+ entry from the soil environment into the root cells is a passive process, due to the negative electrical potential (~ -180mV) of plant cells (Cheeseman, 1982), and Na^+ accumulation into plants is due to the net result of passive influx and active efflux. Unidirectional Na^+ influx is mediated by three different pathways: two protein mediated pathway distinguished by their sensitivity to extracellular Ca^+, and a Na^+ 'leakage' pathway via the apoplast. The relative importance of these pathways varies with different species and growth conditions (Tester and Davenport, 2003). Major candidates for the Ca^{2+} -sensitive Na^+ influx are the non-selective cation channels including the cyclic nucleotide gated channels (the CNGCs) and the putative glutamate activated

channels (the GLRs) (CNGCs, Maathuis and Sanders, 2001; Leng et al., 2002; GLRs, Demidchik et al., 2004). Possible candidates for the Ca^{2+}-insensitive pathways are the Ca^{2+}- insensitive components of non- selective-cation channels (Davenport and Tester, 2000) and members of the KUP, and HAK gene families that encode high affinity K^+ transporters, and possibly mediate Na^+ influx at low affinity levels (Rubio et al., 1995; Tyerman and Skerrett, 1999). Some members of HKT transporters are able to mediate specific high- affinity Na^+ uptake, which might be a common process for most land plants (Haro et al., 2010).

Na^+ that enters the root cell have one of three fates: it can be translocated back to the apoplast; it can be compartmentalized into vacuoles, or it can move from cell to cell before being unloaded into the xylem apoplast and translocated via xylem transpiration stream from root the shoot. Unidirectional Na^+ influx into roots has been recorded within the range of 0.5-2.0 μmol g^{-1} f. wt min^{-1} for several species growing at conditions of 50mM external Na^+ (Tester and Davenport, 2003; Essah et al., 2003). This is significantly higher than Na^+ accumulation rates within plants (about ten- fold), implying substantial efflux of Na^+ across the plasma membrane (Tester and Davenport, 2003). An important candidate gene responsible Na^+ efflux is *AtSOS1*. *AtSOS1* is expressed in epidermal cells at the root tip (Shi et al., 2002) and the mature root zone (Shabala et al., 2005), as well as in the parenchyma cells at the xylem/ symplast boundary of roots (Shi et al., 2002).

Under mild salt stress, *sos1* mutants accumulate less Na^+ in the shoot than wild type plants (Shi et al., 2002). This suggests SOS1 is involved in maintaining low Na^+ level within the root, either by exporting to the environment or to the shoot. Na^+ remaining in roots can be sequestered in the vacuoles by tonoplast antiporter (NHX) family proteins. Comparing different maize varieties differing in salt tolerance, it was found that NHX genes were induced in roots of a variety known to exclude Na^+ from the shoot (Zörb et al., 2004). Similarly, comparing the *NHX* induction in salt tolerant barley (HvNHX1) and in rice that is more salt sensitive revealed *HvNHX1* was more induced in the root, whereas *OsNHX1* more induced in the shoot (Fukuda et al., 2004a, b). This suggests the salt tolerance in barley is related to Na^+ accumulation in root cell vacuoles, thus limiting the amount of Na^+ transported to the shoot.

Control of xylem loading

As Na^+ traffics from root to shoot through xylem transpiration stream, maintaining low Na^+ accumulation in shoot can thus be achieved by minimization of Na^+ entry into the xylem, or by maximizing Na^+ removal from the xylem sap before it reaching the shoot. Retrieval of Na^+ from the xylem as a major controller of shoot Na^+ accumulation has been suggested based on the research around *athkt1;1* mutants. *Athkt1* is a salt- sensitive mutant accumulating significant amount of Na^+ in the shoot tissue and reduced Na^+ in the root (Berthomieu et al., 2003; Mäser et al., 2002; Rus et al., 2004),

therefore AtHKT1;1 was involved in the regulation of Na^+ distribution between roots and shoots. AtHKT1;1 functions as Na^+-selective uniporter when expressed in *Xenopus laevis* oocytes and yeast (Uozumi et al., 2000). Based on the result that HKT1 localized to the plasma membrane of xylem parenchyma cells, reduced Na^+ content in the phloem exudate and elevated Na^+ level in the xylem sap of *hkt1;1* mutants, it was hypothesized HKT1 function in retrieval of Na^+ from xylem parenchyma cells to facilitate Na^+ loading and recirculation via phloem from shoot back to the root (Sunarpi et al., 2005). More recent work using $^{22}Na^+$ labeling to study the individual process contributing Na^+/K^+ accumulation in Arabidoposis root and shoot demonstrates that *AtHKT1* is involved in Na^+ retrieval from xylem back into the roots instead of in phloem recirculation of Na^+ from shoot back into roots (Davenport et al., 2007). Research on two Arabidopsis accession lines (Ts-0 and Tsu-0) which accumulate significantly higher levels of Na^+ in the shoot than Col-0 demonstrates that the reduced expression of *AtHKT1;1* in the root tissue is responsible for the elevated Na^+ accumulation in shoot and this result was supported by the reciprocal grafting experiment between Col-0 and *hkt1;1* plants (Rus et al., 2006).

More evidence for a role of *HKT* in salinity tolerance is from the study in monocots. Quantitative trait locus mapping of rice *SKC1* (shoot K^+ content) has identified *OsHKT1;5*, the close ortholog of *AtHKT1;1*(Ren et al., 2005). Point mutations in *OsHKT1;5*, lead to changes in several amino acids and

enhanced Na^+ transport activity of OsHKT1;5 in the salt- tolerant cultivar Nona Bokra. OsHKT1;5 was localized to xylem parenchyma cells and involved in reducing Na^+ levels in xylem sap (Ren et al., 2005). Similarly the major salinity tolerance QTLs in bread wheat (*Kna1*) and wheat (*Nax1* and *Nax2*) have been correlated with polymorphisms in the copies of *AtHKT1;1* orthologs (*TmHKT7-A1* and *TmHKT7- A2* for *Nax1*; *TmHKT1;5* and *TaHKT1;5* for *Nax2* and *Kna1* respectively.) (Huang et al., 2006; Byrt et al., 2007). The *Nax1* locus mediates Na^+ exclusion from leaves, by removing Na^+ from the xylem of leaf sheath and preventing Na^+ entry into the leaf blade. Both Nax1 and Nax2 were shown to enhance K^+ accumulation in leaf sheaths and blades. (James et al., 2006). Together these studies suggest AtHKT1;1 and its close othlogs in rice (OsHKT1;5), wheat (TmHKT7-A1, TmHKT7-A2 and TmHKT1;5) and bread wheat (TaHKT1; 5) have major functions in mediating Na^+ tolerance and Na^+ exclusion from leaves by removing Na^+ from the xylem sap.

The functional interplay between AtSOS1 and AtHKT1 has been suggested to affect xylem loading/ unloading process and the differential Na^+ distribution in root and shoot (Rus et al., 2004). Research on SlSOS1 revealed its crucial role in the survival of tomato plants in saline soil (Olías et al., 2009). Comparing varieties differing in salt tolerance revealed the more tolerant tomato species accumulate more Na^+ in stems and old leaves, while the more sensitive species accumulate Na^+ mainly in roots (Cuartero and

Fernandez- Muñoz, 1999). *SlSOS1*- silenced plants accumulated significantly less Na^+ in stems than control plants under saline conditions (Olías et al., 2009a). Based on these results a model has been made that besides its main action in the extrusion of Na^+ out of the root, SlSOS1-mediate Na^+ transfer from xylem parenchyma cells to xylem vessels, preferentially from the root. HKT1 then mediate the reverse unloading process of Na^+ from the xylem to the stem before it reaches the shoot. SlSOS1 might also contribute in exclusion of Na^+ from young leaves toward the apoplast (Olías et al., 2009b).

Phloem recirculation of Na^+

Large gaps still remain in our knowledge of phloem recirculation of Na^+, especially its relative importance in shoot Na^+ accumulation and the specific membrane transporters involved in this process. The textbook views tend to support that Na^+ is effectively excluded from the phloem sap to avoid its accumulation in young and meristematic tissues. The challenges of studying phloem recirculation of Na^+ are mainly caused by the difficulty of collecting enough pure phloem exudate for accurate phloem sap measurements. Estimates of xylem and phloem fluxes in barley revealed that phloem export of Na^+ from leaves is only 10% of the import via the xylem (Munns, 2005). Similar Na^+ recirculation rate was obtained in durum wheat using $^{22}Na^+$ labeling in a split root system (James et al., 2006) and in Arabidopsis using $^{22}Na^+$ flux measurements (Davenport et al., 2007). Phloem recirculation of

Na^+ to levels that significantly affect leaf Na^+ accumulation has also been reported in several other species including lupin (Munns et al., 1988), maize (lohaus et al., 2000) and more recently in castor bean (Peuke, 2010). Moreover by comparing a salt- tolerant wild species of tomato (*Lycopersicon pennellii*) with domesticated tomato (Perez- Alfocea et al., 2000) and salt-tolerant *Phragmites communis* with rice (Matsushita and Matoh, 1991) revealed salt- tolerant species exclude Na^+ from phloem to greater extent than salt- sensitive species. Protection of young tissues and meristem region from over-accumulating Na^+ is of crucial importance for plant salt tolerance. ^{14}C labeled experiments indicated lower leaves are responsible for loading carbohydrates to be transported to roots, upper leaves to the shoot apex and photosynthate produced by middle-layer leaves is transported in both directions (Layzell et al.,1981). It has been described that Na^+ transport is targeted to certain leaves to protect the young tissue and meristem region from excessive accumulation of Na^+. Although the role of *HKT* gene in removing Na^+ from the xylem sap has been well defined, the hypothesis made by Sunarpi et al., (2005) that AtHKT1;1 involved in Na^+ loading into phloem vessels needs be considered based on the fact that HKT is also expressed in the shoot. It is possible that HKT is involved in the deposition of Na^+ to specific regions of the shoot to facilitate its loading into phloem (Jame et al., 2006). Recent research on cyclic nucleotide-gated channels (CNGCs) suggests some members of this family might be involved in re-allocation of

Na^+ within the Arabidopsis based on their specific expression pattern within the phloem region (AtCNGC19, Kugler et al., 2009), and salt- dependent phenotype as well as altered K^+/Na^+ ratio in roots and shoots of antisense plants (AtCNGC10, Guo et al., 2008). However, more detailed characterization of these channels is still required.

Part II. Phloem, structures and functions

Phloem is the long- distance route that transports photoassimilates (Chiou and Bush, 1998; Lalonde et al., 1999), mineral elements (Peuke, 2010), amino acids (Urquhart and Joy, 1981) and lipids (Madey et al., 2002) from source to sinks. The sources are mainly photosynthetically active leaves. The storage organs in some cases also act as the source tissues. Tissues that depend on the net import of fixed carbon are considered to be sinks, including roots, young leaves, fruits, seeds, meristematic region and most parenchymatous cells of cortex, pith, xylem and phloem (Evert, 2006). Phloem also transports a large amount of water and may serve as the major source of water for fruits, young leaves and storage organs (Lee, 1990; Araki et al., 2004; Nerd and Neumann, 2004). Recent research has revealed more important and complicated roles for phloem transport. Hormones (Baker, 2000) and flowering signals (Corbesier et al., 2007) are transported through phloem translocation stream. A large number of proteins and RNAs are also identified form phloem exudate, the majority of them the functions remain unknown. Long distance signaling predominantly occurs through the phloem. For this reason phloem plays a major role in inter- organ communication and in the coordination of growth processes within plant. Phloem transport was also found to be the major source for the accumulation of nonessential element such as arsenic (As) in seeds (Carey et al., 2010).

Structures and pathways

The basic components of phloem are sieve elements and various parenchyma cells. Sieve elements are the principal conducting cells. Mature sieve elements are devoid of nucleus, tonoplast, and the wall areas are characterized with pores to increase the degree of symplasmic continuity between vertically or laterally adjoining sieve elements. The remaining organelles (endoplasmic reticulum, plastids and mitochondria) occupy a peripheral position to facilitate mass flow of phloem components. Sieve elements (SEs) are intimately linked with specific parenchyma cells called companion cells (CCs) via numerous specialized plasmodesmata structures- **the pore plasmodesmal units** (**PPU**s) and rely on the companion cells to provide most of the cellular components for their maintenance (Evert, 2006). Derived from the same cambial mother cell, the SE-CC complexes become increasingly symplasmically isolated from the adjacent phloem parenchyma cells during differentiation, which makes the transport phloem independent structure both physiologically and functionally (Van Bel and Van Rijen, 1994). Despite the symplastic isolation, water molecules have been detected exchange freely along the transport path with surrounding tissues (Eschrich et al., 1972; Phillips and Dungan, 1993).

PPUs are different from regular plasmodesmata structure in that they consist of multiple channels on the CC side and a single pore on the SE side (Oparka and Turgeon, 1999). Microinjection of fluorescently labeled probes into

companion cells or sieve elements revealed the size exclusion limit (SEL) between sieve tube – companion cells is around 10-40 KDa (Kempers and van Bel, 1997), significantly larger than the SEL of PD between epidermal cells (Derrick et al., 1990) or mesophyll cells (Wolf et al., 1989) which is at the range of 1 kDa. Diffusion of the fluorescent dyes occurs on both directions between SE and companion cells (Kempers and van Bel, 1997). In consistent, expression of green fluorescence protein (27kDa) specifically in CCs of Arabidopsis revealed the CC-SE trafficking of GFP and its subsequent unloading in sink tissues (Imlau et al., 1999). In research studying the expression of gfp- fusion proteins driven by companion cell specific promoter SUC2, a SEL of 67kDa were detected for PPUs connecting CCs to SEs (Stadler et al., 2005).

The PPU connecting SE with CC might be highly dynamic, depending on tissue type and developmental stages. Upon sink- source transition, SEL of PD decrease significantly, which is accompanied by a developmental switch from simple to branched forms of plasmodesmata (Oparka et al., 1999). Consistently the fusion of FLOWERING LOCUS T (FT) with green fluorescence protein (GFP) when expressed specifically in phloem companion cell, moves from CC into SE and through phloem sap into the shoot apical meristem (SAM) to induce flowering; however when expressed in CCs of minor vein of leaves, the fusion protein was retained in the minor veins (Corbesier et al., 2007). Proteins derived from pumpkin phloem sap

were detected to have the capacity to alter SEL of plasmodesmata (Balachandran et al., 1997). Similarly, viral proteins can manipulate PD connecting SE with CC thus affect the long- distance signaling and carbonhydrate partitioning. Expression of the TMV MP in tobacco phloem region leads to elevated levels of starch and sugars and a decrease in sugar export and dramatic shift of root to shoot ratio (Almon et al., 1997). A complete antioxidant system has been detected in phloem sap, including thioredoxin- h, cytosolic Cu/Zn superoxide dismutase, monodehydroascobate reductase, and peroxidase (Walz et al., 2002; Giavalisco et al., 2006). Their possible function might be to protect phloem especially plasmodesmata structures against reactive oxygen species. Loss of function of a m- type thioredoxin encoding gene led to callose and hydrogen peroxide accumulation and defects in plasmodesmal transport (Benitez- Alfonso et al., 2009). Cadmium at non- toxic concentrations has been detected to specifically block systemic movement of tobacco viruses (Citovsky et al., 1998; Ghoshroy et al., 1998). A cadmium- induced glycine rich protein (cdiGRP) negatively regulates viral systemic spread along phloem (Ueki and Citovsky, 2002), possibly by inducing callose deposits in phloem tissue thus reducing the SEL of PD (Iglesias and Meins, 2000).

Several types of minor veins and sucrose loading strategies

Phloem loading occurs in the minor veins of source leaves. Photoassimilates produced in leaf mesophyll cells diffuse into bundle sheath cells surrounding

phloem. Depending on the density of plasmodesmata linking bundle sheath cells with companion cells within the minor veins, two types of minor veins (Gamalei, 1991) and three different loading strategies have been identified (Rennie and Turgeon, 2009). Type-1 plants have a plasmodesmata density of >10 per μm^2 and type-2 plants have a plasmodesmata density of <1 per μm^2. Plants with plasmodesmata density in between of type 1 and type 2 are called type 1-2a plants (Gamalei, 1991). Arabidopsis thaliana is a type 1-2a species (Haritatos et al., 2000). Type 2 plants are known as apoplastic loaders, with sucrose being the major type of sugar transported within phloem. Sucrose is loaded from the apoplast into SE-CC complex by sucrose-proton cotransport activity that is energized by a plasma membrane H^+-ATPase (Lalonde et al., 2003). The importance of the phloem specific sucrose transporter for apoplastic loading is revealed by experiments including overexpression of apoplastic invertase (Heineke et al., 1992), down regulation of sucrose symporter activity (Burkle et al., 1998; Hackel et al., 2006; Riesmeier et al., 1994) and study of sucrose transporter T- DNA insertion lines(Gottwald et al., 2000; Slewinski et al., 2009). All these experiments led to significant growth defects including sucrose/ starch over-accumulation in source leaves, stunted growth, leaf chlorosis etc.. In some species the phloem sucrose transporter localized to the plasma membrane of sieve elements (Kühn et al., 2003) whereas in other species the sucrose transporter is specifically expressed in the companion cells (Arabidopsis

thaliana, Stadler and Sauer, 1996; Gottwald et al., 2000; *Plantago major*, Stadler et al., 1995). The type 1 species are regarded as symplastic loaders. Some type 1 species have specialized companion cells called intermediary cells characterized by especially large cell size with dense cytoplasm, extensive labyrinth of endoplasmic reticulum, numerous small vacuole, rudimentary plastids and highly branched plasmodesmata leading into them (Turgeon et al., 1993). The presence of intermediary cells is always accompanied by raffinose and stachyose being transported as the major form of sugar within the phloem. A polymer trap mechanism has been proposed to explain this process (Turgeon, 1991; Haritatos et al., 1996). Sugar synthesized in the mesophyll cells diffuse via plasmodesmata through bundle sheath cells and into the intermediary cells. Within the intermediary cells, sucrose is synthesized into raffinose and stachyose. The size of raffinose and stachyose is too large for them to diffuse back to the bundle sheath cells. From the intermediary cells they diffuse into sieve tubes to be transported into the sinks. There are some type 1 plants that also transport sucrose as the major form of sugar- the third strategy. Sucrose diffuses down the concentration gradient from mesophyll cells to sieve tube- companion cell complexes for long distance transport (Turgeon & Medville, 1998). This passive loading strategy is more widespread than previously thought, especially in trees (Rennie and Turgeon, 2009).

Phloem translocation and unloading

The mechanism of assimilate flow from the source to sinks is widely accepted to follow the osmotically generated pressure flow mechanism, originally proposed by Ernst Münch (1930) and modified by others (Crafts and Crisp, 1971; Eschrich et al., 1972; Young et al., 1973; van Bel, 1993). Sucrose loading into the source tissue leads to an increase in solute concentration, and a decrease in water potential, as a result water flows into the source tissue by osmosis. An opposite effect occurs in the sink tissue accompanied by sucrose unloading. Assimilates and other compounds thus flow along the pressure gradient from the source to the sink. Photoassimilates leak along the pathway (Hayes et al., 1987; Minchin and Thorpe, 1987). Sucrose transporters are expressed along the whole transport phloem, possibly involved in the recovery of leaked solutes from flanking tissues (Sauer, 2007; Srivastava et al., 2008). The process of phloem unloading remains largely unknown. Symplastic unloading is thought to predominate in most sink tissues (such as roots and developing leaves). Unloading of GFP from the phloem terminal and post- phloem diffusion has been detected in the root apical meristem of transgenic Arabidopsis plants (Stadler et al., 2005) and in cortical tissues destined to develop as nodules in Medicago (Complainville et al., 2003). Apoplastic unloading however has also been reported in sink tissues and some developmental stages. Energy dependent unloading process might be involved in unloading into the developing seeds of cereal and leguminous species (Patrick, 1990). A shift of phloem unloading from

symplastic to apoplastic pathway has been reported before onset of fruit ripening in grape berry (Zhang et al., 2006). Similarly, a transition from symplasmic connection to surrounding cells to symplasmic isolation has been reported in Arabidopsis inflorescence meristem before flowering initiation (Gisel et al., 1999; 2002). Viola et al. (2001) reported that tuberization of potato stolons is accompanied by a switch from apoplastic to symplasmic unloading. Transgenic research provided strong evidence that sucrose transporters are involved in apoplastic unloading based on the tuber- specific repression of potato StSUT1 expression leading to retarded development of tubers (Kühn et al., 2003).

Relationship between K^+ and sucrose loading/unloading

Potassium and sucrose are the major osmotic solutes in the phloem. 50% of K^+ transported to the shoot tissue is redistributed via phloem (Peuke, 2010). K^+ recirculation via phloem translocation to the root is thought to act as a signal that controls K^+ secretion into the root xylem and by feedback K^+ absorption from the soil (Drew and Saker, 1984; Marschner et al., 1996). Moreover as a major cation in the phloem K^+ stimulates sugar loading into the phloem (Giaquinta, 1980; Peel and Rogers, 1982). Mild K^+ deficiency has been shown to suppress assimilate translocation (Vreugdenhil, 1985). The most well know mechanism is from the research on the phloem specific K^+ channel AtAKT2/3 (Marten et al., 1999). AKT2/3 is predominantly expressed in the vasculature of the source tissue. Gene transcription induced by light

and high CO_2 concentration, indicating the positive regulation of photosynthesis (Deeken et al., 2000). *AKT2/3* endodes a weakly rectifying, voltage independent and proton- blocked K^+ channel (Marten et al., 1999). Compared with that of the wild type plants, the phloem exudate of *akt2/3-1* mutant has reduced sucrose concentration and exhibits a reduced K^+ dependence of the phloem membrane potential. When co-expressed with sucrose transporter *AtSUC2* in *Xenopus oocytes* AKT2/3 effectively inhibits membrane potential depolarization upon sucrose application. However K^+ concentration within phloem sap was not significantly influenced by loss of function *AKT2/3* mutations, suggesting AKT2/3 is more involved in maintaining phloem tissue membrane potential in a K^+ dependent manner rather than loading K^+ into the phloem (Deeken et al., 2002). VFK1 is an AKT2/3 homolog isolated from *Vicia faba*. In situ RT-PCR revealed its specific expression within the phloem tissue, with the expression predominantly in sink tissues and the stem. Like AKT2/3 VFK1 expression is induced in the light. When source leaves were forced to form sink tissues, the channel mRNA increased more than two fold. In developing seeds the expression of *VFK1* is tightly correlated with *VfSUT1* with the transcript maximum occurs at the beginning of the storage stage and decrease during maturation. Feeding fructose instead of sucrose or glucose doubled VFK1 gene expression and increased the K^+ channel activity, and as a result K^+ channel dominated the electrical properties of the sieve element plasma membrane. Since fructose

is the product of apoplastic invertase, a tight correlation between sucrose and K^+ unloading from the phloem and positive regulation of K^+ channel activity by sucrose unloading is suggested (Ache et al., 2001).

Proteins

Besides facilitating the cell-to- cell exchange of metabolites and mineral elements, PD also mediate the trafficking of macromolecules such as proteins and RNAs. Proteins that move through PD are defined as non- cell-autonomous proteins (NCAPs). Analyses of phloem exudates from multiple species (pumpkin, Lin et al., 2009; rape, Biavalisco et al., 2006; rice, Aki et al., 2008; castor bean, Barnes et al., 2004; cucumber, Walz et al., 2004) revealed a large population of NCAPs within phloem sap. The presence NCAPs is also supported by grafting experiment, analysis of cucumber scion sieve tube contents detected pumpkin stock- derived phloem sap proteins (Golecki et al., 1998). The functions of most phloem-sap derived proteins remain unidentified. The identified proteins are divided into several types: RNA binding proteins possibly involved in unfolding and refolding of RNA during trafficking (Jorgensen et al., 1998; Yoo et al., 2004), molecular chaperones to assist the delivery of protein “cargo” (Aoki et al., 2002), proteins involved in ubiquitin- mediated proteolysis, protein synthesis and stress response etc. (Lin et al., 2009). Heavy metal binding proteins including ferredoxin, copper homeostasis factor, metallothioneins have been detected in phloem sap of several species, underlining the importance of this class of proteins in the

function of SEs (Giavalisco et al., 2006; Barnes et al., 2004; Krüger et al., 2002). Their functions might be involved in antioxidant defense; redox reactions and phloem- mediated metal reallocation (Biavalisco et al., 2006). The most significant example of non-cell- autonomous protein that serves as long-distance phloem mobile signal is *FLOWERING LOCUS T* (FT). Study in Arabidopsis, pumpkin and rice indicates FT is the long-sought florigen, with the mRNA transcripts expressed in the vascular region of leaves in response to photoperiod however FT protein is translocated through the phloem translocation stream to the shoot apical meristem to induce flowering (Corbesier et al., 2007; Lin et al., 2007; Tamaki et al., 2007).

The findings that many phloem sap proteins are larger than 100 kDa (Balachandran et al., 1997; Walz et al., 2004) and the protein profiles identified from phloem sap are uniquely different from those of the surrounding tissues (Giavalisco et al., 2006; Lin et al., 2009) suggested that protein trafficking from CC to SE is a regulated process. Evidence is provided from the study of pumpkin (*Cucurbita maxima*) phloem sap protein CmPP36. This phloem mobile protein contains a plasma membrane- anchoring domain at the N- terminal. Following the cleavage of this 5 kDa membrane- targeting domain, the ΔN- CmPP36 moves into the phloem translocation stream. Microinjection experiments demonstrated that ΔN- CmPP36, but not CmPP36 is able to interact with plasmodesmata to mediate its cell- to- cell trafficking (Xoconostle-Cázares et al., 2000). Additional evidence comes from

the characterization of a sequence motif from a sub- class of non- cell-autonomous chaperones, which allowed these Hsc70 chaperones to engage in cell- to- cell translocation. When this sequence motif was used to replace the equivalent domains in human Hsp70 chaperone, the engineered chaperone regained the ability to move from cell to cell (Aoki et al., 2002). An endoplasmic reticulum- localized *Nicotiana tabacum* NON-CELL-AUTONOMOUS PATHWAY PROTEIN1 (NtNCAPP1) has the capacity to interact with approximately 30% of pumpkin phloem sap proteins. Transgenic plant expressing an engineered dominant negative form of NCAPP1, lacking the N- terminal membrane- anchoring domain displayed developmental changes- probably due to selective blockage of intercellular trafficking of specific NCAPs. This also support the model that NCAP delivery to plasmodesmata is both selective and regulated (Lee et al., 2003). The selective translocation of phloem sap proteins is also demonstrated by selective movement of CmPP16-1 into roots. Biotin- labeled probes including NCAPs, CmPP16-1 and CmPP16-2 were introduced directly into a SE and their subsequent translocation monitored. While both CmPP16-1 and CmPP16-2 moves to leaf tissues, only CmPP16-1 moves into the root. This property was abolished if CmPP16-1 was purified before reintroduction into sieve tube system. However reconstitution experiments involving CmPP16-1 and specific pumpkin phloem sap fractions restored this selective delivery of CmPP16-1 to the roots. This suggests the selective movement CmPP16-1 is

mediated by other phloem specific protein complex (Aoki et al., 2005).

Besides the selective transport, unregulated, diffusion- based movement might also account for some of proteins that enter the sieve tube system. Since CC expression of GFP and GFP- fusion proteins shows the diffusion of GFP and GFP- fusion proteins into SE translocation stream to be transported to the sinks (Stadler et al., 2005). As GFP is not plant origin, it's unlikely that they enter SE via a selective pathway. The relative importance of the non-selective process in phloem protein trafficking remains to be determined.

RNAs

The non-cell-autonomous nature of some RNAs has received much attention recent years, especially for those acting as potential long- distance signals (review by Kehr and Buhtz, 2008). Studies based on mRNA profiling of phloem tissue (Asano et al., 2002; Brandt et al., 1999; Ivashikina et al., 2003) and direct analysis of transcripts in phloem transpiration stream (Haywood et al., 2005; Xoconostle-Cázares et al., 1999; Deeken et al., 2008) detected a high population of RNAs that transport through phloem. The phloem sieve tubes as ideal place for RNA transport is also supported by the result that no detectable RNase activity detected in phloem sap (Sasaki et al., 1998; Doering- Saad et al., 2002). Three major types of RNA molecules are systematically transported, RNA viruses, endogenous plant mRNAs and small non-coding RNAs (Voinnet and Baulcombe, 1997; Mlotshwa et al., 2002). Most virus genomes are single strand RNAs. Local spread of virus

occurs from cell to cell via PD. Within vascular tissue viruses generally traffic by mass flow at rate similar to nutrient movement (Schneider et al., 1965; Santa Cruz, 1999) although selectivity of some forms has been reported in the systemic movement of *potato spindle tuber viroid* (PSTVd) (Zhu et al., 2001, 2002). Applying cadmium at non- toxic concentration to plants specifically blocks systemic movement of virus (Citovsky et al., 1998; Ghoshroy et al., 1998). This also supports the passive diffusion of virus RNA within the phloem. Viruses contain specific movement proteins (MPs) that have the ability to bind and unfold single stranded RNAs (Citovsky et al., 1990; Citovsky and Zambryski, 1991). MPs can increase the SEL of PD (Ding et al., 1992) and thus facilitate intercellular translocation of virus (Lucas, 2006). Another important factor for virus movement is the coat protein (CP). In some virus types, CPs are required for virus long- distance transport (Scholthof, 2005). Study of endogenous phloem proteins (CsPP2, CmPP2 and CmmLec17) in cucumber and melon revealed their interactions with viral RNAs and involved in virus translocation (Gomez and Pallas, 2004; Gomez et al., 2005). Phloem protein cmPP16 shares sequence homology with viral MPs and has been detected to interact with several RNA molecules (including some viral RNAs and its own mRNA) and facilitate RNA movement into the phloem by increasing the SEL of PD (Xoconostle-Cázares et al., 1999).

The first observation of mRNA presence in SE is from the study that mRNA of

sucrose transporter 1 (SUT1) in *Solanaceae* localized in SEs and PD connecting SEs to CCs (Kühn et al., 1997). Phloem transport of *CmNACP* mRNA in pumpkin was demonstrated by grafting experiments between pumpkin and cucumber plants (Ruiz- Medrano et al., 1999). Recent research has demonstrated mRNA transcripts as long- distance signals involved in the integration of whole- plant development. Potato tuber induction is controlled by *stBEL1* like transcription factors. *BEL1* like mRNA transcripts are localized to phloem cells, and grafting experiment revealed *StBEL5* transcripts move across graft unions to stolon tips correlated with enhanced tuber production. The untranslated regions of *StBEL5* mRNA is involved in mediating long- distance transport (Banerjee et al., 2006; 2009). *GIBBERELLIC ACID INSENSITIVE* (*GAI)* is an important negative regulator of GA signaling. Grafting experiments in Arabidopsis and tomato plants demonstrated the traffic of ∆*DELLA- gai* transcripts (gain- of- function allele of *GAI*) across graft union and induced leaf-shape phenotypes in scion leaves. Detailed analysis of wild- type scion grafted to ∆*DELLA- gai* stocks revealed the presence of ∆*DELLA- gai* transcripts in young leaves but not in developing fruits. This indicated the translocation of *GAI* transcripts is a selective process rather than a result of mass flow (Haywood et al., 2005).

RNA silencing signals can also spread systematically. This was first shown in the grafting experiment where silencing signals moved through grafted union and induced post- transcriptional gene silencing (PTGS) in non- silenced

scion tissues (Palauqui et al., 1997). Non- toxic concentration of cadmium treatment inhibited systemic silencing spread, indicating translocation of silencing signal might be a passive process from source to sinks (Ueki and Citovsky, 2001). The identity of the systemic signal still remains elusive. siRNA originating from a transgene or a virus infection is a possible candidate for this phloem mobile silencing signal. siRNA molecules are possibly transported through phloem as single strands of 19-25nt and their traffic is regulated by a small RNA binding protein CmRSRP1 (Yoo et al., 2004). The other small RNA species found in the phloem are microRNAs (miRNAs) (Yoo et al., 2004). miRNAs are endogenous 21-24 nt long molecules that act as negative regulators of gene expression in different developmental processes (Rhoades et al., 2002). Several studies have demonstrated miRNAs as functional long- distance signals. miR395 has been implicated in being a shoot- derived, phloem- mobile signal involved in root sulfate assimilation by targeting ATP sulphorylases (APS1, APS3 and APS4) (Jones- Rhoades and Bartel, 2004). Another example is miR172, which promotes tuberization and flowering when overexpressed in potato plants. miR172 is present in vascular bundles and its effect on tuberization is graft transmissible. miR172 promotes tuberization probably via upregulation of BEL5 in leaves and stolons (Martin et al., 2009).

Study on *nakr1-1*, a mutant accumulates Na^+ and K^+ and with multiple developmental defects

Research presented in this thesis represents a study that connect phloem function with Na^+ homeostasis in Arabidopsis plants based on systematic study of a Na^+ and K^+ accumulation mutant *nakr1-1*. Elemental analyses had been performed on various parts of *nakr1-1* including rosette leaves, roots and seeds. Contribution of various processes on Na^+ accumulation in rosette leaves was studied using techniques including reciprocal grafting and xylem sap elemental analyses. Traditional linkage mapping together with DNA chip based mapping were used to identify *nakr1-1* mutation. The expression of *AtNaKR1* at the tissue level and its cellular localizations were studied using NaKR1-GUS and NaKR1-GFP constructs driven by *AtNaKR1* promoter. Based on the specific localization of NaKR1 protein in the phloem tissue and proximal root meristem, detailed studies of phloem function, phloem cell identities, root meristem defects were performed in *nakr1-1* mutant. The bolting times of *nakr1-1* mutant under different floral induction conditions were also recorded. Together these results provide evidence that a heavy- metal binding protein AtNaKR1 is important for phloem function and that phloem recirculation plays an important role in maintaining low Na^+ accumulation in rosette leaves of Arabidopsis plants.

2. *Arabidopsis* AtNaKR1 is a Phloem Mobile Metal-binding Protein Necessary for Phloem Function and Root Meristem Maintenance

ABSTRACT

The *SODIUM POTASSIUM ROOT DEFECTIVE 1* (*NaKR1*) encodes a soluble metal binding protein that is specifically expressed in companion cells of the phloem. The *nakr1-1* mutant phenotype includes high Na^+, K^+, Rb^+ and starch accumulation in leaves, short roots, late flowering and decreased long-distance transport of sucrose. Using traditional and DNA microarray-based deletion mapping, a 7 bp deletion was found in an exon of *NaKR1* that caused a premature stop. The mutant phenotypes were complemented by the native gene and by GFP and GUS fusions driven by the native promoter. NAKR1-GFP was mobile in the phloem, it moved into sieve elements and into a novel symplasmic domain of the root meristem. Grafting experiments revealed that the high Na^+ accumulation was mainly due to loss of NaKR1 function in the leaves. This supports a role for the phloem in recirculating Na^+ to the roots to limit Na^+ accumulation in leaves. The onset of root phenotypes coincided with NaKR1 expression after germination. Short root length was primarily due to a decrease in cell division rate in the root meristem indicating a role for NaKR1 expression in the phloem in root meristem maintenance.

INTRODUCTION

Plant vascular tissue consists of two parallel pathways for long distance transport: the xylem and phloem. The xylem transports water and mineral nutrients from roots to the shoot. The phloem transports sugars and other metabolites, proteins and RNA from photosynthetic tissues to sinks such as roots, developing leaves, flowers, seeds and storage tissues (reviewed by Lough and Lucas, 2006). In angiosperms, the main unit of the phloem is the companion cell/sieve element complex (CC/SE). Sieve elements that form the conduits for transport are highly differentiated cells that lack many of the normal intracellular organelles such as mitochondria and a nucleus. Companion cells are connected to sieve elements via plasmodesmata; they provide metabolic support and synthesize RNAs and proteins that are transported in sieve elements. In addition to the basic function of the phloem in transporting reduced carbon to sink tissues, the phloem performs a variety of important roles in plants. Genes specifically expressed in the phloem have been identified (Brady et al., 2007; Zhang et al., 2008), but the functions of relatively few phloem-expressed genes have been analyzed.

The classic theory that the phloem in leaves has a significant function in promoting Na^+ tolerance (Greenway and Munns, 1980) does not have much support from molecular genetic studies. Based on the phenotype of *sas2* mutants, Na^+ transporter AtHKT1 was proposed to function in the phloem (Berthomieu et al., 2003). However, the current consensus is that AtHKT1 mainly functions to remove Na^+ from the xylem, thus limiting Na^+ accumulation in leaves

(Mäser et al., 2002; Sunarpi et al., 2005; Rus et al., 2006). The extent and mechanism of Na^+ translocation in the phloem remains unknown and has been identified as a current research topic that is important for understanding Na^+ tolerance (Munns and Tester, 2008). More is known about the function of K^+ in the phloem. K^+, along with sugars, serves as one of the major osmotica in phloem sap. K^+ efflux via AKT2/3 also serves to repolarize the membrane potential during sucrose uptake (Deeken et al., 2002).

One main function of the phloem is the transport of fixed carbon from photosynthetic tissues to sink tissues such as growing leaves, roots, flowers and seeds. *atsuc2* mutants are specifically defective in sucrose transport into the phloem and have a severe phenotype that includes dwarf stature, starch accumulation in leaves and anthocyanin accumulation (Gottwald et al., 2000). The severity of the *atsuc2* phenotype indicates the importance of companion cell function but provides limited information about other roles of the phloem such as the control of flowering, K^+ and Na^+ translocation, and control of meristem functions.

Plasmodesmata (PD) are essential for phloem function. Companion cells and sieve elements are connected by specialized PD with high size exclusion limit (SEL) of at least 67 kDa (Stadler et al., 2005). Observing cell-to-cell movement of GFP fusion proteins has been instrumental in identifying symplasmic domains: groups of cells connected by PD. GFP fusions of 36-67 kDa expressed under the control of the companion cell specific AtSUC2 promoter were translocated in the phloem and entered the protophloem but did not move throughout the root tip,

although free GFP (27 kDA) was able to move throughout the root tip (Stadler et al., 2005). This sets a SEL of 27-36 kDa for PD connecting cells of the root tip with protophloem cells. Little is known concerning the specificity or sequence requirements for protein transit through PD (Lucas et al., 2009).

In this paper, the cloning of the *NaKR1* gene, the analysis of the *nakr1-1* mutant phenotype, localization, phloem transport, and metal binding properties of the NaKR1 protein are presented. The results provide evidence for Na^+ recirculation in the phloem, a function for the phloem in root meristem maintenance, and a novel symplasmic domain in the root tip.

RESULTS

nakr1-1 has high K^+, Na^+ and Rb^+ in leaves

In previous work an *Arabidopsis thaliana* fast neutron-induced mutant (136:31) was identified based on differences in elemental composition in leaves as determined by ICP-MS analysis (Lahner et al., 2003). When isolated, the mutant showed a complex phenotype with high Li, Mg, K, As and low Mn compared with wild type (Col-0). After backcrossing twice to Col-0 a single recessive allele was resolved that resulted in high Na, K and Rb (a chemical analog of K) (Fig. 1) accumulation in leaf tissue. The mutant and Col-0 plants were grown under various soil conditions and the high Na^+ and K^+ phenotypes were consistent. Fig. 2A-C shows results from a typical experiment where plants were grown under conditions described by Lahner et al. (2003). The mutant accumulated around 3-fold higher Na^+ and 2-fold higher K^+ and Rb^+ compared to

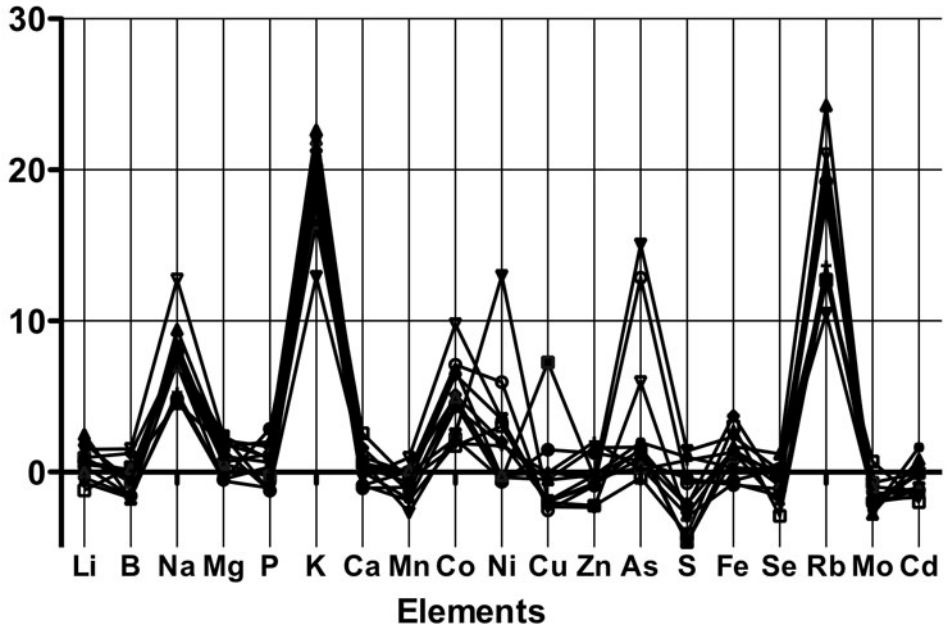

Figure 1. Leaves of *nakr1-1* contain higher Na^+, K^+ and Rb^+ than Col-0. Arabidopsis *nakr1-1* and Col-0 plants were grown in conditions as described in Lahner et al. (2003). Rosette leaves were sampled after 5-6 weeks of growth and elemental analysis was performed by ICP-MS. Differences in content of the mutant compared to Col-0 for each element analyzed are plotted as Z-values (standard deviations) for individual plants. The zero line indicates the average for Col-0 grown in the same tray.

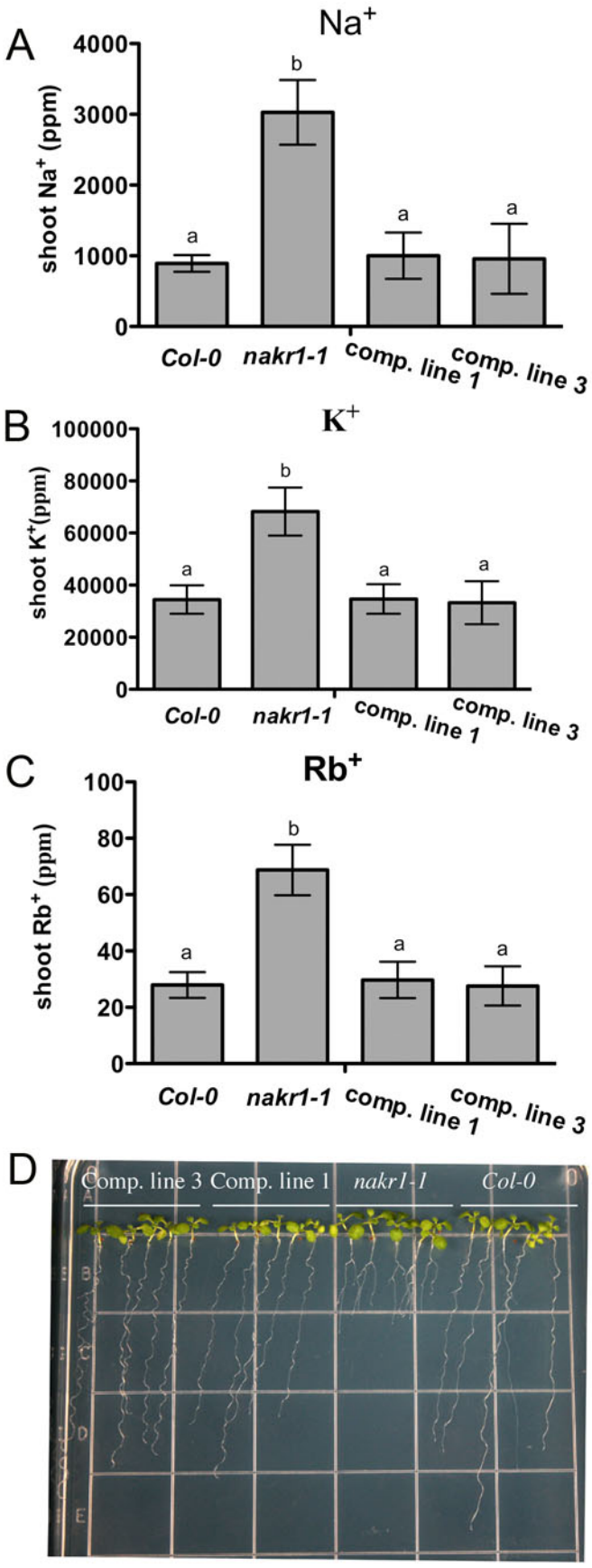

Figure 2. *nakr1-1* Na, K and Rb accumulation phenotypes and root growth defects were complemented by a NaKR1 whole-gene construct. (A to C) Concentrations of shoot Na^+, K^+ and Rb^+ in Col-0, *nakr1-1* and complemented lines 1 and 3 (T2 generation) were determined by ICP-MS. Plant growth and sample collection was according to Lahner et al. (2003). Values are the average elemental content of 12 individual plants of the same genotype. Error bars represent mean ± SD. Student's t-test was performed and the different letters indicate significant difference with $p < 0.05$. (D) Eight day-old seedlings grown vertically on ATS media. From left to right are two complementation lines, *nakr1-1* and Col-0. Note that *nakr1-1* had significantly reduced primary root growth.

Col-0. The mutant also showed defects in primary root growth (Fig. 2D). Therefore, we renamed the mutant *nakr1-1* for *high Na, high K, root defective 1*.

NaKR1 encodes a heavy metal coordinating protein

A mapping population was created after backcrossing *nakr1-1* once to Col-0; the mutant was crossed with Landsberg erecta (Ler-0) and 300 F_2 progeny with short primary roots were selected. The primary root growth defect in *nakr1-1* is illustrated in Fig. 2D. Using PCR-based mapping, *NaKR1* was localized within a region of 90kb (514.5-604.6kb) at the top of chromosome 5. To identify the mutation, DNA microarray-based deletion mapping was used. Genomic DNA was prepared from two populations (*nakr1-1* mutants and Col-0) and hybridized to *A. thaliana* ATTILE 1.0R arrays. A single deletion of 7 base pairs was identified within At5g02600 (Fig. 3), which caused a frame shift mutation (Fig. 4A and B) and premature truncation of the C-terminal 183 amino acids (Fig. 4C). Transformation of *nakr1-1* with a 2817 bp genomic construct containing a 689 bp promoter and 5'UTR, all the exons and introns and 1005 nucleotide sequence after the stop codon (Fig. 4A) complemented the root growth defects (Fig. 2D) as well as the Na^+ (Fig. 2A), K^+ (Fig. 2B) and Rb^+ (Fig. 2C) over-accumulation phenotypes. This confirmed the identity of the *NaKR1* gene. Four T-DNA insertion lines were examined with insertions in the *NaKR1* promoter region (SALK_022426) or downstream of the coding region (SALK_033325, SALK_049519 and FLAG_633FO3), however none displayed a phenotype.

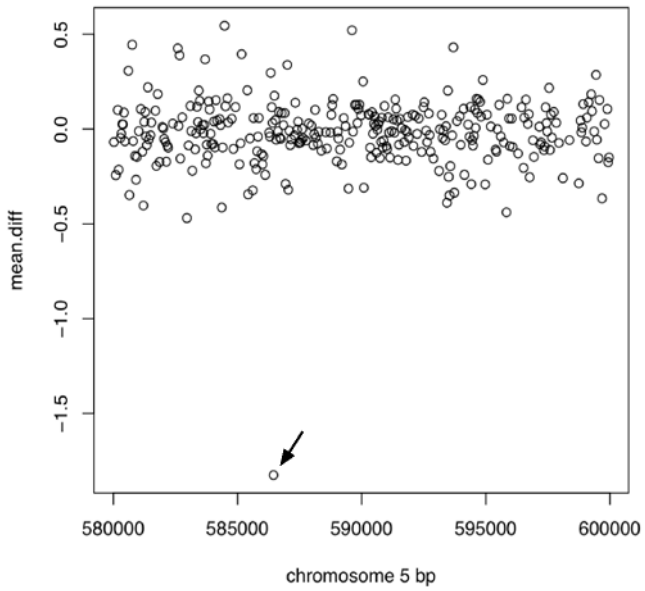

Figure 3. Identification of a 7 bp deletion in At5g02600. *nakr1-1* and Col-0 WT genomic DNA was hybridized to Arabidopsis thaliana ATTILE 1.0R arrays. The vertical axis is the difference between the mean hybridization of *nakr1-1* and Col-0. Horizontal axis is the base pair position on chromosome 5. The data points represent hybridization to individual 25- mer features on the *A. thaliana* ATTILE 1.0R chip. Microarray data have been submitted to the GEO database with accession:

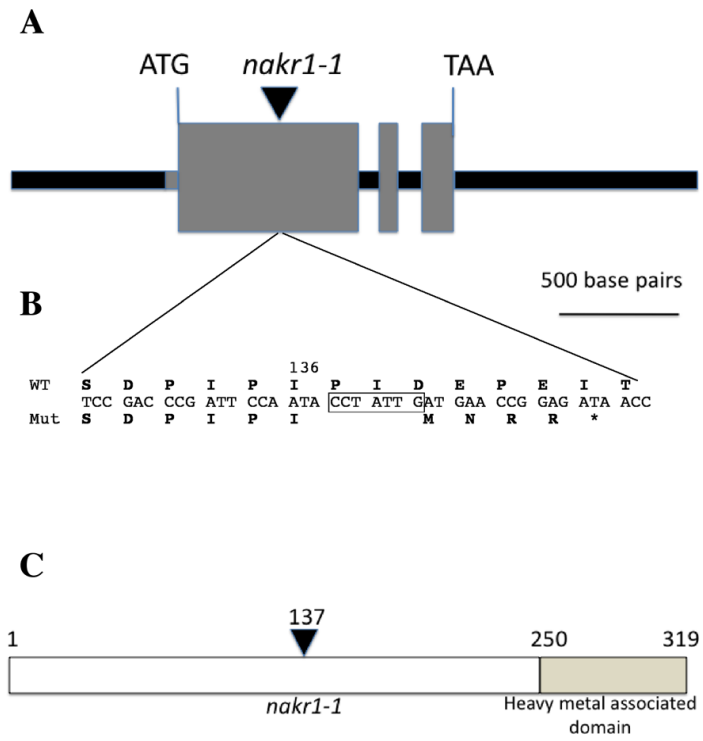

Figure 4. *NaKR1* gene and protein structure.
(A) The gene structure of *NaKR1* (used for complementation), with the positions of the initiation and stop codon highlighted. From left to right are the promoter region and 5′ UTR (the black and gray box in front of ATG), 3 exons, 2 introns and 3′ UTR. The black arrowhead indicates the position of *nakr1-1* mutation. (B) A deletion of 7 base pairs in nakr1-1 in the first exon, indicated by the boxed sequence caused a frame shift and premature truncation of C-terminal amino acid sequences. (C) The protein structure of NaKR1, with a C-terminal heavy metal associated domain and an N-terminal region with little similarity with other functional domains. Amino acid position 137 indicates the first changed position in the mutant protein.

NaKR1 is predicted to encode a soluble protein of 319 amino acids, with a heavy metal associated domain (HMA domain, pfam 00403.6) of 59 amino acids at the C-terminal end (Fig. 4C). No homology was found between the N-terminal region of NaKR1 and proteins of known function. Two *Arabidopsis thaliana* genes of unknown function share high homology with NaKR1 in the C-terminal domain (At2g37390 is 79% identical and At3g53530 is 72% identical) and lower homology in the N-terminal domain (At2g37390 is 36% identical and At3g53530 is 32% identical). The HMA domain has been found in all organisms, in proteins that transfer/bind heavy metals, including small metallochaperones, heavy metal transporters and enzymes that use heavy metals as cofactors. The conserved sequence L(M)XCXXC is believed to be a Cu binding site, in which the two cysteines coordinate metal directly; this motif was also observed in transport proteins that specifically transport Zn^{2+}, Ni^{+} and Hg^{+} (Bull and Cox, 1994; Dykema et al., 1999; Suzuki et al., 2002).

The HMA domain of NaKR1 shares 47% and 45% identity with *A. thaliana* Cu chaperones AtATX1 and AtCCH, respectively. The homolog in yeast (*Saccharomyces cerevisiae*) *ATX1* has been well characterized (Lin and Culotta, 1995; Lin et al., 1997; Pufahl et al., 1997) and found to be involved in both Cu transport and defense against oxidative stress. When overexpressed in a yeast strain lacking the superoxide dismutase gene *SOD1*, both *AtATX1* and *AtCCH* can protect the mutant from active oxygen toxicity in a Cu dependent manner (Himelblau et al., 1998; Puig et al., 2007). In our experiments, overexpression of *NaKR1* or the C terminal region alone (containing the HMA domain) failed to

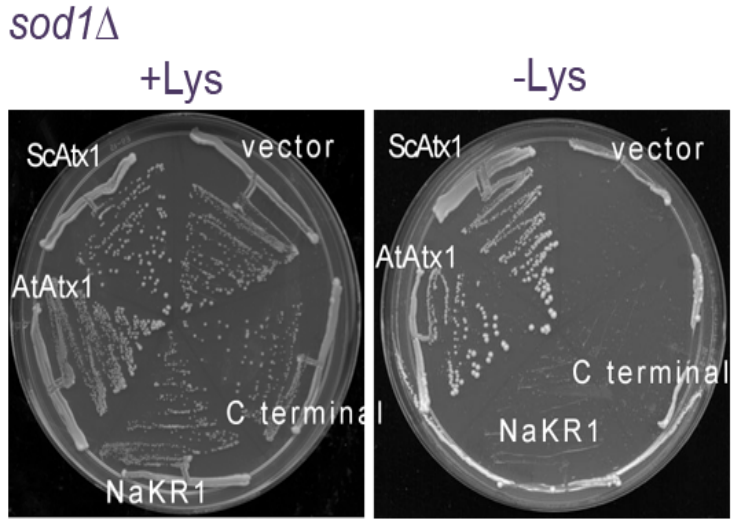

Figure 5. *AtNaKR1* and the C- terminal HMA domain failed to rescue the lysine auxotrophy phenotype of *sod1*Δ mutant. Lysine auxotrophy is an indication for reactive oxygen toxicity. Yeast *sod1*Δ cells transformed with p426GPD vector (vector) alone or *Saccharomyces cerevisiae* ATX1 (ScATX1), Arabidopsis ATX1 (AtATX1), AtNaKR1 and the C- terminal region (containing the HMA domain) were assayed for growth on SC-Ura and SC lacking lysine medium.

complement the reactive oxygen toxicity phenotype of yeast *sod1Δ* mutant (Fig. 5), indicating that the HMA domain of NaKR1 functions differently than AtATX1/AtCCH when expressed in yeast.

To test for possible metal binding, NaKR1 was expressed in *Escherichia coli* as a fusion to maltose binding protein (MBP). The purified MBP-NaKR1 fusion protein is shown in Fig. 6A. The identity of the purified MBP-NaKR1 fusion protein was confirmed by mass spectrometry analysis. Forty unique peptides were detected covering 48.5% of the fusion protein sequence (Fig. 7). Several heavy metals were detected in the purified protein sample using ICP-MS analysis (Fig 6B). Higher Zn, Cu, Fe, Ni and Co was associated with the MBP-NaKR1 fusion protein compared to the MBP control. The molar ratio of protein to metals was around 3:1 (Fig. 6C) indicating that NaKR1 protein is a metal binding protein. A mutated version of the *NaKR1* whole gene construct in which two conserved Cys residues in the HMA domain were changed to Gly failed to complement *nakr1-1* phenotypes (data not shown). This indicates that metal binding is essential for NaKR1 function in the plant.

NaKR1 **is specifically expressed in the phloem**

To study the expression pattern, a whole gene GUS fusion (*NAKR1*pro:*NAKR1-GUS*) was expressed in Col-0 and 10 independent transformants were analyzed. No GUS staining was found in embryos or imbibed (but not germinated) seeds (Fig. 8A). At 1 day after germination (dag), GUS staining was observed in 10% of the seedlings. GUS activity was found in the

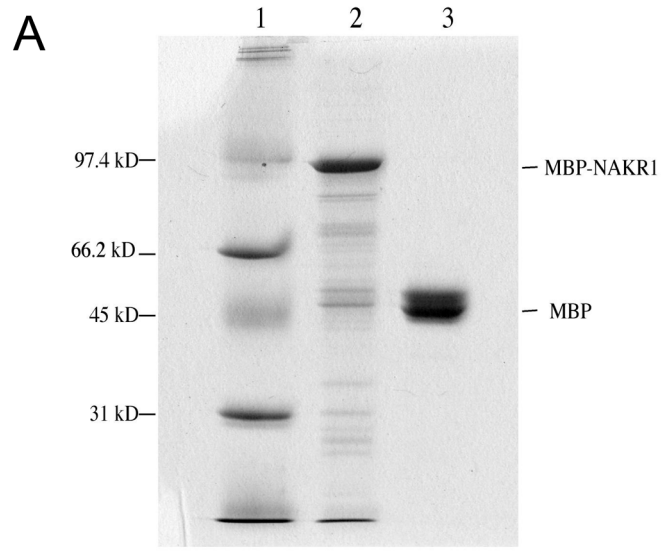

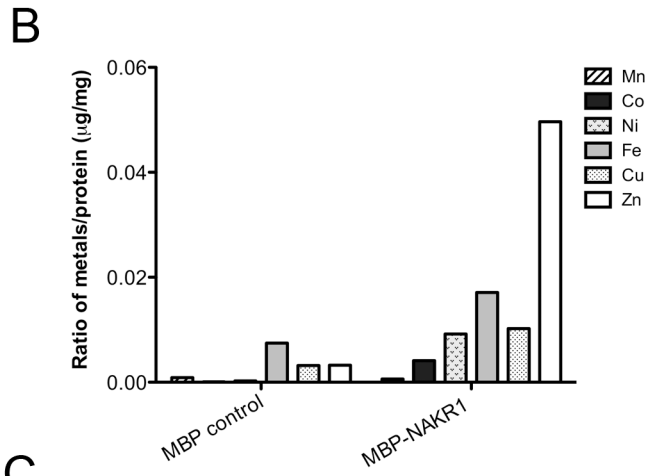

C

Metal Elements	Mn	Co	Ni	Fe	Cu	Zn	Total
Metal/Protein ratio (mol/mol)	0.0025	0.0672	0.0156	0.0343	0.0352	0.1683	0.3231

Figure 6. Purified MBP-NaKR1 fusion protein binds heavy metals. MBP-NaKR1 or MBP (control) were expressed in *E. coli* BL21-AI and purified using amylose resin. (A) Coomassie-stained polyacrylamide gel (12%) showing 3 µg purified MBP-NaKR1 (lane 2) and 3 µg maltose binding protein (lane 3). Lane 1 contained low range SDS-PAGE standards (Bio-Rad). (B) Metal content of the purified protein samples MBP-NaKR1 and MBP. Average metal concentration from two independent experiments is presented. The metal concentrations were determined by ICP-MS analysis (C) Molar ratio of heavy metal to protein in purified MBP-NaKR1 samples. The metal concentrations were determined by ICP-MS analysis and protein concentrations by amino acid analysis. The values represent the average of results from two independent experiments.

MKTEEGKLVIWINGDKGYNGLAEVGKKFEKDTGIKVTV
EHPDKLEEKFPQVAATGDGPDIIFWAHDRFGGYAQSGL
LAEITPDKAFQDKLYPFTWDAVRYNGKLIAYPIAVEAL
SLIYNKDLLPNPPKTWEEIPALDKELKAKGKSALMFNL
QEPYFTWPLIAADGGYAFKYENGKYDIKDVGVDNAGAK
AGLTFLVDLIKNKHMNADTDYSIAEAAFNKGETAMTIN
GPWAWSNIDTSKVNYGVTVLPTFKGQPSKPFVGVLSAG
INAASPNKELAKEFLENYLLTDEGLEAVNKDKPLGAVA
LKSYEEELAKDPRIAATMENAQKGEIMPNIPQMSAFWY
AVRTAVINAASGRQTVDEALKDAQTNSSSNNNNNNNNN
NLGIEGRISEFLNQTSLYKKAEGPSRPEGDITMLCASQ
ASTTTLCSTMDQTSQPSSSSSATIRLGGRAIDRHNPII
RDGRRLTPPPSPNLNPSSSSSSTYHTPLMTRLGLESSE
QKRLAKRKSKKGDSDVGKSPVSCFSSDTPQGSSRYLLS
NPVFFDGFVDSDPIPIPIDEPEITKADDLNNFHEDRLI
INASKYLSTSASFLEKKQPDFFEGFLDYEPVLSPDNPF
SEPTKASPTASLSSLEDKDVSSPDFKFSPPPPPPPSPP
QSSPPSPPEKNSSSDQVVVLRVSLHCKGCAGKVKKHLS
KLKGVTSYNIDFAAKKVTVTGDVTPLTVLASISKVKNA
QFWPEIIQK

Figure 7. The identity of the purified MBP-NaKR1 fusion protein was confirmed by mass spectrometry analysis. Expression of MBP-NaKR1 in *Escherichia coli* strain BL21-AI was induced by adding IPTG to the liquid culture. Cell lysate was incubated with amylose resin and MBP-tagged proteins eluted with 10mM maltose and digested with trypsin. The underlined sequences were the unique peptides detected by LC-MS/MS analysis.

vasculature of the root-hypocotyl junction, and to a lesser extent in the hypocotyl (Fig. 8B). At 2 dag GUS activity was found in the vascular tissue throughout the seedling (Fig. 8C). In more mature plants, strong GUS staining was found in vascular tissue in rosette (Fig. 8D) and cauline leaves (Fig. 8E). In floral tissue, GUS staining was mainly localized to the sepals and the filaments of the flowers and the pedicel of the siliques (Fig 8F and 8G). Cross sections of roots (Fig. 8H) and leaf petioles (Fig. 8I) revealed expression in the phloem region of the vasculature, but not in the xylem.

NaKR1 (At5g02600) expression was previously reported to be companion cell specific. This is based on microarray results and cDNA library analysis of mRNA transcripts isolated from purified companion cell protoplasts, nuclei or isolated phloem tissue (Brady et al., 2007; Deeken et al., 2008; Zhang et al., 2008). In the work by Zhang et al (2008), *NaKR1* was among the top 12 transcripts most enriched in companion cell nuclei. Furthermore, the *NaKR1pro:histoneB2-GFP* (called NPCC6 in that study) was expressed in *A. thaliana* and shown to specifically label companion cells.

In our experiments, expression of histoneB2-GFP driven by the *NaKR1* promoter labeled nuclei within the phloem of roots (Fig. 9A), confirming results of Zhang et al. (2008). In the root tip, histoneB2-GFP fluorescence was only found within the phloem (Fig. 9B). Sieve plates stained with aniline blue were identified in SE adjacent to cells containing histoneB2-GFP fluorescence in nuclei (Fig. 9C). This confirms that NaKR1 is expressed in companion cells. A whole gene GFP fusion (*NaKR1pro:NaKR1-GFP*) complemented the *nakr1-1* mutant

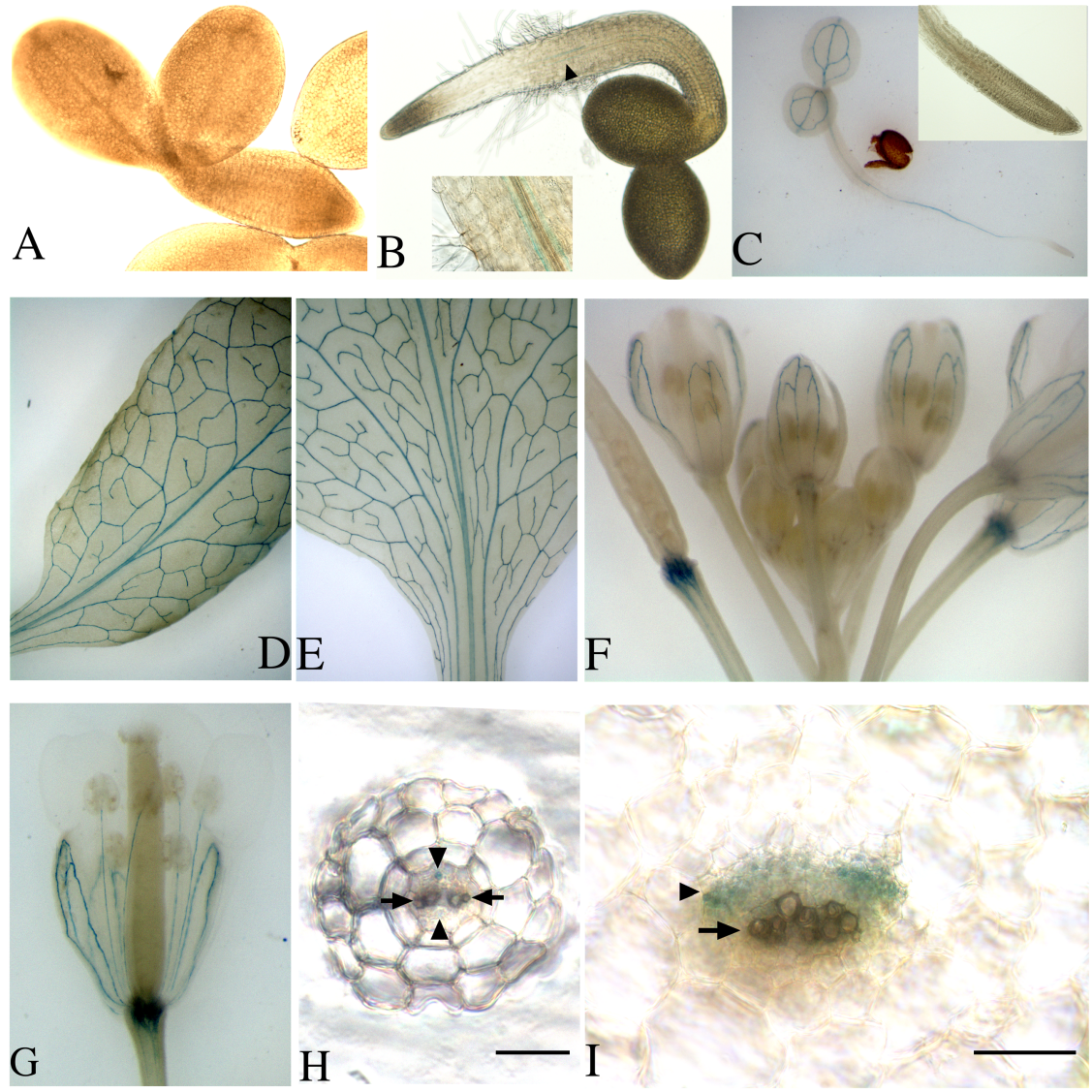

Figure 8. Expression pattern of *NaKR1pro:NaKR1-GUS* specifically in the phloem region of the vasculature. (A) No GUS expression was detected in imbibed seeds prior to germination. Seed coat was removed to facilitate observation. (B) GUS staining was visible in the vasculature of a 1 dag seedling in the region of root- hypocotyl boundary (indicated by arrow). (C) 2 dag seedling. (D) Mature rosette leaf. (E) Cauline leaf. (F) Floral tissue. Note that the strongest staining is in the pedicel of developing siliques and in the sepals. (G) Sepals and stamen filaments in an opening flower. (H) Cross section of a young root after GUS staining. The positions of the phloem and xylem region are indicated (by the arrowheads and arrows, respectively). Note that GUS expression was found in the phloem cells. (I) Cross section of a rosette leaf petiole after GUS staining. The position of the phloem and the xylem regions of the main vasculature are indicated as in (H). Note that GUS expression was limited to the phloem tissue.

phenotypes (Fig. 10), indicating that the NaKR1-GFP fusion protein is functional. Confocal microscopy was performed on the T_2 generation seedlings. Within the root, GFP fluorescence was found in two parallel cell files on both side of the xylem within the vasculature, indicating phloem localization (Fig. 9D). At the root tip, NaKR1-GFP fluorescence was observed in cells proximal to the zone of cell division in both primary (Fig. 9E) and lateral (Fig. 9F) roots. Fluorescence was apparent in both the cytosol and nucleus (Fig. 9E inset). Since expression of the *NaKR1* gene is specific to companion cells (Fig. 9B and Stadler et al., 2005; Zhang et al., 2008), our results indicate that the NaKR1-GFP fusion protein is mobile through plasmodesmata into sieve elements and unloaded into some cells of the root meristem. As a control, GFP fluorescence in seedlings of the same age transformed with *pSUC2:GFP* was analyzed. *AtSUC2* is specifically expressed in companion cells and GFP fluorescence was observed in the phloem and within 2 cell layers surrounding the phloem in the mature region of roots (Fig. 9G) as previously reported (Stadler et al., 2005). Free GFP diffused through the symplast into the whole root meristem (Fig. 9H) (Stadler et al., 2005; Benitez-Alfonso et al., 2009). Compared to free GFP (27 kDa), NaKR1-GFP (61 kDa) was more restricted to the phloem in mature roots. This is similar to results for multiple soluble GFP fusions of 36-67 kDa analyzed by Stadler et al., (2005). NaKR1-GFP in the root tip showed significant cell-to-cell translocation but was more restricted than free GFP.

To test whether NaKR1 protein mobility was essential for its function, NaKR1pro:NaKR1-GUS was used to transform *nakr1-1*. The larger size of

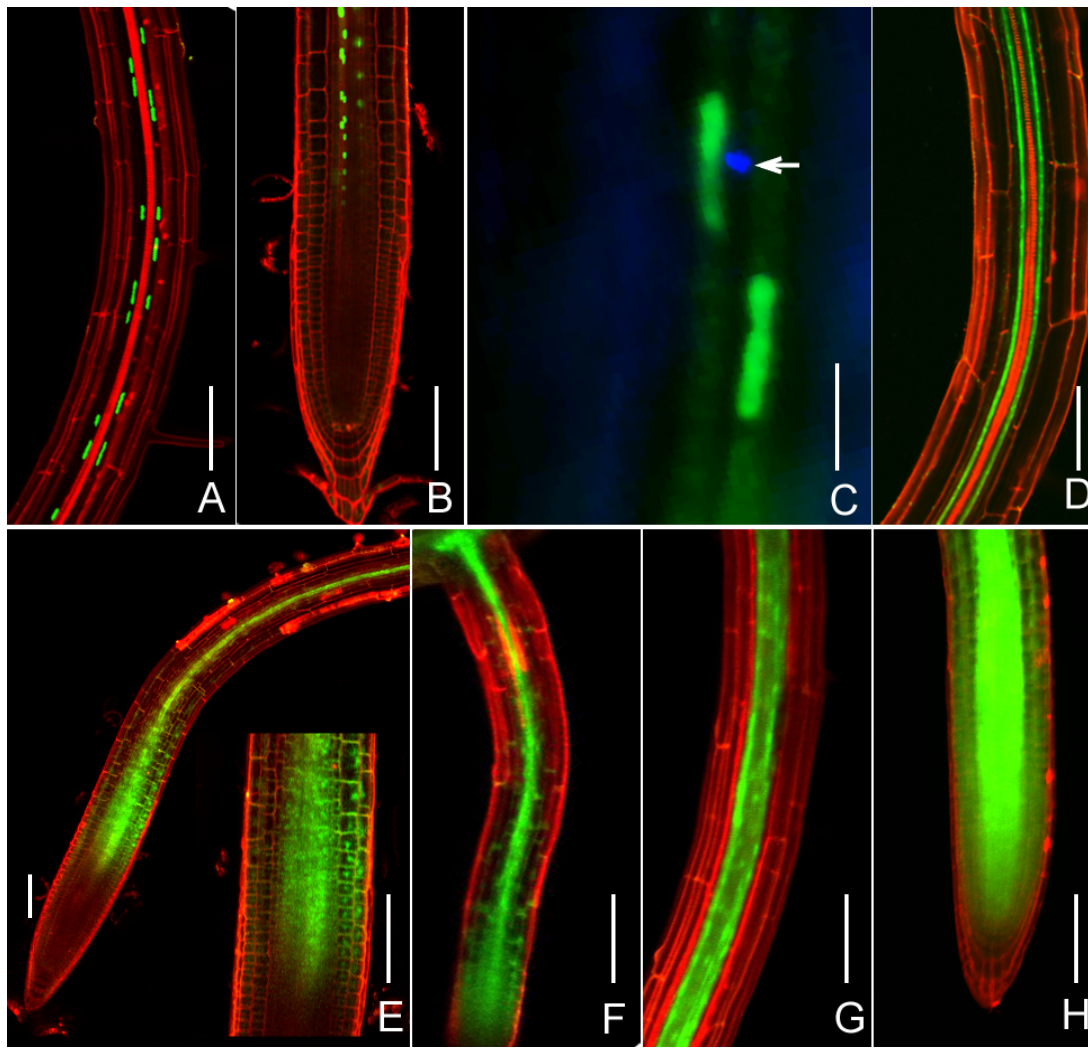

Figure 9. *NaKR1* is expressed in companion cells and NaKR1-GFP is phloem mobile. Confocal images (except in C) of Arabidopsis tissue stained briefly with propidium iodide. (A) NaKR1pro:histone2B-GFP localization in CC nuclei of Col-0 primary root. (B) NaKR1pro:histone2B-GFP localization in the proximal meristem region of the primary root meristem. (C) Epifluorescence image of NaKR1pro:histone2B-GFP expression in Col-0 root. Aniline blue staining shows sieve plate (indicated by arrow) of the adjacent SE. (D) NaKR1pro:NaKR1-GFP expression in mature, complemented *nakr1-1* root. (E) NaKR1pro:NaKR1-GFP fluorescence in the proximal meristem region of a primary root of complemented *nakr1-1*. Inset is magnified meristem region. (F). NaKR1pro:NaKR1-GFP expression in the lateral root of complemented *nakr1-1*. (G) Free GFP expressed using the AtSUC2 promoter showing fluorescence in the mature primary root of Col-0. (H) Expression of free GFP under AtSUC2 promoter in a primary root meristem of Col-0.

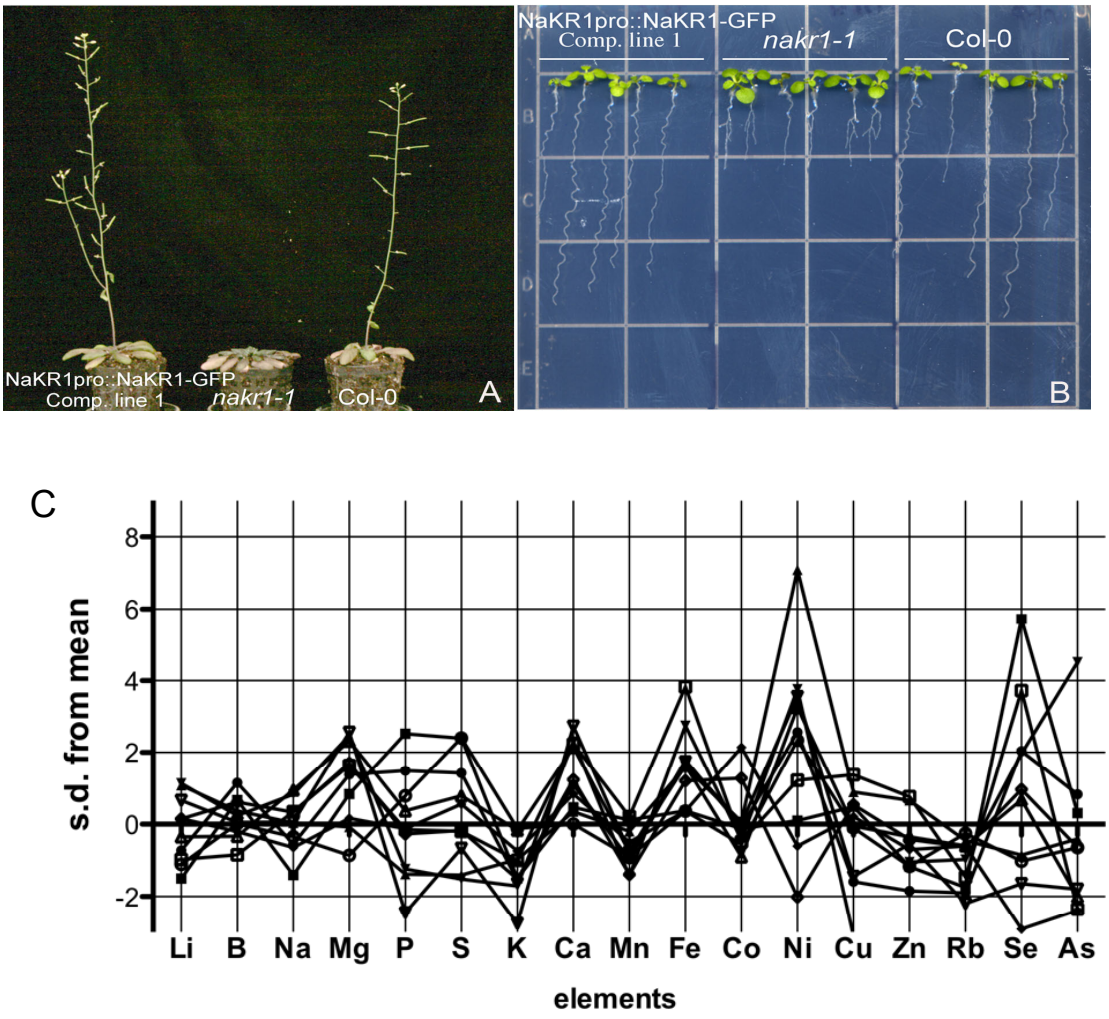

Figure 10. *nakr1-1* developmental and $Na^+/K^+/Rb^+$ accumulation defects were complemented with NaKR1pro::NaKR1-GFP. (**A**). From left to right, *nakr1-1* expressing NaKR1pro::NaKR1-GFP, *nakr1-1* and Col-0. Plants were grown in the same tray under long day growth conditions. (**B**). Seedlings grown vertically on ATS media. From left to right: *nakr1-1* transformed with NaKR1pro::NaKR1-GFP, *nakr1-1* and Col-0. **(C)**. Differences in leaf elemental content between individual NaKR1-GFP complementation lines and the average of Col-0 plants were plotted as z-values (standard deviation). Wild type and complemented lines were grown in the same tray.

NaKR1-GUS (102 kDa) compared to NaKR1-GFP (61 kDa) was expected to limit NaKR1-GUS mobility through PD. Of 24 primary transformants, 20 showed full complementation of both root defects and the late flowering phenotype (Fig. 11). GUS staining patterns in the complemented lines were similar to the expression pattern described in Col-0 background plants (Fig. 8). This indicated that the post-phloem trafficking of NaKR1 protein within the root meristem was not essential for the function of *NaKR1* in root growth.

Based on the result that *NaKR1* expressed specifically within the phloem region, a detailed characterization of the vasculature of Col-0 and *nakr1-1* mutant was performed. The general pattern of cell layers within the vasculature of *nakr1-1* mutant was normal. Based on the results of transmission electron microscopy, no difference in subcellular structure was detected for *nakr1-1* compared with Col-0 in the mature phloem region (Fig. 12). The phloem specific gene *APL* (*ALTERED PHLOEM DEVELOPMENT*) is essential for maintaining phloem cell identity. The expression of *APLpro:GFP:APL* was used to study phloem cell identity as the fusion protein specifically labels companion cells and developing protophloem/metaphloem cells (Bonke et al., 2003). No difference was detected in the expression of GFP-APL in Col-0 and *nakr1-1* plants, indicating the phloem differentiation process proceeded normally in the *nakr1-1* mutant (Fig. 13).

nakr1-1 is defective in phloem loading or translocation

The accumulation of starch in leaves of the mutant was analyzed as a test for phloem function. Previous work has shown that reduced phloem loading leads to

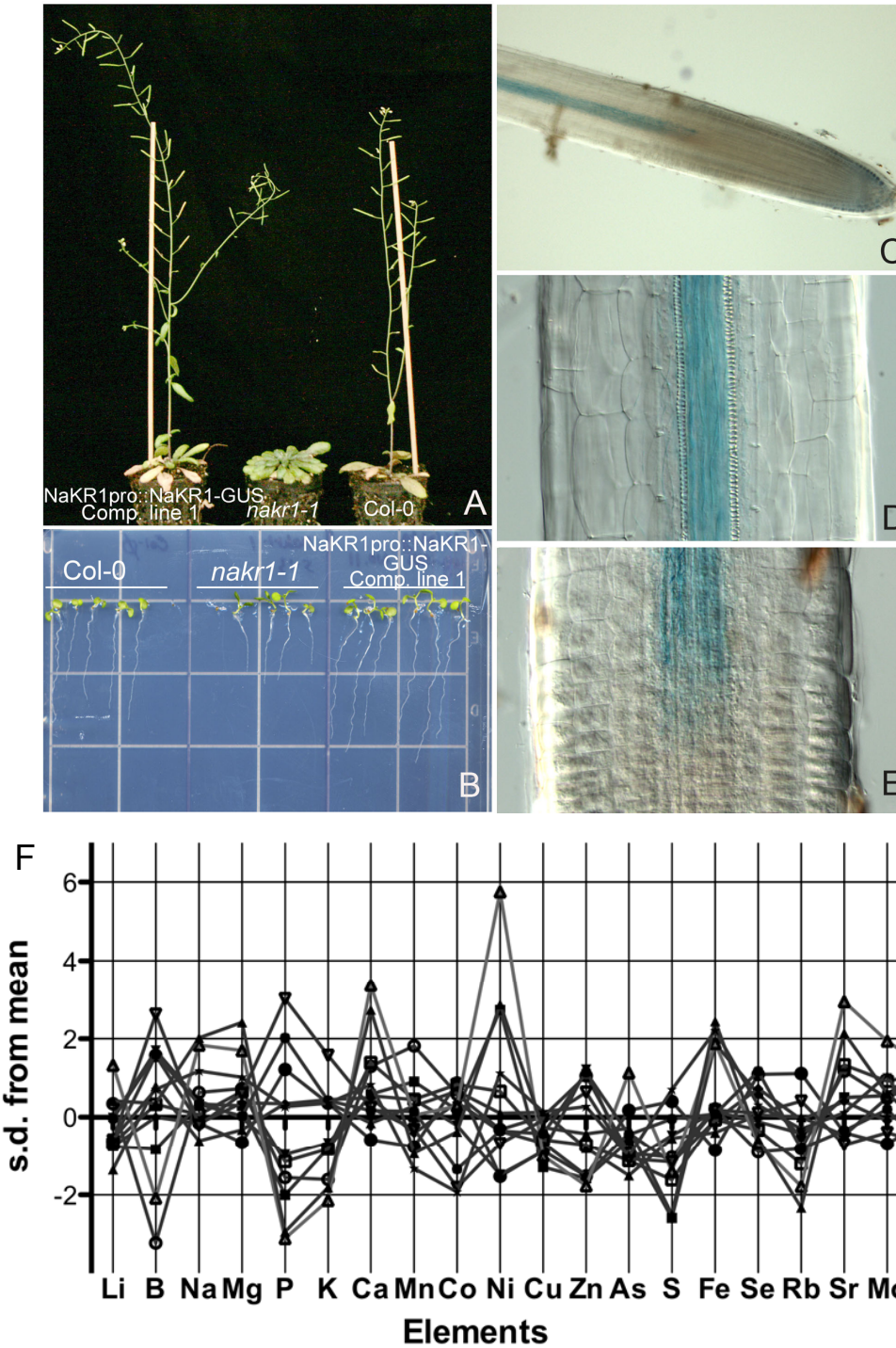

Figure 11.*nakr1-1* developmental and $Na^+/K^+/Rb^+$ accumulation defects were complemented with NaKR1pro::NaKR1-GUS. (A). From the left to the right, *nakr1-1* plant expressing NaKR1pro::NaKR1-GUS, *nakr1-1* and Col-0 grown in the same tray under long day growth conditions. (B). Seedlings grown vertically on ATS plate. From the left to the right: *nakr1-1* plants complemented with NaKR1pro::NaKR1-GUS, *nakr1-1* mutants and Col-0. (C-E). GUS staining of root tip (C), mature root (D) and the proximal region of root meristem (E). **(**F**)**. Differences in leaf elemental content between complementation lines and the mean of wild- type Col-0 plants were plotted as z-values (standard deviation).

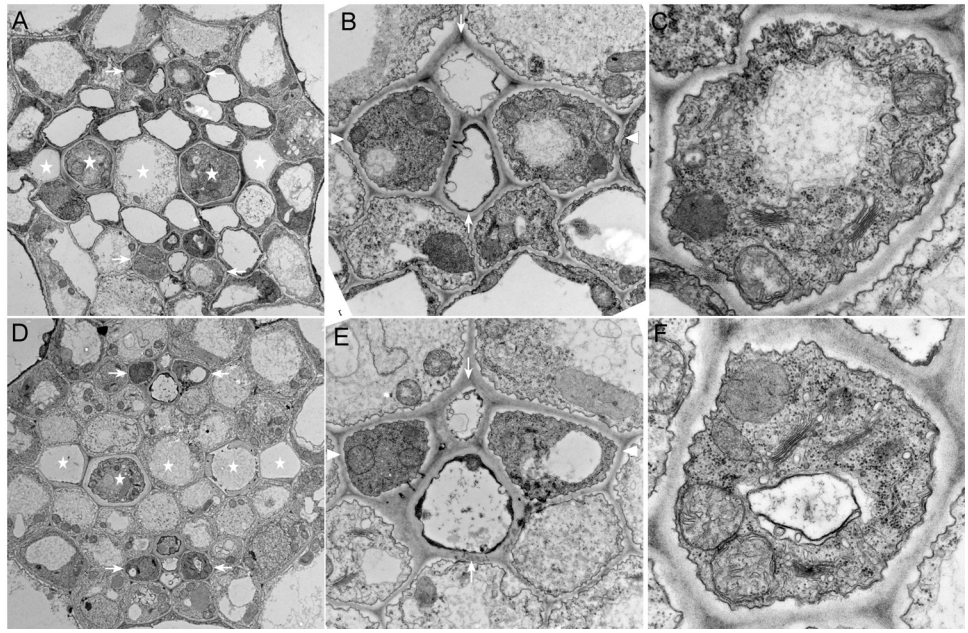

Figure 12. Cellular structures of SE/CC complex were not affected by the *nakr1-1* mutation as shown by transmission electron microscopy. (A) and (D), vascular region of Col-0 (A) and *nakr1-1* (D) roots. Xylem cells and phloem companion cells were labeled with asterisks and arrows, respectively. (B) and (E), SE/CC complex of WT (B) and *nakr1-1* mutant (E), with the arrowheads pointing to the companion cells and the arrows pointing the protophloem (top) and metaphloem cells (bottom) respectively. (**C**) and (**F**), the cellular structure of companion cells

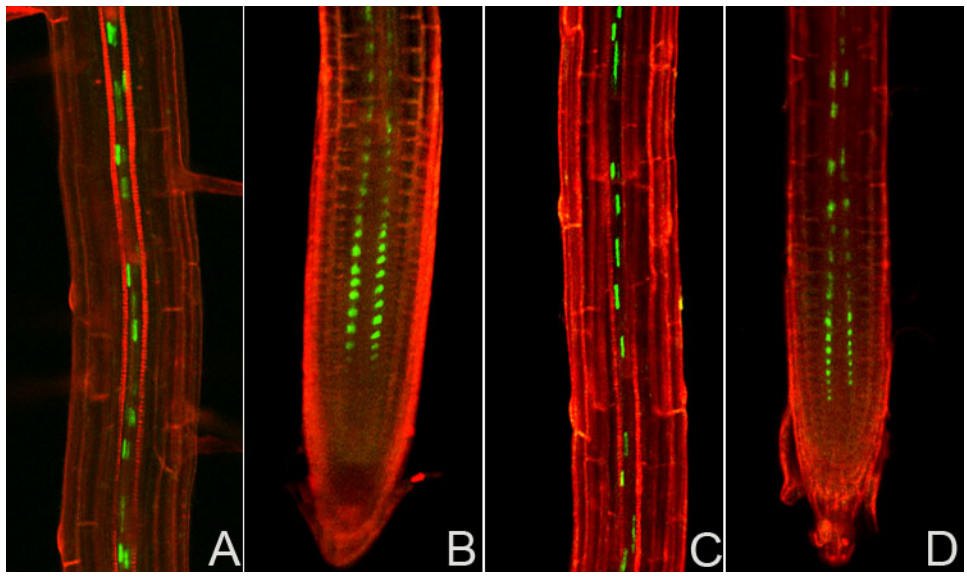

Figure 13. The differentiation of protophloem/ metaphloem cells and companion cells was not affected by the *nakr1-1* mutation. The expression of APLpro::GFP-APL in Col-0 and *nakr1-1* was analyzed by confocal microscopy. (A) and (C), Expression of APLpro::GFP-APL in mature roots of Col-0 (A) and *nakr1-1* mutant (C). The GFP fluorescence specifically labeled the companion cells. (B) and (D). Expression of APLpro::GFP-APL in root meristem of Col-0 (B) and *nakr1-1* mutant (D), with the GFP fluorescence specifically localized in developing metaphloem and protophloem cells.

starch accumulation in leaves (Riesmeier et al., 1994; Gottwald et al., 2000; Ma et al., 2009). Leaves of short-day grown plants were collected at the beginning and end of the day and stained with I_2/KI solution. In the *nakr1-1* mutant, a significant amount of starch was retained at the end of the night (Fig. 14A). Starch was quantified during the 8h/16h light/dark cycle (Fig. 15). *nakr1-1* accumulated around 4-fold more starch in leaves compared to wild type during the day. By the end of the following dark period, 30% of the starch remained in *nakr1-1* compared to undetectable amounts of starch in Col-0. When the plants were kept in continuous darkness for 3 days, leaf starch in the wild type decreased completely while *nakr1-1* retained leaf starch even after 88h of darkness (Fig. 15A). When plants were illuminated for 8h following 88h of continuous darkness, the starch accumulation rate was twice as high in the mutant compared to WT (Fig. 15B). This indicated that the starch over-accumulation phenotype was caused by a higher accumulation rate during the day and a decreased ability to deplete leaf starch during the night.

Considering that NaKR1 is expressed in companion cells, it was likely that the starch excess phenotype of *nakr1-1* was caused by a defect in phloem loading or translocation. To test this possibility, sucrose translocation from source to sink was analyzed in *nakr1-1* and Col-0. Plants were grown in Turface to facilitate access to the root system. A 2 µl aliquot of ^{14}C- sucrose was applied to wounded, fully expanded rosette leaves (Fig. 14B and D). Plants were then incubated for 30 minutes to allow translocation. After dissection and drying, the plants were exposed to X-ray film for 5 days. As shown in the autoradiographs, in both *nakr1-*

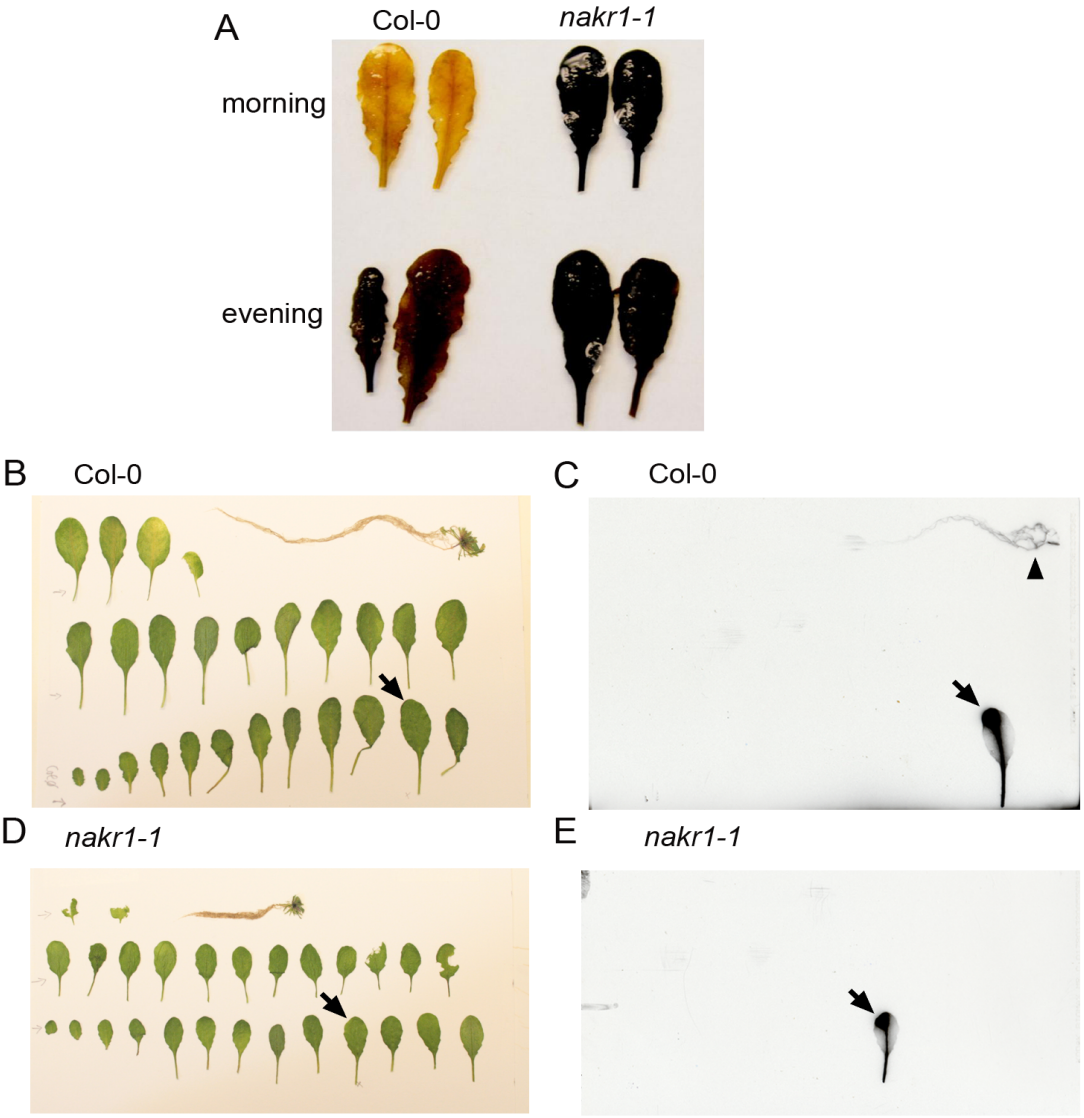

Figure 14. *nakr1-1* mutants are defective in phloem function. (A) I2/KI staining of Col-0 and *nakr1-1* leaves, sampled at the beginning and end of the day. Col-0 and *nakr1-1* plants were grown in the same tray under short-day conditions for 12 weeks. Mature healthy leaves were sampled for I2/KI staining and starch quantification. (B-E) Autoradiography of Col-0 and *nakr1-1* plants exposed to ^{14}C-sucrose. Plants were grown in Turface. One fully expanded rosette leaf was labeled with 2 µl of ^{14}C-sucrose (indicated by arrows). After 30 min, the application site was rinsed, plants were dissected, dried overnight at 20°C and exposed to film for 5 days. Arrowhead in C indicates appearance of radioactivity in the root of Col-0.

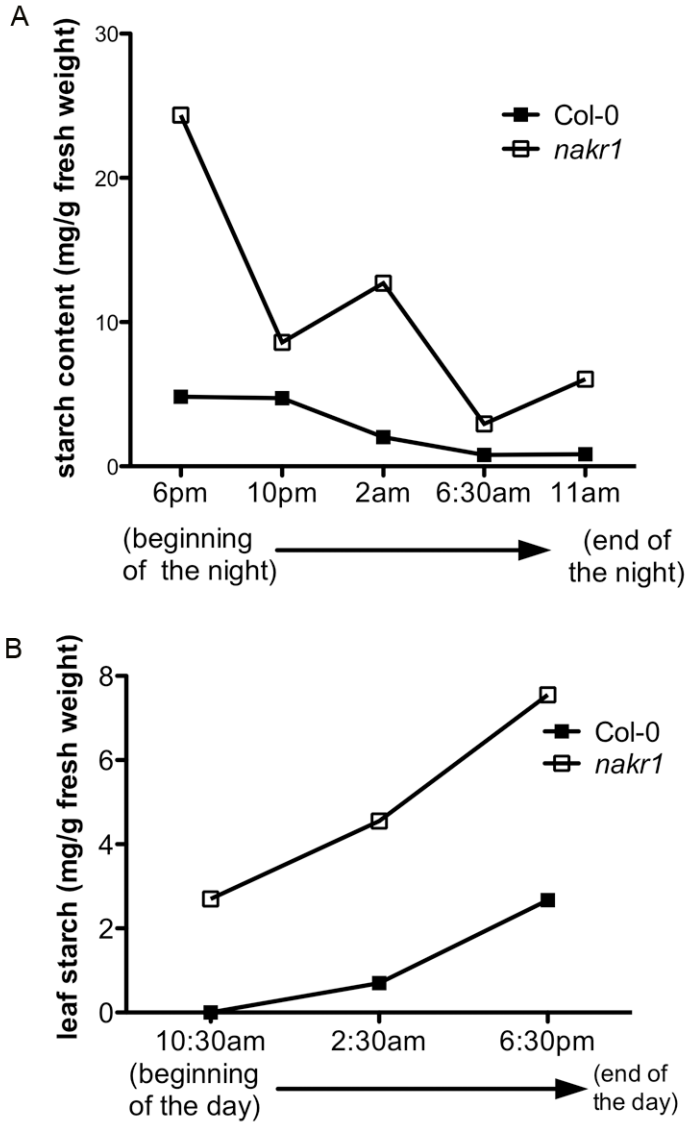

Figure 15. Quantification of starch in Col-0 and *nakr1-1.* (**A**) Leaf starch of *nakr1-1* and Col-0 at different time points during the night. The values at each time point are means from two independent experiments. (**B**) Starch quantification during the day after 3 days of continuous darkness. A higher starch accumulation rate was detected in *nakr1-1* than in Col-0.

1 and Col-0 radioactivity is present in the labeled leaf. In Col-0, radioactivity was translocated to the root system (Fig. 14C). However, no radioactivity was observed in the root system of the *nakr1-1* mutant (Fig. 14E). The results indicate that the *nakr1-1* mutant is defective in phloem loading or translocation.

The K^+ and Na^+ over-accumulation phenotype is mainly caused by shoot defects

To begin to analyze how the *nakr1-1* defect in phloem translocation was related to the Na^+ and K^+ accumulation phenotypes, reciprocal grafts were made between *nakr1-1* and wild type plants. The working hypothesis was that if a defect in phloem loading caused Na^+ and K^+ accumulation in leaves then plants with mutant shoots grafted to wild-type roots would show high Na^+ and K^+ accumulation similar to the mutant. Grafted and control plants were grown in Turface (Turface Athletics). Self-grafting did not affect the visible phenotype of the plants; *nakr1-1* shoots grafted to *nakr1-1* roots produced plants with small root and shoot structure (Fig. 16A), similar to non-grafted *nakr1-1* mutants growing in the same conditions (data not shown). When Col-0 shoots were grafted to *nakr1-1* roots, the plants produced larger shoot architecture with short roots (Fig. 16A), indicating that the defect in root growth was caused by loss of NaKR1 function in the roots. Leaf K^+ and Na^+ levels were tested for all the grafted combinations using ICP-MS analysis. The self-grafted *nakr1-1* and Col-0 plants displayed K^+ and Na^+ accumulation similar to the control *nakr1-1* mutants and Col-0, respectively (Fig. 16B-C). This indicates the grafting per se had little

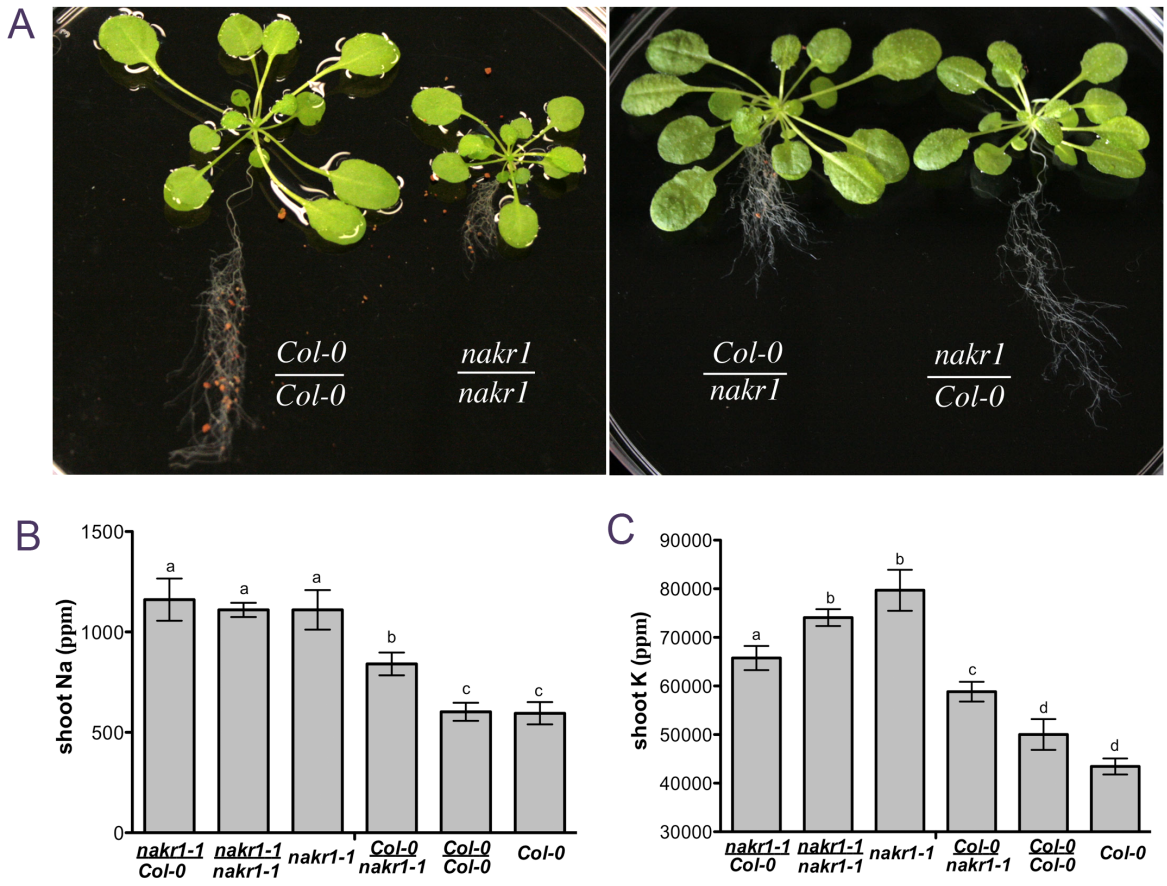

Figure 16. Grafting experiment followed by ICP-MS analysis indicated that the Na^+/K^+ overaccumulation phenotype of *nakr1-1* was mainly caused by the loss of function of NaKR1 in the shoot tissue. (A) The different grafting types. From left to right are Col-0 shoot- Col-0 root, *nakr1-1* shoot- *nakr1-1* root, Col-0 shoot- *nakr1-1* root, and *nakr1-1* shoot- Col-0 root. (B) Shoot Na^+ content in different grafting types and control plants. Data are presented as mean ± SE. (C) Shoot K^+ content presented as presented as mean ± SE, n =9-12 plants for grafting between Col-0 and *nakr1-1* and n=5 for self-grafting types and control plants (Col-0 and *nakr1-1*). Student's t-test was performed and different letters indicated p values <0.01.

effect on K^+ and Na^+ accumulation. Mutant shoots grafted to wild type roots showed leaf Na^+ levels similar to that of the mutant. Plants with wild type shoots grafted to mutant roots also showed Na^+ content in leaves higher than wild type, although lower than in mutant plants (Fig. 16B). The results indicate that high Na^+ in *nakr1-1* is mainly caused by loss of NaKR1 function in the shoot and that loss of NaKR1 in the roots also contributes.

The K^+ levels of mutant shoot/wild type root plants and wild type shoot/mutant root plants were intermediate between the self-grafted mutant and wild type plants. However mutant shoot/wild type root plants still had higher K^+ in leaves than the wild type shoot/mutant root plants. These results suggest that the K^+ accumulation phenotype was also caused by both root and shoot defects; however the effect of loss of *NaKR1* in the shoot predominated (Fig. 16C). Similar results were obtained when the different grafted types and control plants were grown in soil (Fig. 17).

To test the effect of root K^+/Na^+ uptake on their accumulation in the shoot, xylem sap was collected from Col-0 and *nakr1-1* mutant plants grown in the same soil conditions and K^+ and Na^+ concentration analyzed by ICP-MS analysis. Similar Na^+ concentrations were detected in *nakr1-1* and Col-0 xylem samples (Fig. 18A) and lower K^+ concentration was detected in the xylem sap samples of *nakr1-1* plants than those of Col-0 plants (Fig. 18B). These results indicated K^+/Na^+ over-accumulation in the shoot tissue of *nakr1-1* mutant was not caused by increased Na^+/K^+ uptake from the mutant roots or increased K^+/Na^+ concentration within the xylem sap.

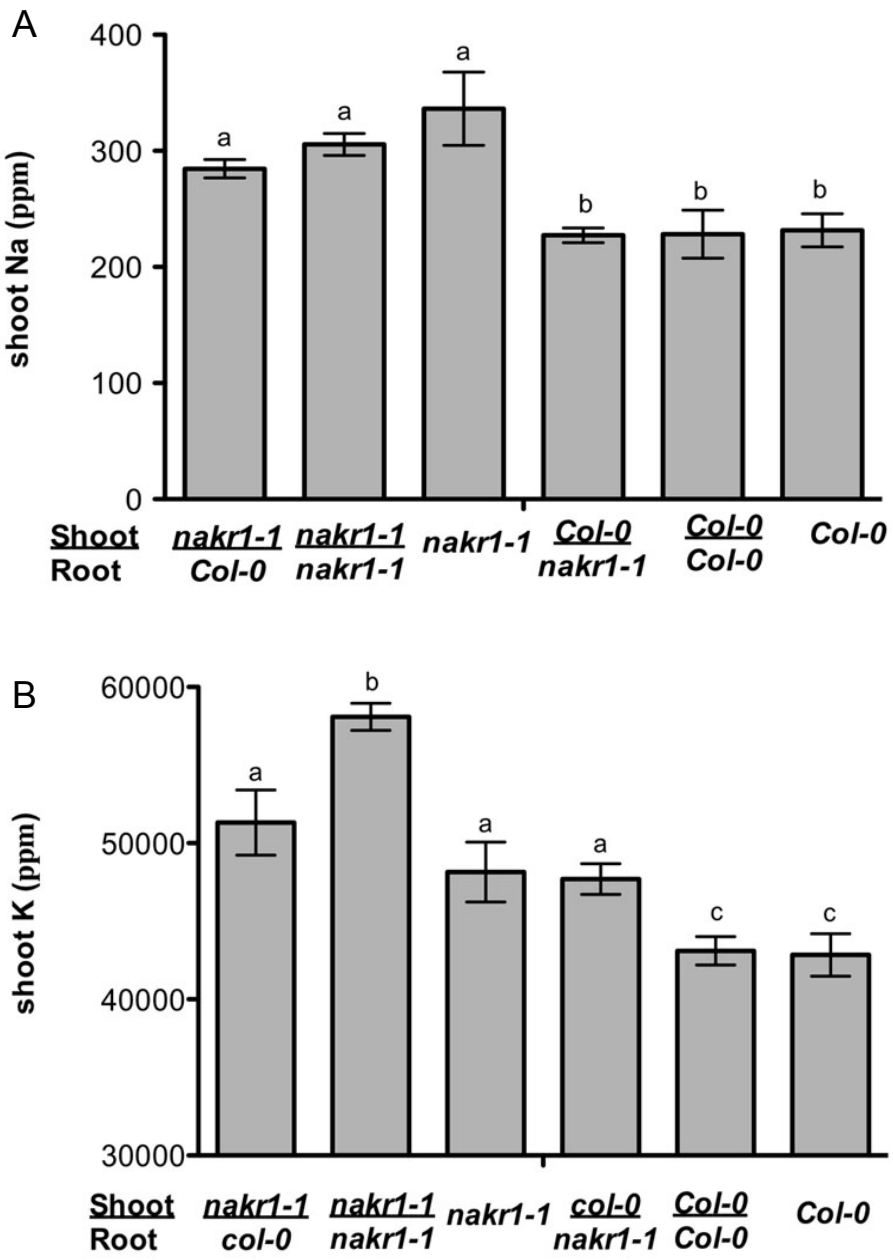

Figure 17. The effect of reciprocal grafting of Col-0 and *nakr1-1* on leaf Na^+ and K^+ content. (A) Leaf Na^+ content analyses of different grafting types (indicated in the figure) and control plants grown in LG_3 soil. (B) Leaf K^+ content of the same plants in (A). Na^+ and K^+ were assayed by ICP-MS. Data are presented as mean ± SE, n= 9-12 plants for the reciprocal grafting types and n=5 for self-grafted plants and control plants.

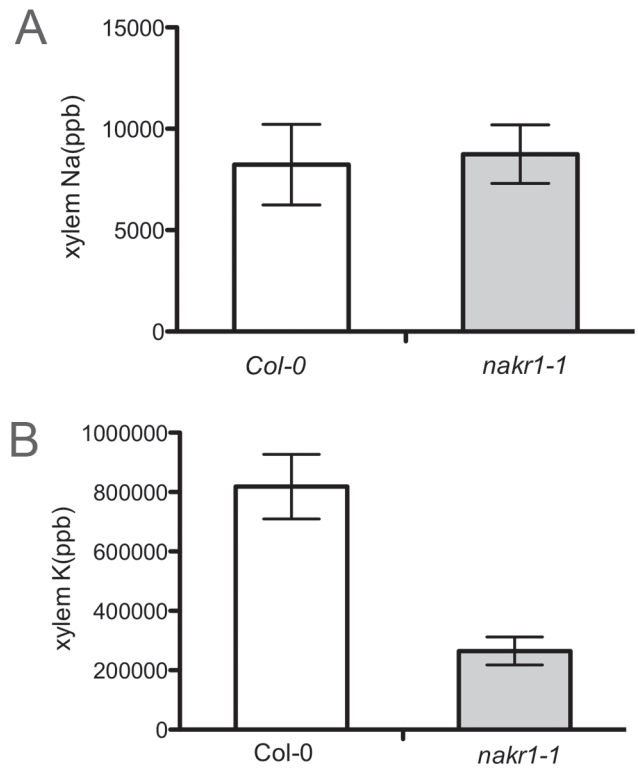

Figure 18. *nakr1-1* plants displayed similar Na^+ content and less K^+ in xylem sap than Col-0 plants. (A) Na^+ content (ppb) in the xylem sap of *nakr1-1* and Col-0 plants. (B) K^+ content (ppb) in the xylem sap of *nakr1-1* and Col-0 plants. Na^+ and K^+ concentrations were determined by ICP-MS analysis of xylem sap collected as inflorescence stem exudates from plants grown under the same conditions. Each value was represented as mean ± SE, n = 7-12 plants.

NaKR1 is necessary for root meristem maintenance after germination

nakr1-1 showed a severe root growth phenotype shortly after germination that involved short primary roots and increased lateral root growth (Fig. 2D). When grown on normal ATS plates for one week, the primary root length of *nakr1-1* seedlings was 50% of the wild type roots (Fig. 2D). The size of the *nakr1-1* root meristem region decreased dramatically during the first 7 dag as determined by analysis of propidium iodide-stained roots using confocal microscopy (Figs. 19A, 19C). In comparison, meristem size remained more stable in wild type seedlings (Figs. 19A, 19C), and a decrease in the number of meristematic cells did not occur in wild type *A. thaliana* until 3-4 weeks after germination (Baum et al., 2002). The elongation zone of *nakr1-1* seedlings at 7 dag was typically reduced to 3 cells in length (Fig. 19A). The length of fully elongated cortex cells was also measured (Fig. 19B). *nakr1-1* had a smaller cell length than the wild type. Thus, the short roots of *nakr1-1* were the result of both fewer cells in the root and a smaller cell size.

To determine whether the root meristem defects originated from an abnormality in embryo development, embryos of different stages were dissected from developing seeds of *nakr1-1* and Col-0. No obvious differences between the wild type and *nakr1-1* were found in early embryo stages (data not shown). This result was supported by the finding that *nakr1-1* seeds can germinate normally on both plates and soil, as well as GUS staining results showing that *NaKR1* gene was expressed only after germination (Fig. 8A). The root meristem defect in

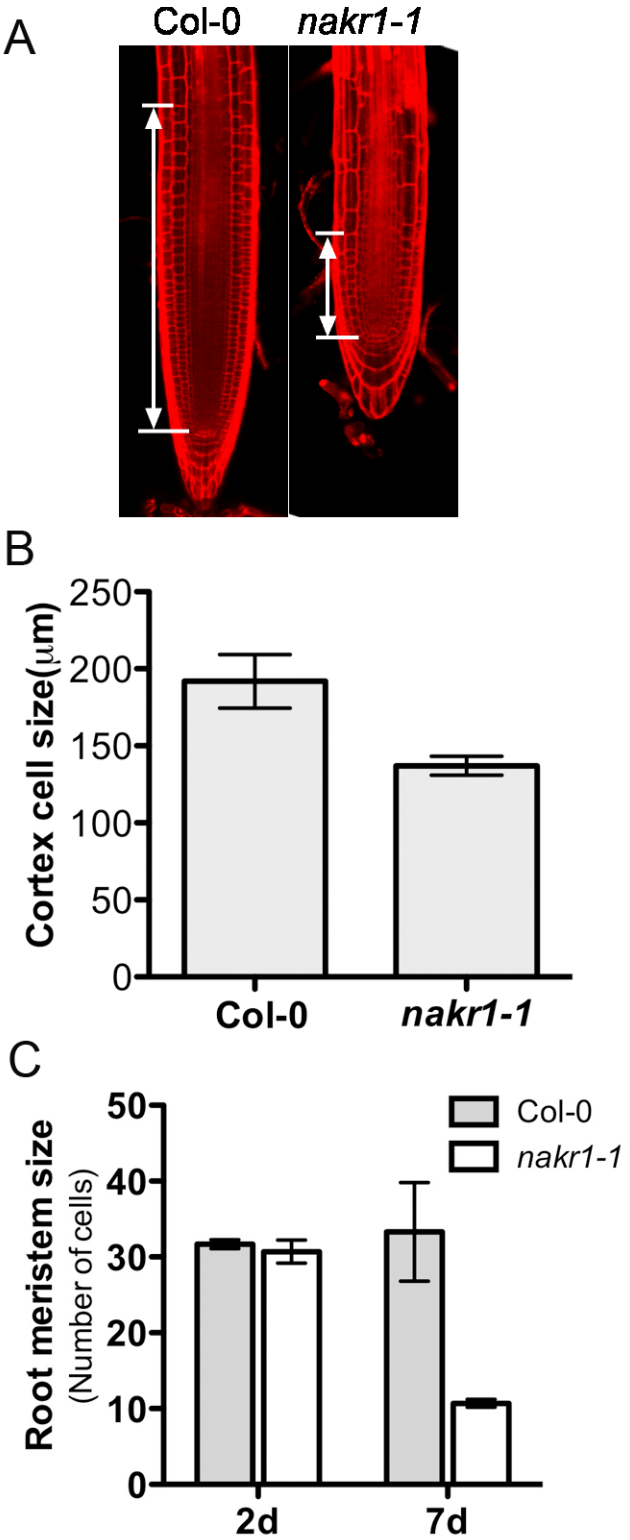

Figure 19. Root phenotypes of *nakr1-1* mutant. (A) Confocal images of Col-0 and *nakr1-1* primary roots at 7 dag stained with propidium iodide. The smaller root meristematic zone of *nakr1-1* compared to Col-0 is indicated. (B) Fully elongated cortex cell length measured in Col-0 and nakr1-1. (C) The size of the root meristem in Col-0 and *nakr1-1* seedlings at 2 and 7 dag was measured by counting the number of cells within the cortex cell files from the quiescent center to the first elongated cortex cell. Compared to Col-0, the size of the root meristem in *nakr1-1* was reduced significantly at 7 dag.

seedlings was investigated using a quiescent center marker, starch accumulation in root columella cells and the expression of cyclin:GUS in the root apical meristem (RAM). At 7 dag, *nakr1-1* seedlings showed much lower expression of quiescent center marker JYB1234 (Fig. 20A). At 3 dag, *nakr1-1* seedlings showed similar cyclin:GUS expression pattern as the wild type (Fig. 20C), however, by 4 dag the number of cells expressing cyclin:GUS in the RAM decreased significantly in some *nakr1-1* roots compared to wild type (Fig. 20C). Within the first 3 dag, no difference was detected in starch accumulation within root columella cells (Fig. 20B). From 4 dag, starch accumulation in the outermost columulla cell layer disappeared in *nakr1-1* roots, as a result only 3 layers of columella cells exhibited starch accumulation compared to 4 layers in the wild type roots (Fig. 20B). At 7 dag 90% of *nakr1-1* roots had only 2-3 layers of columella cells accumulating starch versus 4-5 layers in Col-0 primary roots (data not shown). Abnormality of starch accumulation in *nakr1-1* root columella cells is consistent with defects in quiescent center (QC) cells. However, no sign of differentiation in *nakr1-1* columellar stem cells was detected as revealed by the absence of stainable starch granules within columellar stem cell layer in *nakr1-1* mutant (Fig. 20B). The growth of primary roots within Col-0 and *nakr1-1* mutants was recorded for the first two weeks after germination (Fig. 20D). Clear differences between Col-0 and *nakr1-1* root growth was not observed until 4 dag when primary roots grew at a slower but constant rate. These results suggest that defects in *nakr1-1* root apical meristem occurred at 3-4 dag.

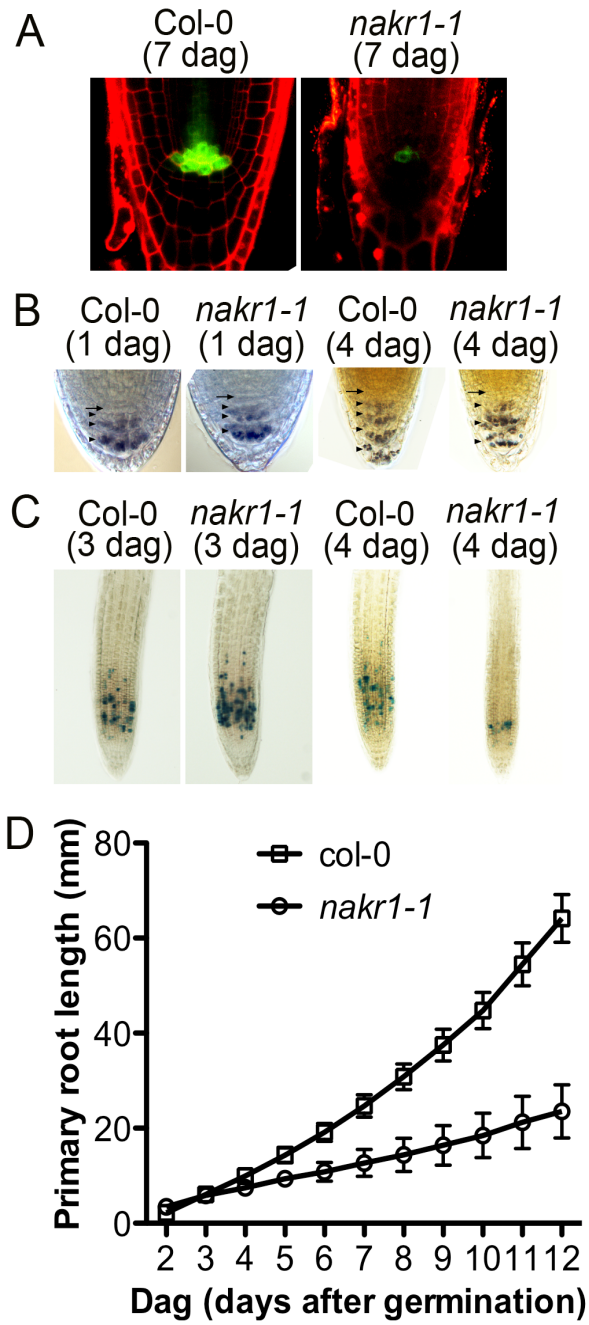

Figure 20. Root defects in *nakr1-1* appeared after germination. (A) Expression of quiescent center marker JYB1234 in Col-0 and *nakr1-1* primary roots at 7 dag. (B) Starch accumulation pattern in root columella cells of Col-0 and *nakr1-1* seedlings at 1 and 4 dag. The position of columella cell layers and columella stem cells were labeled with arrowheads and arrows, respectively. Note, at 4 dag Col-0 roots showed starch staining in 4 layers of columella cells while *nakr1-1* roots showed starch in only 3 layers. (C) Cyclin:GUS expression in Col-0 and *nakr1-1* roots at 3 dag and 4 dag. (D) Primary root growth of *nakr1-1* and Col-0 within the first two weeks after germination. 20% of *nakr1-1* primary roots stopped growing within the first week, and their primary roots were not measured in the second week. Col-0 and *nakr1-1* seedlings were grown vertically on ATS plates under long day conditions (16h day/ 8h night). Experiments were repeated 3 times under the same conditions. The Y- axis value at each time point represents mean ± SD.

nakr1-1 is a late flowering mutant especially in long-day conditions

In the early stage of vegetative growth, *nakr1-1* rosette leaves appeared at the same rate as wild type. *nakr1-1* leaves were slightly smaller and had shorter petioles than Col-0. After the wild type plants bolted, *nakr1-1* mutants continued to form new rosette leaves, displaying a late flowering phenotype (Fig. 21A). In *A. thaliana* several different promotion pathways control floral induction. The autonomous pathway responds to endogenous signals at specific developmental stages. The photoperiod and vernalization pathways respond to environmental stimuli such as light and temperature. The gibberellic acid (GA) pathway plays a relatively independent role in floral transition under non-inductive photoperiods (Araki, 2001). Among these pathways, the photoperiod pathway is largely dependent on phloem activity, since the signals induced by photoperiod, CONSTANS (CO) and its downstream target FLOWERING LOCUS T (FT) are expressed in the vasculature and the mobile flowering signal FT needs to be transported through the phloem to the meristem (Corbesier et al., 2007; Mathieu et al., 2007). Floral transition time of *nakr1-1* and Col-0 was measured under different floral promotion conditions. In long day conditions (16h day/ 8h night, 55μE light intensity), wild type plants began to bolt at 31±2 dag, after forming 13.5±0.5 rosette leaves; *nakr1-1* mutants required 55.5±4.5 days to bolt, and by that time 42.5±4.5 rosette leaves had developed (Fig. 21C). *nakr1-1* and Col-0 bolted at similar times in short day conditions (8h day/16h night, 55μE light intensity; Fig 21C). Wild type plants took 99±2.5 days to bolt, whereas *nakr1-1* plants took 112±5 days to bolt. The effects of vernalization and GA_3 treatment

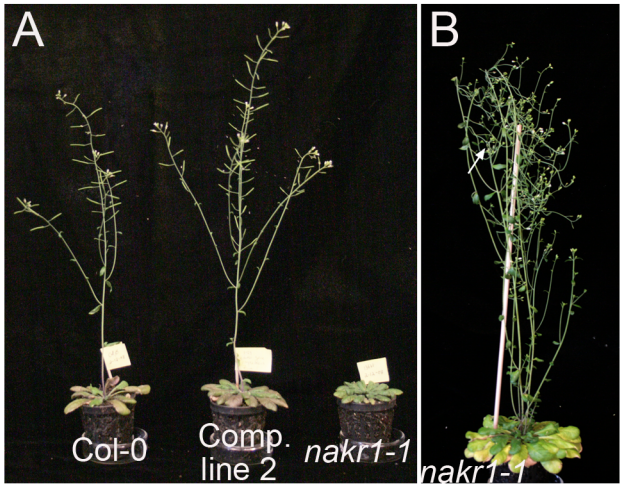

C

Growth conditions /Treatment	Col-0		*nakr1-1*	
	Bolt time (days)	Number of rosette leaves	Bolt time (days)	Number of rosette leaves
Long day conditions (16h day/ 8h night)	31± 2	13.5±0.5	55.5±4.5	42.5± 4.5
Long day (16h day/ 8h night)+ vernalization treatment	16±0.5	9±1	24±3	14.5±1.5
Short day (8h day/16h night) + GA_3 treatment	73±4	35.5±3.5	77±5	36±5
Short day (8h day/ 16h night)	99±2.5	n.d.	112±5	n.d.

Figure 21. *nakr1-1* displayed a strong late flowering phenotype, most significantly in long-day growth conditions. (A) The late-flowering phenotype of *nakr1-1* was complemented by NaKR1 whole gene construct. Col-0, *nakr1-1* and complementation line 2 (T2 generation) were grown in long day conditions within the same tray. The image was taken 45 days after sowing. (B) A flowering *nakr1-1* mutant after 90 days of growth in long day conditions. The white arrow indicates the position of the primary shoot meristem. Note that the mutant showed a loss of apical dominance and set seeds poorly. (C) Bolting time of *nakr1-1* and Col-0 under different growth conditions. Days after sowing and the number of rosette leaves were expressed as mean ± SD.

were also tested. Both treatments accelerated flowering in *nakr1-1*, although in both conditions the mutant plants still required slightly longer time to bolt (Fig. 21C). Therefore, *nakr1-1* mutants were mainly affected in the photoperiod pathway. This is consistent with a phloem defect in the *nakr1-1* mutant.

In addition to extended vegetative growth, *nakr1-1* also showed elongated reproductive growth and significant late senescent phenotypes. Abundant flowers were made in this period, but the early flowers set seeds poorly. The main stem displayed loss of apical dominance (Fig. 21B) in both short and long day conditions and the floral meristem in the primary shoot died before producing any flowers. The same phenomenon also appeared in the floral meristems of lateral branches. During vegetative and reproductive growth, *nakr1-1* plants over-accumulated anthocyanins, which gave leaves and stems dark purple pigmentation (data not shown).

DISCUSSION

The *nakr1-1* mutant phenotype included elevated Na^+, K^+, and Rb^+ in leaves, short roots, elevated starch accumulation during the day, decreased long-distance transport of sucrose, and late flowering under long-day conditions. The *NaKR1* gene was identified (At5g02600) and encodes a soluble protein of 34.5 kDa with a conserved HMA domain in the C-terminal half. NaKR1 expression was specific to companion cells as previously reported (Zhang et al., 2008). NaKR1-GFP was mobile in the phloem and was detected in the proximal root meristem region.

The specificity of NaKR1 expression in companion cells and the observation that long-distance sucrose transport in the phloem is affected indicated that elevated Na^+ and K^+ in *nakr1-1* leaves is likely to be due to a defect in phloem transport of these ions in the mutant. However the cause of this decrease in ion translocation is not clear. Transport of K^+ and sucrose in the phloem are linked as evidenced by the phenotype of mutants of K^+ channel AKT2/3 (Deeken et al., 2002) that are affected in sucrose concentration in the phloem. In theory, any defect in companion cells that limits ATP production or plasma membrane H^+-ATPase activity would be expected to decrease both sucrose and K^+ loading into the phloem.

The *nakr1-1* phenotypes cannot be fully explained by a decrease in phloem loading in leaves as demonstrated in reciprocal grafting experiments. Reduced root growth, as well as elevated Na^+ and K^+ in leaves, was found when either the root or shoot lacked NaKR1. While NaKR1-GFP was found to be mobile in the phloem, a NaKR1-GUS fusion that complemented all *nakr1-1* phenotypes did not translocate outside of the phloem. Therefore, all of the phenotypes observed for the *nakr1-1* mutant are due to a lack of NAKR1 in the phloem. This does not rule out additional functions that require post phloem NaKR1 mobility; functions that may be redundant with other metal binding domain proteins.

These results contribute to our understanding of phloem function in long distance transport of K^+, Na^+ and sugars, flowering time, and maintenance of the root meristem. They raise questions regarding 1) cell-to-cell movement of

protein; 2) the significance of Na^+ and K^+ recirculation in the phloem from leaves to roots; and 3) the function of the phloem in controlling root growth.

NaKR1 movement through plasmodesmata

NaKR1 expression was reported to be specific to companion cells in microarray experiments performed with fluorescently labeled protoplasts (Brady et al., 2007). When companion cell nuclei were labeled with histoneB2-GFP, NaKR1 was identified as one of the 12 most companion cell-specific transcripts (Zhang et al., 2008). HistoneB2-GFP targets GFP to nuclei in cells where translation occurs, and when driven by the NaKR1 promoter, was specific to companion cells (Zhang et al., 2008). We confirmed the companion cell localization of NaKR1pro:histoneB2-GFP (Fig 9A and B). This localization was also supported by NaKR1pro:NAKR1-GUS expression in Col-0 which was restricted to vascular tissue (Fig. 8). Interestingly, NaKR1-GFP driven by the native promoter produces a different localization consistent with transport through plasmodesmata. In mature parts of the root, NaKR1-GFP fluorescence was observed in files of cells consistent with sieve elements and appeared similar to other soluble GFP fusions that move from companion cells into sieve elements (Stadler et al., 2005). NaKR1-GFP was more restricted to sieve elements in mature regions of roots compared to free GFP, which is able to move 1-2 cell layers laterally (Fig 9G and Stadler et al., 2005). Free GFP, expressed in companion cells driven by the AtSUC2 promoter, can move out of the transport phloem in mature regions of the root, is unloaded from the protophloem and moves throughout the root tip,

indicating that these cells are connected by plasmodesmata (Fig 9H and Stadler et al., 2005). NaKR1-GFP movement was restricted to an area of the root tip below the transition zone of the root meristem. Since NaKR1-GFP was only translocated to a portion of the root tip, in contrast to free GFP, this identifies a new symplasmic domain in the root tip. In a previous study, the smallest GFP protein fusions (ubiquitin-GFP is 36 kDa) did not move from the protophloem into cells of the root tip (Stadler et al., 2005). Our results indicate that control of protein transport through plasmodesmata is not only restricted by size (SEL) and that NaKR1 contains a signal sequence required for transit through PD.

Maize KNOTTED1 (KN1) was the first protein identified to function non-cell-autonomously (Lucas et al., 1995). Trafficking of KN1 through plasmodesmata requires an internal signal contained in the homeodomain (Kim et al., 2005) and the trafficking is essential for KN1 function in maintaining stem cell populations in plant shoots (Kim et al., 2003). NaKR1 shares no homology with the KN1 homeobox domain and the presence of a signal sequence in NaKR1 remains to be tested.

Phloem and Na^+/K^+ homeostasis

The *nakr1-1* mutant overaccumulates Na^+ and K^+ in leaves. In theory, the amount of K^+ and Na^+ in leaves is determined by several distinct processes: Na^+/K^+ uptake from the soil, long distance transport to the shoot via the xylem, and redistribution through the phloem. The function of xylem-localized HKT1 in limiting Na^+ translocation to the shoot has been established (Mäser et al., 2002;

Sunarpi et al., 2005; Rus et al., 2006; Davenport et al., 2007). The possible function of the phloem in recirculating Na^+ back to the roots has remained less clear (Horie et al., 2009). As shown here, the specificity of NAKR1 expression in companion cells combined with the *nakr1-1* high K^+ and Na^+ phenotypes indicates a role for the phloem in determining leaf K^+ and Na^+ accumulation.

NaKR1 is expressed in the phloem throughout the plant. We hypothesized that K^+ and Na^+ are loaded into the phloem in leaves and that NaKR1 is required. To test this, reciprocal grafting experiments were done with *nakr1-1* and Col-0. The results (Fig. 16) showed that lack of NaKR1 in the shoot resulted in a Na^+ concentration in leaves as high as in *nakr1-1*. However, a lack of NaKR1 in roots also resulted in leaf Na^+ that was higher than in Col-0. The results indicate that companion cell function in both the root and shoot contributes to the limitation of Na^+ accumulation in shoots.

The effect of the *nakr1-1* mutation on K^+ accumulation was similar. In grafting experiments, the lack of NaKR1 in either the root or shoot led to K^+ accumulation in leaves. Differences in K^+ concentration between source and sink tissues has been detected and are thought to contribute to the turgor gradient (Vreugdenhil et al., 1985; Fischer, 1987; Fromm and Eschrich, 1989; Hayashi and Chino, 1990) that drives phloem sap movement (Mengel and Haeder, 1977; Lang, 1983). The K^+ channel *AKT2/3* is specifically expressed in the phloem and functions in controlling the membrane potential (Marten et al., 1999; Deeken et al., 2000; Lacombe et al., 2000). The *akt2/3-1* mutant exhibited reduced sucrose concentration in the phloem sap but K^+ concentration was not significantly

affected (Deeken et al., 2002). Transporters functioning in loading K^+ into the phloem remain to be identified. The grafting experiments indicated that NaKR1 is required in both the shoot and the root for K^+ recycling in the phloem. The requirement in the shoot may be related to phloem loading of K^+. In the root, NaKR1 may be required for phloem unloading. Lower K^+ concentration observed in the xylem sap in *nakr1-1* is consistent with this hypothesis.

nakr1-1 affects phloem translocation, starch accumulation and flowering

nakr1-1 accumulated more starch in leaves during the day. This is consistent with a decrease in phloem loading of sucrose as exemplified by the effects of antisense inhibition of *StSUT1* in potato (Riesmeier et al., 1994), *AtSUC2* insertional mutants in *A. thaliana* (Gottwald et al., 2000), and *tdy1* mutants of maize (Ma et al., 2009). The ability of *nakr1-1* to translocate ^{14}C sucrose was tested in intact plants. When ^{14}C-sucrose was applied to Col-0 leaves, radioactivity was detected in roots within 30 minutes. With *nakr1-1*, no radioactivity was detected in roots indicating that phloem loading or translocation is defective in the mutant.

Consistent with a defect in phloem function, the *nakr1-1* mutant displayed a large delay in flowering under long-day conditions. This is consistent because the phloem functions in producing and translocating FT protein (Corbesier et al., 2007) a mobile signal that induces flowering. In contrast, *nakr1-1* responded normally to other conditions that promote flowering such as GA_3 treatment or vernalization and to conditions that delay flowering such as short days.

NaKR1 expression and root phenotypes

Considering the short root phenotype of *nakr1-1*, it was important to compare the timing of *NaKR1* expression and onset of the phenotype to determine if NaKR1 is important for root development. Using a NaKR1-GUS fusion driven by the *NaKR1* promoter, the earliest expression was identified at 1 dag in the vascular tissue at the root-hypocotyl junction. No expression was detected in developing embryos or in seeds before germination. Therefore, *NaKR1* is not expressed in the earliest protophloem cells that differentiate in mature embryos (Bauby et al., 2007). By 2 dag *NaKR1* expression was observed in vascular tissue throughout the seedlings. The earliest expression of *NaKR1* coincides well with the onset of phenotypes in the root. By 3 dag, root growth was measurably slower and the cell division rate in the meristematic region was less. By 4 dag, differences were observed in starch accumulation in the root distal region. Overall, the results indicate that *NaKR1* is important for root meristem maintenance rather than root development.

The NaKR1pro:NaKR1-GUS construct complemented the *nakr1-1* mutant phenotypes. This construct only produced GUS staining in the phloem. This indicates that NaKR1 functions at a distance from areas of the root displaying a phenotype, for example in the quiescent center and in the zone of cell division. The root phenotypes in *nakr1-1* could be due to a defect in supply of photosynthate to the roots. Interestingly, results from reciprocal grafting experiments (Fig. 16), indicated that a lack of NaKR1 in the roots was

responsible for the short root phenotype. This indicates a specific function for companion cells in the root in maintenance of the root meristem.

NaKR1 function as a metal binding protein

A NaKR1 fusion protein was expressed in *E. coli*, purified and shown to bind Zn, Cu, Fe, Ni and Co. A mutated version of NaKR1 in which the two metal-coordinating cysteines were changed to glycine failed to complement *nakr1-1* phenotypes. This indicates that metal binding is important for NaKR1 function. HMA domain proteins have been identified in the phloem sap of *Brassica napus* and *Cucurbita maxima* (Giavalisco et al., 2006; Lin et al., 2009). In *A. thaliana*, HMA domain protein *AtCCH* is found in the phloem and is thought to transport Cu out of senescing tissues (Himelblau et al., 1998; Mira et al., 2001). *nakr1-1* growth was not affected by varying heavy metal (Fe^{2+}, Cu^{2+} and Zn^{2+}) concentrations in the growth medium (data not shown). Overall, the results suggest that metal binding is important for NaKR1 function in companion cells. We cannot rule out additional NaKR1 functions that require NaKR1 mobility in the phloem that are redundant with other related HMA domain-containing proteins also known to be present in the phloem such as AtCCH1.

Conclusions

The NaKR1 gene encodes a soluble, cytoplasmic heavy metal binding protein that is specifically expressed in companion cells of the phloem in *A. thaliana*. The *nakr1-1* mutant displayed a number of phenotypes that are consistent with

defects in phloem function: higher starch accumulation in the mesophyll, defective long-distance transport of ^{14}C-sucrose, accumulation of K^+ and Na^+ in leaves, and late flowering under long day conditions. The *nakr1-1* mutation also caused a short root phenotype, primarily due to a lower rate of cell division. NaKR1-GFP was found to move cell-to-cell through plasmodesmata, which may indicate that it functions non-cell autonomously.

METHODS

Plant material

A. thaliana ecotypes *Columbia* (Col-0) and *Landsberg erecta* (Ler-0) seeds were obtained from the ABRC. The mutant line 136:31 (Lahner et al., 2003) was backcrossed twice to Col-0 and renamed *nakr1-1*. *Cyclin1pro:GUS* (in Col-0) was obtained from Dr. William Gray (University of Minnesota). The *SUC2pro:GFP* marker line (in Col-0) was obtained from Dr. David Jackson (Cold Spring Harbor Laboratory). *APLpro:APL:GFP* (in Ler-0) was obtained from Dr. Ykä Helariutta (University of Helsinki, Finland). These marker lines were crossed with *nakr1-1* mutants and the F_2 progeny with short roots and containing these constructs (selected by the expression of GUS or GFP) were selected. *NaKR1pro:HTB2:GFP* (NPCC6) was provided by Dr. David W. Galbraith (University of Arizona).

Plant Growth on Vertical Plates

Seeds were surface sterilized, stratified for 2 days in the dark at 4°C and placed on square petri dishes containing ATS medium (Lincoln et al., 1990) supplemented with 0.05% MES (w/v), 0.5% (w/v) sucrose and 0.8% (w/v) Phytoagar (Caisson Laboratory Inc.), pH 5.7. The petri dishes were placed vertically in a growth room under controlled conditions (16h/8h day/ night cycle, 22°C, 60 $\mu mol \cdot m^{-2} \cdot S^{-1}$).

Plant Growth in Soil

Plants were grown in plastic trays with sterilized LG3 (Sun Gro Horticulture, Canada) or BM2 (Berger, Canada). *A. thaliana* seeds were sowed on the top of the soil. To facilitate seeds germination, the trays were kept for 4 days at 4°C before transferred to the growth room. Plants were grown at long day (16h/8h day/ night cycle, 22°C, 55- 70 $\mu mol \cdot m^{-2} \cdot S^{-1}$) or short day (8h/ 16h day/ night cycle, 22°C, 55- 70 $\mu mol \cdot m^{-2} \cdot S^{-1}$) conditions. Trays were regularly rotated and watered twice a week from the bottom of the tray with DI H_2O, and fertilized once with All Purpose Plant Food (Vigoro). For vernalization experiments, seeds were plated on ATS medium and incubated at 4°C for 6 weeks before being transferred to soil and grown under long day conditions until flowering. To test GA_3 effects, plants were grown under short day conditions for one month before they were sprayed with 100μM GA_3 once per week until flowering.

Identification of the *nakr1-1* mutation

For map-based cloning, *nakr1-1* mutants were crossed with Ler-0 and F_2 progeny with short primary roots were selected after 3 weeks of growth on ATS plates. PCR primers were designed for mapping based on the polymorphism information provided by Monsanto SNP and Ler Collections from the TAIR website (http://www.arabidopsis.org). A genomic DNA pool from 30 mutants was created for bulk segregant analysis and the mutation was revealed to be at the top of chromosome 5. Three hundred mutant plants were used for fine mapping. Progeny were collected from those F_2 mutants with recombination sites close to the mutation region, and grown on ATS plates to confirm they were homozygous mutants.

DNA microarray-based deletion mapping was performed to identify the mutation. Three genomic DNA pools were created from the Col-0 plants, and three from a *nakr1-1* mutant population using DNeasy Plant Mini Kit (Qiagen). For each pool the genomic DNA was from 10-15 plants. Genomic DNA was labeled, and hybridized to Affymetrix ATTILE 1.0R arrays. Probes with no sequence differences should show no difference in hybridization between *nakr1-1* and Col-0. Deletions linked to NaKR1, were identified by decreased hybridization signals that were consistent in all three *nakr1-1* hybridized samples. Microarray data have been submitted to the GEO database with accession: GSE24385.

The *nakr1-1* mutation was confirmed by sequencing PCR products amplified from *nakr1-1* genomic DNA using primer pairs F: (5'- CAC TCC TCC ACC TTC CCC AAA CCT TAA T- 3') and R: (5'- GTC TCC CGT CAC GGT AAC CTT CTT

TGC T-3'). A dCAPs marker (Neff et al., 1998) was designed to discriminate *nakr1-1* and wild type Col-0 genotype using PCR primer pairs F: (5'- CGG TTA GCG AAG AGG AAG AGC AAG AAA GG-3') and R: (5'- TTA AAT CAT CAG CTT TGG TTA TCT CCG GTC CAT-3'). The amplified Col-0 genomic DNA could be specifically digested by the enzyme BccI; the amplified *nakr1-1* genomic DNA was not recognized by BccI. Co-segregation of the mutation sequence with mutant phenotypes was further confirmed by genotype analysis of a segregating population containing 108 plants using the dCAPs marker.

Plasmid Construction and Plant Transformation

NaKR1 whole gene sequence (including promoter, exons, introns and 3'UTR) were amplified from wild type Col-0 genomic DNA by using primer pairs F(5'-GCC TTT GTG AAA TCG ATT TGA GTT AGA A-3'), R (5'-GGT CAT CTG TAA AGG TAA GTC TAT ATG G-3'). The resulting 2424-bp PCR product (*NaKR1;1*) was cloned into the Gateway entry vector pCR8/GW/TOPO (Invitrogen). A LR gateway recombination reaction (Invitrogen) between the vectors *pCR8/NaKR1;1* with pMDC123 (Curtis and Grossniklaus, 2003) was performed to sub-clone *NaKR1;1* into the binary vector. To make the constructs *NaKR1pro:NaKR1:GUS* and *NaKR1pro:NaKR1:GFP* , *NaKR1* gene sequence (including the promoter, coding and non-coding region, without TAA stop codon) was PCR amplified using primer pairs F(5'- GCC TTT GTG AAA TCG ATT TGA GTT AGA A-3') and R (5'- CTT CTG AAT AAT CTC AGG CCA AAA CTG A-3'). The 1809-bp PCR product (*NaKR1;2*) was cloned into pCR8/GW/TOPO and by LR recombination

reaction into the binary vectors pMDC164 and pMDC107 (Curtis and Grossniklaus, 2003).

Agrobacterium tumefaciens was transformed by electroporation (Micropulser^{TM}, BIO-RAD). Col-0 and *nakr1-1* plants were transformed using the floral dip method (Weigel and Glazebrook, 2002). Transformants containing the construct *pMDC123/NaKR1;1* were selected based on Basta resistance. Transformants expressing *NaKR1pro:NaKR1:GUS* and *NaKR1pro:NaKR1:GFP* were hygromycin resistant and were selected by growing seeds on 0.5 Murashige and Skoog medium (CAISSON Laboratories, Inc.) supplemented with 1% phytoagar, 0.05% MES, 2% sucrose and hygromycin (30mg/L for seeds of Col-0 background and 10mg/L for seeds of *nakr1-1* background), pH 5.7.

NaKR1 cDNA clone in the Gateway entry vector (pENTR223.1) was obtained from the Salk Institute Genomic Analysis Laboratory. For expression in *E.coli* cells, the cDNA fragment was recombined with the expression vector pRARE_MAL_DEST by LR reaction (Invitrogen), and *pRARE MAL DEST/ NaKR1* was introduced into *E. coli* strain BL21-AI by electroporation. A control plasmid was made by LR recombination between an empty pCR8/GW/TOPO vector and pRARE_MAL_DEST to remove the CcdB gene and Kanamycin resistance marker between the AttR1/AttR2 sites.

GUS staining

GUS staining was performed according to the method described by (Quaedvlieg et al., 1998). Plant tissues were vacuum infiltrated in X-Gluc solution (Research

Products International) twice for 5 minutes each, followed by incubation at 37°C for 16h and cleared with 70% ethanol at 65°C for 1h before whole- mount samples in 70% ethanol for microscopy. For cross-sections the stained samples (without clearing) were embedded in 4% agarose and 50µm sections were made using a Vibratome 1000 Plus Sectioning System.

Microscopy

Confocal laser microscopy was performed using C1 Spectral Imaging Confocal Microscope (Nikon) and EZ-C1 acquisition and analysis software. For propidium iodide staining of cell walls, seedlings were removed from the growth medium, stained briefly in 10µg/mL propidium iodide and the whole plants were mounted in water. The excitation wavelength for propidium iodide was 561nm and emission wavelength collected at 570-610 nm. For GFP fluorescence, the excitation wavelength was 488nm and the emission wavelength collected at 505-545 nm. A z-series of scans was collected to obtain a transverse section view.

GUS expression images were collected using the MZFLIII dissection microscope (Leica) and Hoffman Modulation contrast microscope (Nikon), and Qcapture acquisition software. DIC images of root meristems and starch accumulation in root columellar cells and epifluorescence images of GFP and aniline blue staining were captured using DM5000B microscope (Leica) and Leica Applicaion Suite Software (version 2.4.0 R1).

For starch staining of columellar cells, whole seedlings were fixed overnight in FAA solution (50% ethanol, 5% formaldehyde, and 10% acetic acid), rinsed

briefly in 50% ethanol twice and stained in a mixture of glycerol: chloral hydrate: I_2/KI (containing 30% glycerol (v/v), 8% chloral hydrate (w/v), 0.04% I_2 (w/v) and 0.2% KI (w/v)) for 1h and mounted in 50% glycerol for DIC imaging. For aniline blue staining, seedlings were incubated in 2.5% aniline blue (Fischer Scientific) dissolved in 0.5M K_3PO_4 solution (pH 9.5) for 5 minutes before mounted in 0.5M K_3PO_4 for observation using a fluorescence microscope with UV filter.

NaKR1 **cDNA expression in** ***E. coli*** **and protein purification for ICP-MS analysis**

E. coli strain BL21-AI containing the construct *pRARE_MAL_DEST/ NaKR1* or *pRARE_MAL_DEST* (with CcdB gene and KAN resistance gene removed) was inoculated into small LB liquid culture containing 100mg/L ampicillin and incubated overnight at 37°C at 200 rpm. Overnight cultures (10ml) were inoculated into 1L of LB medium for further amplification. When the culture reached OD_{600} of 0.5- 0.7, IPTG was added (to a final concentration of 0.5mM) and the culture was allowed to grow for another 3-4 hours before harvest. Protein purification was according to the pMAL™ protein purification protocol (New England BioLabs Inc.) with minor modifications. The cell culture was disrupted by sonication and the MBP-NaKR1 fusion protein and MBP protein were purified by mixing cell supernatant with amylose resin (NEB Inc.) at the ratio of 20:1 (v:v), incubated at 4°C for 0.5h. The resin was washed with PBS (0.8% NaCl, 0.02% KCl, 0.144% Na_2HPO_4 and 0.024% KH_2PO_4, pH7.4) and eluted 10mM of maltose

in PBS. The protein products collected from 3 independent experiments were combined for one ICP-MS analysis.

The purified protein sample was digested with trypsin (50:1 ratio in 25-100mM ammonium bicarbonate at 37°C overnight) followed by reduction with 10mM DTT and alkylated with iodoacetamide. The sample was analyzed by LC-MS/MS on a ThermoFinnigan. (ABI, Inc., Foster City, CA) LTQ ion trap mass spectrometer (MS). LC was preformed on a Michrom BioResources Paradigm AS1 with an inline C^{18} 12 cm column, packed in-house (Michrom BioResources, Auburn, CA). All MS/MS samples were analyzed using Sequest (ThermoFinnigan, San Jose, CA) and X! Tandem (www.thegpm.org). The search used a FASTA file for Arabadopsis containing more than 174668 entries including known contaminants as well as the sequence of the MBP-NAKR1 fusion protein. Scaffold (version Scaffold-01_05_14, Proteome Software Inc., Portland, OR) was used to validate MS/MS-based peptide and protein identifications. Peptides were manually confirmed to NaKR1 to insure that all peaks were assigned.

Xylem sap collection

Col-0 and *nakr1-1* plants were grown in soil under long day conditions until bolting and the inflorescence stems reached 7- 10 cm in length. Rosette leaves were removed with scissors and inflorescence stems cut with a razor blade. The plants were covered to maintain humidity. The first two drops of xylem sap were discarded and subsequent drops of xylem sap were collected from each plant with micropipettes (Drummond) (Shi et al., 2002; Sunarpi et al., 2005). Samples

were dried overnight at 95°C and dissolved in 5% of HNO_3 solution. Sodium and potassium content was measured by ICP-MS.

Grafting analysis

Reciprocal grafting between the shoot and root from different *A. thaliana* seedlings was performed. Medium and grafting method were according to Rus et al. (2006). Seeds were germinated and grown vertically on plates containing 0.5x MS macro- and micro- nutrients, vitamins (Caisson Laboratories, Inc.), fungicide benomyl, IAA, BA and 1.2% phytoagar in controlled conditions (16h/8h light/ dark cycle, 22°C, 55 $\mu mol \cdot m^{-2} \cdot S^{-1}$). Four- to five-day old seedlings were grafted on the plate under a dissection microscope. The grafted plants were grown vertically on the same plate for one week and successful graft unions were transferred to LG3 soil or Turface (Turface Athletics) and grown under short day conditions (8h/16h light/ dark cycle, 22°C, 70 $\mu mol \cdot m^{-2} \cdot S^{-1}$) for another five weeks. Two to three fully expanded rosette leaves of similar age were sampled from each plant, rinsed three times in DI H_2O, and dried in the oven (90°C) overnight and dry weight of each sample was recorded. Plants grown in Turface were watered twice per week with 0.25x Hoagland solution (Sigma) and iron supplement (4.15mg/L (4.5 μM) sodium ferric EDDHA) from the bottom. Grafted unions were checked two weeks after transfer to the soil/Turface, as well as after harvesting the rosette leaves. The individuals with adventitious roots formed above the grafted union were discarded.

^{14}C sucrose loading

Phloem loading of sucrose was analyzed essentially as described (Srivastava et al., 2008). Before the start of the experiment [U-^{14}C] sucrose stock (21.8 GBq/mmol, MP Biomedicals) was dried to remove the ethanol and then resuspended at a final solution of 0.5 mM [U-^{14}C] sucrose in 10 mM MES, pH 5.5, 1 mM $CaCl_2$. 11- week- old Col-0 and *nakr1-1* plants grown in Turface under short day conditions were used. On each plant the tip of a fully expanded rosette leaf was crimped with forceps and 2 µl of the [U-^{14}C] sucrose applied. Plants were maintained at 20 °C under high moisture conditions for the duration of the experiment. After 30 min the remaining sucrose drop was removed and the application site rinsed with buffer (10 mM MES, pH 5.5, 1 mM $CaCl_2$). The labeled plants were dissected immediately and rosette leaves, stem and roots from each plant were pressed flat between Whatman 3M filter paper until dry. The dried plant parts were attached to card stock using double-sided tape and then exposed to KODAK BioMax MR Film for 5 days.

Leaf Starch analysis

Arabidopsis plants were grown for 3 months in short day conditions and fully expanded rosette leaves were sampled. For starch staining, leaves were cleared in 70% ethanol at 70°C and stained in I_2/KI solution for 15 min at room temperature. Starch quantification was according to the method of Smith and Zeeman (2006) with minor modifications. 0.2g of fresh leaves were sampled from each plant, boiled in 80% ethanol (5 times × 3 min) to remove soluble sugar. The remained pellet was ground in water and adjusted to a final volume of 1.5-2 mL.

From each sample, 0.1 mL (×4) of homogenate was collected and boiled in water bath for 20 minutes and the gelatinized samples were digested with 6 units of α-amyloglucosidase (dissolved in 200 mM Na acetate, pH 5.5) and 1.2 units of α-amylase (dissolved in 3.2 M ammonium sulfate, pH 7.0) at 37°C for 4h. The glucose content of each tube was measured by glucose Trinder assay (Sigma Diagnotics). The glucose concentration of each sample was determined based on the absorbance monitored at 495nm using Microplate Scanning Spectrophotometer (Power Wave 340, BIO-TER) and the standard curve produced using a series of glucose standards (0.011mg/mL, 0.051mg/mL, 0.11mg/mL, 0.51mg/mL, 1mg/mL).

3. CONCLUSIONS

This dissertation work was done to identify important genes involved in Na^+/K^+ homeostasis of Arabidopsis plants. Using ICP- MS analyses of leaf tissue combined with traditional and DNA- chip based mapping, a gene encoding a heavy- metal- associated domain containing protein has been identified, which we named *AtNaKR1*. Loss of function of *AtNaKR1* mutation caused Na^+/K^+ accumulation phenotypes and multiple developmental defects including short primary roots, late flowering and loss of apical dominance. *AtNaKR1* is specifically expressed in phloem companion cells. *nakr1-1* mutation affects phloem function of carbohydrates partitioning between source and sinks and sucrose loading. K^+ and Na^+ accumulation phenotypes are also attributed to phloem function defects, based on grafting followed by ICP-MS analyses of rosette leaves and elemental analyses of xylem sap samples. Interestingly, although phloem translocation is responsible for the long- distance transport of multiple mineral elements, *nakr1-1* mutation specifically affects K^+ and Na^+ redistribution. This is supported by the result of elemental analyses of *nakr1-1* seeds, in which K^+ is one of the few elements the contents of which significantly reduced than the control seeds, and most other elements remain relatively unchanged or increased compared to wild- type seeds. K^+ is the major cation within the phloem sap and is involved in maintaining the osmotic gradient between the source and sinks. K^+ and sucrose loading/unloading processes are functionally interrelated. Whether these can partially explain the specific effect of *nakr1-1* mutation on K^+/Na^+ homeostasis still requires further research.

Phloem translocation stream forms a long- distance signaling system connecting distant organs with meristimatic regions. The result *nakr1-1* is a late flowering mutant and the late flowering phenotype most dramatic in long day growth conditions suggest *nakr1-1* mutation also affect the transport of florigen, a phloem mobile signal. Analyzing the root meristem region of *nakr1-1* seedlings revealed root defects occurred at 3DAG. The earliest expression of *NaKR1* was detected at 1DAG, thus the root defect might be an indirect result of *NaKR1* mutation. Whether the root defects is simply the result of nutritional deficiency or involve signaling processes (requiring normal phloem function) still requires further research. Comparing the expression pattern of *NaKR1pro::histone:GFP* with that of *NaKR1pro::NaKR1:GFP* revealed that NaKR1 protein is phloem mobile and it is further unloaded into part of the root meristem region. However this mobility seems nonessential for any of the phenotypes recorded for *nakr1-1* mutant, because *nakr1-1* was fully complemented by the construct *NaKR1pro::NaKR1-GUS*, and NaKR1-GUS was not mobile within the meristem region. However, the possibility cannot be excluded that the protein mobility might exert some unknown functions, or its function is redundant with similar proteins expressed in the root meristem region.

Elemental analysis of MBP-NaKR1 protein purified from *Escherichia coli* revealed it's a heavy metal binding protein. Point mutation analysis confirmed the heavy- metal binding domain is essential for its function. Heavy metal binding proteins that coordinate Fe^{3+}, Cu^{+} have been identified from phloem sap

in previous studies. Their functions varied from maintaining the reduced state of heavy metals in phloem sap to sequestration of heavy metals from old, senescent tissues. None of them however when mutated caused severe phenotype as *nakr1-1*, suggesting AtNaKR1 might have peculiar functions. The next step might be to characterize the exact type of heavy metals it coordinates and proteins AtNaKR1 interact with.

4. REFERENCES

Ache P., Becker D., Deeken R., Dreyer I., Weber H., Fromm J., and Hedrich R. (2001). VFK1, a *Vicia faba* K(+) channel involved in phloem unloading. Plant J. **27,** 571-580.

Aki T., Shigyo M., Nakano R., Yoneyama T., and Yanagisawa S. (2008). Nano scale proteomics revealed the presence of regulatory proteins including three FT-Like proteins in phloem and xylem saps from rice. Plant Cell Physiol. **49,** 767-790.

Allen GJ and Sanders D (1994). Osmotic stress enhances the competence of Beta vulgaris vacuoles to respond to isositol 1,4,5- triphosphate. Plant J. **6,** 687-695.

Almon E., Horowitz M., Wang H.L., Lucas W.J., Zamski E., and Wolf S. (1997). Phloem-Specific Expression of the Tobacco Mosaic Virus Movement Protein Alters Carbon Metabolism and Partitioning in Transgenic Potato Plants. Plant Physiol. **115,** 1599-1607.

Aoki K., Kragler F., Xoconostle-Cazares B., and Lucas W.J. (2002). A subclass of plant heat shock cognate 70 chaperones carries a motif that facilitates trafficking through plasmodesmata. Proc. Natl. Acad. Sci. U. S. A. **99,** 16342-16347.

Aoki K., Suzui N., Fujimaki S., Dohmae N., Yonekura-Sakakibara K., Fujiwara T., Hayashi H., Yamaya T., and Sakakibara H. (2005). Destination-selective long-distance movement of phloem proteins. Plant Cell **17,** 1801-1814.

Apse M.P., Aharon G.S., Snedden W.A., and Blumwald E. (1999). Salt tolerance conferred by overexpression of a vacuolar Na(+)/H(+) antiport in Arabidopsis. Science **285,** 1256-1258.

Apse M.P., Sottosanto J.B., and Blumwald E. (2003). Vacuolar cation/H(+) exchange, ion homeostasis, and leaf development are altered in a T-DNA insertional mutant of AtNHX1, the Arabidopsis vacuolar Na(+)/H(+) antiporter. Plant J. **36,** 229-239.

Araki T., Eguchi T., Wajima T., Yoshida S., and Kitano M. (2004). Dynamic analysis of growth, water balance and sap fluxes through phloem and xylem in a tomato fruit: Short- term effect of water stress. Environ. Control Biol. **42,** 225-240.

Araki T. (2001). Transition from vegetative to reproductive phase. Curr. Opin. Plant Biol. **4,** 63-68.

Asano T., Masumura T., Kusano H., Kikuchi S., Kurita A., Shimada H., and Kadowaki K. (2002). Construction of a specialized cDNA library from plant cells isolated by laser capture microdissection: toward comprehensive analysis of the genes expressed in the rice phloem. Plant J. **32,** 401-408.

Baker DA (2000). Long- distance vascular transport of endogenous hormones in plants and their role in source- sink regulation. Isr. J. Plant Sci. **48,** 199-203.

Balachandran S., Xiang Y., Schobert C., Thompson G.A., and Lucas W.J. (1997). Phloem sap proteins from Cucurbita maxima and Ricinus communis have the capacity to traffic cell to cell through plasmodesmata. Proc. Natl. Acad. Sci. U. S. A. **94,** 14150-14155.

Banerjee A.K., Chatterjee M., Yu Y., Suh S.G., Miller W.A., and Hannapel D.J. (2006). Dynamics of a mobile RNA of potato involved in a long-distance signaling pathway. Plant Cell **18,** 3443-3457.

Banerjee A.K., Lin T., and Hannapel D.J. (2009). Untranslated regions of a mobile transcript mediate RNA metabolism. Plant Physiol. **151,** 1831-1843.

Barnes A., Bale J., Constantinidou C., Ashton P., Jones A., and Pritchard J. (2004). Determining protein identity from sieve element sap in Ricinus communis L. by quadrupole time of flight (Q-TOF) mass spectrometry. J. Exp. Bot. **55,** 1473-1481.

Bashir K, Inoue H, Nagasaka S, Takahashi M, Nakanishi H, Mori S, Nishizawa NK. (2006). Cloning and characterization of deoxymugineic acid synthase genes from graminaceous plants. J. Biol. Chem. **281**, 32395-32402

Batelli G., Verslues P.E., Agius F., Qiu Q., Fujii H., Pan S., Schumaker K.S., Grillo S., and Zhu J.K. (2007). SOS2 promotes salt tolerance in part by interacting with the vacuolar H(+)-ATPase and upregulating its transport activity. Mol. Cell. Biol. **27,** 7781-7790.

Bauby H., Divol F., Truernit E., Grandjean O., and Palauqui J.C. (2007). Protophloem differentiation in early Arabidopsis thaliana development. Plant Cell Physiol. **48,** 97-109.

Baum SF, Dubrovsky JG, and Rost TL (2002). Apical organization and maturation of the cortex and vascular cylinder in Arabidopsis thaliana (Brassicaceae) roots. Am. J. Bot. **89,** 908-920.

Benitez-Alfonso Y., Cilia M., San Roman A., Thomas C., Maule A., Hearn S., and Jackson D. (2009). Control of Arabidopsis meristem development by thioredoxin-dependent regulation of intercellular transport. Proc. Natl. Acad. Sci. U. S. A. **106,** 3615-3620.

Berthomieu P., Conejero G., Nublat A., Brackenbury W.J., Lambert C., Savio C., Uozumi N., Oiki S., Yamada K., Cellier F., Gosti F., Simonneau T., Essah P.A., Tester M., Very A.A., Sentenac H., and Casse F. (2003). Functional analysis of AtHKT1 in Arabidopsis shows that Na(+) recirculation by the phloem is crucial for salt tolerance. EMBO J. **22,** 2004-2014.

Bhandal IS and Malik CP (1988). Potassium estimation, uptake, and its role in the physiology and metabolism of flowering plants. Int. Rev. Cytol. **110,** 205-254.

Blaha G, Stelzl U, Spahn CMT, Agrawal RK, Frank J, and Nierhaus KH (2000). Preparation of functional ribosomal complexes and effect of buffer conditions on tRNA positions observed by cryoelectron microscopy. Methods Enzymol. **317,** 292-309.

Blumwald E., Aharon G.S., and Apse M.P. (2000). Sodium transport in plant cells. Biochem. Biophys. Acta **1465,** 140-151.

Bonke M., Thitamadee S., Mahonen A.P., Hauser M.T., and Helariutta Y. (2003). APL regulates vascular tissue identity in Arabidopsis. Nature **426,** 181-186.

Brady S.M., Orlando D.A., Lee J.Y., Wang J.Y., Koch J., Dinneny J.R., Mace D., Ohler U., and Benfey P.N. (2007). A high-resolution root spatiotemporal map reveals dominant expression patterns. Science **318,** 801-806.

Brandt S., Kehr J., Walz C., Imlau A., Willmitzer L., and Fisahn J. (1999). Technical Advance: A rapid method for detection of plant gene transcripts from single epidermal, mesophyll and companion cells of intact leaves. Plant J. **20,** 245-250.

Brett C.L., Tukaye D.N., Mukherjee S., and Rao R. (2005). The yeast endosomal Na+K+/H+ exchanger Nhx1 regulates cellular pH to control vesicle trafficking. Mol. Biol. Cell **16,** 1396-1405.

Bull P.C. and Cox D.W. (1994). Wilson disease and Menkes disease: new handles on heavy-metal transport. Trends Genet. **10,** 246-252.

Burkle L., Hibberd J.M., Quick W.P., Kuhn C., Hirner B., and Frommer W.B. (1998). The H+-sucrose cotransporter NtSUT1 is essential for sugar export from tobacco leaves. Plant Physiol. **118,** 59-68.

Byrt C.S., Platten J.D., Spielmeyer W., James R.A., Lagudah E.S., Dennis E.S., Tester M., and Munns R. (2007). HKT1;5-like cation transporters linked to Na(+) exclusion loci in wheat, Nax2 and Kna1. Plant Physiol. **143,** 1918-1928.

Carey A.M., Scheckel K.G., Lombi E., Newville M., Choi Y., Norton G.J., Charnock J.M., Feldmann J., Price A.H., and Meharg A.A. (2010). Grain unloading of arsenic species in rice. Plant Physiol. **152,** 309-319.

Caspar T, Lin TP, Kakefuda G, Benbow L, Preiss J, Somerville C. (1991). Mutants of Arabidopsis with altered regulation of starch degradation. Plant Physiol. **95**, 1181-1188.

Cheeseman JM (1982). Pump- leak sodium fluxes in low salt corn roots. J. Mem. Biol. **70,** 157-164.

Cheng N.H., Pittman J.K., Zhu J.K., and Hirschi K.D. (2004). The protein kinase SOS2 activates the Arabidopsis H(+)/Ca(2+) antiporter CAX1 to integrate calcium transport and salt tolerance. J. Biol. Chem. **279,** 2922-2926.

Chiou T.J. and Bush D.R. (1998). Sucrose is a signal molecule in assimilate partitioning. Proc. Natl. Acad. Sci. U. S. A. **95,** 4784-4788.

Citovsky V., Knorr D., Schuster G., and Zambryski P. (1990). The P30 movement protein of tobacco mosaic virus is a single-strand nucleic acid binding protein. Cell **60,** 637-647.

Citovsky V. and Zambryski P. (1991). How do plant virus nucleic acids move through intercellular connections? Bioessays **13,** 373-379.

Citovsky V., Ghoshroy S., Tsui F., and Klessig D. (1998). Non-toxic concentrations of cadmium inhibit systemic movement of turnip vein clearing virus by a salicylic acid-independent mechanism. Plant J. **16,** 13-20.

Complainville A., Brocard L., Roberts I., Dax E., Sever N., Sauer N., Kondorosi A., Wolf S., Oparka K., and Crespi M. (2003). Nodule initiation involves the creation of a new symplasmic field in specific root cells of medicago species. Plant Cell **15,** 2778-2791.

Corbesier L., Vincent C., Jang S., Fornara F., Fan Q., Searle I., Giakountis A., Farrona S., Gissot L., Turnbull C., and Coupland G. (2007). FT protein movement contributes to long-distance signaling in floral induction of Arabidopsis. Science **316,** 1030-1033.

Crafts AS., Crisp CE (1971). Phloem transport in plants. Freeman, San Francisco.

Cuartero J and Fernandez- Muñoz R (1999). Tomato and salinity. Sci. Hort. **78,** 83-125.

Curtis M.D. and Grossniklaus U. (2003). A gateway cloning vector set for high-throughput functional analysis of genes in planta. Plant Physiol. **133,** 462-469.

Davenport R.J. and Tester M. (2000). A weakly voltage-dependent, nonselective cation channel mediates toxic sodium influx in wheat. Plant Physiol. **122,** 823-834.

Davenport R.J., Munoz-Mayor A., Jha D., Essah P.A., Rus A., and Tester M. (2007). The Na(+) transporter AtHKT1;1 controls retrieval of Na(+) from the xylem in Arabidopsis. Plant. Cell. Environ. **30,** 497-507.

Deeken R., Sanders C., Ache P., and Hedrich R. (2000). Developmental and light-dependent regulation of a phloem-localised K+ channel of Arabidopsis thaliana. Plant J. **23,** 285-290.

Deeken R., Geiger D., Fromm J., Koroleva O., Ache P., Langenfeld-Heyser R., Sauer N., May S.T., and Hedrich R. (2002). Loss of the AKT2/3 potassium channel affects sugar loading into the phloem of Arabidopsis. Planta **216,** 334-344.

Deeken R., Ache P., Kajahn I., Klinkenberg J., Bringmann G., and Hedrich R. (2008). Identification of Arabidopsis thaliana phloem RNAs provides a search criterion for phloem-based transcripts hidden in complex datasets of microarray experiments. Plant J. **55,** 746-759.

Demidchik V., Essah P.A., and Tester M. (2004). Glutamate activates cation currents in the plasma membrane of Arabidopsis root cells. Planta **219,** 167-175.

Derrick PM, Barker H, and Oparka KJ (1990). Effect of virus infection on symplastic transport of fluorescent tracers in Nicotiana clevelandii leaf epidermis. Planta **181,** 555-559.

Ding B., Haudenshield J.S., Hull R.J., Wolf S., Beachy R.N., and Lucas W.J. (1992). Secondary plasmodesmata are specific sites of localization of the tobacco mosaic virus movement protein in transgenic tobacco plants. Plant Cell **4,** 915-928.

Doering-Saad C., Newbury H.J., Bale J.S., and Pritchard J. (2002). Use of aphid stylectomy and RT-PCR for the detection of transporter mRNAs in sieve elements. J. Exp. Bot. **53,** 631-637.

Drew MC and Saker LR (1984). Uptake and long-distance transport of phosphate, potassium and chloride in relation to internal ion concentrations in barley: evidence for a non- allosteric regulation. Planta **160,** 500-507.

Dubcovsky J, Santa Maria G, Epstein E, Luo M-C, and Dvoøák J. (1996). Mapping of the K(+)/Na(+) discrimination locus KnaI in wheat. Theor. Appl. Genet. **92,** 448-454.

Dykema P.E., Sipes P.R., Marie A., Biermann B.J., Crowell D.N., and Randall S.K. (1999). A new class of proteins capable of binding transition metals. Plant Mol. Biol. **41,** 139-150.

Eschrich W, Evert RF, and Young JH (1972). Solution flow in tubular semipermeable membranes. Planta **107,** 279-300.

Essah P.A., Davenport R., and Tester M. (2003). Sodium influx and accumulation in Arabidopsis. Plant Physiol. **133,** 307-318.

Fischer DB (1987). Changes in the concentration and composition of peduncle sieve tube sap during grain filling in normal and phosphate-deficient wheat plants. Aust. J. Plant Physiol. **14,** 147-156.

Flowers TJ, Hajibagheri MA, and Yeo AR (1991). Ion accumulation in the cell walls of rice plants growing under saline conditions- evidence for the Öertli hypothesis. Plant Cell Environ. **14,** 319-325.

Fromm J and Eschrich W (1989). Correlation of ionic movements with phloem unloading and loading in barley leaves. Plant Physiol. Biochem. **27,** 577-585.

Fukada A, Chiba K, Maeda A, Nakamura A, Maeshima M, and Tanaka Y (2004a). Effect of salt and osmotic stresses on the expression of genes for the vacuolar H(+)- pyrophophatase, H(+)-ATPase subunit A, and Na(+)/H(+) antiporter from barley. J. Exp. Bot. **55,** 585-594.

Fukada A, Nakamura A, Tagiri A, Tanaka H, Miyao A, Hirochika H, and Tanaka Y (2004b). Function, Intracellular Localization and the Importance in Salt Tolerance of a Vacuolar Na(+)/H(+) Antiporter from Rice. Plant Cell Physiol. **45,** 146-159.

Fukada-Tanaka S., Inagaki Y., Yamaguchi T., Saito N., and Iida S. (2000). Colour-enhancing protein in blue petals. Nature **407,** 581,.

Gamalei Y (1991). Phloem loading and its development related to plant evolution from trees to herbs. Trees **5,** 50-64.

Gaxiola R.A., Rao R., Sherman A., Grisafi P., Alper S.L., and Fink G.R. (1999). The Arabidopsis thaliana proton transporters, AtNhx1 and Avp1, can function in cation detoxification in yeast. Proc. Natl. Acad. Sci. U. S. A. **96,** 1480-1485.

Gaxiola R.A., Li J., Undurraga S., Dang L.M., Allen G.J., Alper S.L., and Fink G.R. (2001). Drought- and salt-tolerant plants result from overexpression of the AVP1 H(+)-pump. Proc. Natl. Acad. Sci. U. S. A. **98,** 11444-11449.

Ghoshroy S., Freedman K., Lartey R., and Citovsky V. (1998). Inhibition of plant viral systemic infection by non-toxic concentrations of cadmium. Plant J. **13,** 591-602.

Giaquinta R (1980). Mechanism and control of phloem loading of sucrose. Ber. Dtsch. Bot. Ges. **93,** 187-201.

Giavalisco P., Kapitza K., Kolasa A., Buhtz A., and Kehr J. (2006). Towards the proteome of Brassica napus phloem sap. Proteomics **6,** 896-909.

Gil-Mascarell R., Lopez-Coronado J.M., Belles J.M., Serrano R., and Rodriguez P.L. (1999). The Arabidopsis HAL2-like gene family includes a novel sodium-sensitive phosphatase. Plant J. **17,** 373-383.

Gisel A., Barella S., Hempel F.D., and Zambryski P.C. (1999). Temporal and spatial regulation of symplastic trafficking during development in Arabidopsis thaliana apices. Development **126,** 1879-1889.

Gisel A., Hempel F.D., Barella S., and Zambryski P. (2002). Leaf-to-shoot apex movement of symplastic tracer is restricted coincident with flowering in Arabidopsis. Proc. Natl. Acad. Sci. U. S. A. **99,** 1713-1717.

Golecki B, Schulz A, Carstens- Behrens U, and Kollmann R (1998). Evidence for graft transmission of structural phloem proteins or their precursors in heterografts of Cucurbitaceae. Planta **206,** 630-640.

Gomez G. and Pallas V. (2004). A long-distance translocatable phloem protein from cucumber forms a ribonucleoprotein complex in vivo with Hop stunt viroid RNA. J. Virol. **78,** 10104-10110.

Gomez G., Torres H., and Pallas V. (2005). Identification of translocatable RNA-binding phloem proteins from melon, potential components of the long-distance RNA transport system. Plant J. **41,** 107-116.

Gorham J (1990). Salt tolerance in the Triticeae: Ion discrimination in rye and triticale. J. Exp. Bot. **41,** 609-614.

Gottwald J.R., Krysan P.J., Young J.C., Evert R.F., and Sussman M.R. (2000). Genetic evidence for the in planta role of phloem-specific plasma membrane sucrose transporters. Proc. Natl. Acad. Sci. U. S. A. **97,** 13979-13984.

Greenway H and Munns R (1980). Mechanisms of salt tolerance in nonhalophytes. Ann. Rev. Plant Physiol. **31,** 149-190.

Guo K.M., Babourina O., Christopher D.A., Borsics T., and Rengel Z. (2008). The cyclic nucleotide-gated channel, AtCNGC10, influences salt tolerance in Arabidopsis. Physiol. Plant. **134,** 499-507.

Hackel A., Schauer N., Carrari F., Fernie A.R., Grimm B., and Kuhn C. (2006). Sucrose transporter LeSUT1 and LeSUT2 inhibition affects tomato fruit development in different ways. Plant J. **45,** 180-192.

Halfter U., Ishitani M., and Zhu J.K. (2000). The Arabidopsis SOS2 protein kinase physically interacts with and is activated by the calcium-binding protein SOS3. Proc. Natl. Acad. Sci. U. S. A. **97,** 3735-3740.

Haritatos E, Medville R, and Turgeon R (1996). Raffinose oligosaccharide concentrations measured in individual cell and tissue types in Cucumis melo L. leaves: Implications for phloem loading. Planta **198,** 614-622.

Haritatos E., Medville R., and Turgeon R. (2000). Minor vein structure and sugar transport in Arabidopsis thaliana. Planta **211,** 105-111.

Haro R., Banuelos M.A., and Rodriguez-Navarro A. (2010). High-affinity sodium uptake in land plants. Plant Cell Physiol. **51,** 68-79.

Hasegawa P.M., Bressan R.A., Zhu J.K., and Bohnert H.J. (2000). Plant Cellular and Molecular Responses to High Salinity. Annu. Rev. Plant Physiol. Plant Mol. Biol. **51,** 463-499.

Hayashi H and Chino M (1990). Chemical composition of phloem sap from the uppermost internode of the rice plant. Plant Cell Physiol. **31,** 247-251.

Hayes PM, Offler CE, and Patrick JW (1985). Cellular structures, plasma membrane surface areas and plasmodesmatal frequencies of the stem of Phaseolus vulgaris L. in relation to radial photosynthate transfer. Ann. Bot. **56,** 125-138.

Haywood V., Yu T.S., Huang N.C., and Lucas W.J. (2005). Phloem long-distance trafficking of GIBBERELLIC ACID-INSENSITIVE RNA regulates leaf development. Plant J. **42,** 49-68.

Haywood V., Yu T.S., Huang N.C., and Lucas W.J. (2005). Phloem long-distance trafficking of GIBBERELLIC ACID-INSENSITIVE RNA regulates leaf development. Plant J. **42,** 49-68.

Heineke D., Sonnewald U., Bussis D., Gunter G., Leidreiter K., Wilke I., Raschke K., Willmitzer L., and Heldt H.W. (1992). Apoplastic expression of yeast-derived invertase in potato : effects on photosynthesis, leaf solute composition, water relations, and tuber composition. Plant Physiol. **100,** 301-308.

Himelblau E., Mira H., Lin S.J., Culotta V.C., Penarrubia L., and Amasino R.M. (1998). Identification of a functional homolog of the yeast copper homeostasis gene ATX1 from Arabidopsis. Plant Physiol. **117,** 1227-1234.

Hirayama T., Ohto C., Mizoguchi T., and Shinozaki K. (1995). A gene encoding a phosphatidylinositol-specific phospholipase C is induced

by dehydration and salt stress in Arabidopsis thaliana. Proc. Natl. Acad. Sci. U. S. A. **92,** 3903-3907.

Horie T., Hauser F., and Schroeder J.I. (2009). HKT transporter-mediated salinity resistance mechanisms in Arabidopsis and monocot crop plants. Trends Plant Sci. **14,** 660-668.

Huang S., Spielmeyer W., Lagudah E.S., James R.A., Platten J.D., Dennis E.S., and Munns R. (2006). A sodium transporter (HKT7) is a candidate for Nax1, a gene for salt tolerance in durum wheat. Plant Physiol. **142,** 1718-1727.

Iglesias V.A. and Meins F.,Jr (2000). Movement of plant viruses is delayed in a beta-1,3-glucanase-deficient mutant showing a reduced plasmodesmatal size exclusion limit and enhanced callose deposition. Plant J. **21,** 157-166.

Imlau A., Truernit E., and Sauer N. (1999). Cell-to-cell and long-distance trafficking of the green fluorescent protein in the phloem and symplastic unloading of the protein into sink tissues. Plant Cell **11,** 309-322.

Ishimaru Y, Masuda H, Bashir K, Inoue H, Tsukamoto T, Takahashi M, Nakanishi H, Aoki N, Hirose T, Ohsugi R, Nishizawa NK. (2010). Rice metal-nicotianamine transporter, OsYSL2, is required for the long-distance transport of iron and manganese. The Plant J. **62**, 379-390.

Ishitani M., Liu J., Halfter U., Kim C.S., Shi W., and Zhu J.K. (2000). SOS3 function in plant salt tolerance requires N-myristoylation and calcium binding. Plant Cell **12,** 1667-1678.

Ivashikina N., Deeken R., Ache P., Kranz E., Pommerrenig B., Sauer N., and Hedrich R. (2003). Isolation of AtSUC2 promoter-GFP-marked companion cells for patch-clamp studies and expression profiling. Plant J. **36,** 931-945.

James RA, Rivelli AR, Munns R, and von Caemmerer S (2002). Factors affecting CO2 assimilation, leaf injury and growth in salt- stressed durum wheat. Funct. Plant Biol. **29,** 1393-1403.

James R.A., Davenport R.J., and Munns R. (2006). Physiological characterization of two genes for Na+ exclusion in durum wheat, Nax1 and Nax2. Plant Physiol. **142,** 1537-1547.

Jones-Rhoades M.W. and Bartel D.P. (2004). Computational identification of plant microRNAs and their targets, including a stress-induced miRNA. Mol. Cell **14,** 787-799.

Jorgensen R.A., Atkinson R.G., Forster R.L., and Lucas W.J. (1998). An RNA-based information superhighway in plants. Science **279,** 1486-1487.

Karley AJ and White PJ. (2009). Moving cationic minerals to edible tissues: potassium, magnesium, calcium. Curr. Opin. Plant Biol. **12,** 291-298.

Katiyar-Agarwal S., Zhu J., Kim K., Agarwal M., Fu X., Huang A., and Zhu J.K. (2006). The plasma membrane Na(+)/H(+) antiporter SOS1 interacts with RCD1 and functions in oxidative stress tolerance in Arabidopsis. Proc. Natl. Acad. Sci. U. S. A. **103,** 18816-18821.

Kehr J. and Buhtz A. (2008). Long distance transport and movement of RNA through the phloem. J. Exp. Bot. **59,** 85-92.

Kempers R and van Bel AJE (1997). Symplasmic connections between sieve element and companion cell in the stem phloem of Vicia faba L. have a molecular exclusion limit of at least 10kDa. Planta **201,** 195-201.

Kim B.G., Waadt R., Cheong Y.H., Pandey G.K., Dominguez-Solis J.R., Schultke S., Lee S.C., Kudla J., and Luan S. (2007). The calcium sensor CBL10 mediates salt tolerance by regulating ion homeostasis in Arabidopsis. Plant J. **52,** 473-484.

Kim J.Y., Yuan Z., and Jackson D. (2003). Developmental regulation and significance of KNOX protein trafficking in Arabidopsis. Development **130,** 4351-4362.

Kim J.Y., Rim Y., Wang J., and Jackson D. (2005). A novel cell-to-cell trafficking assay indicates that the KNOX homeodomain is necessary and sufficient for intercellular protein and mRNA trafficking. Genes Dev. **19,** 788-793,.

Knight H., Trewavas A.J., and Knight M.R. (1997). Calcium signalling in Arabidopsis thaliana responding to drought and salinity. Plant J. **12,** 1067-1078.

Kovtun Y., Chiu W.L., Tena G., and Sheen J. (2000). Functional analysis of oxidative stress-activated mitogen-activated protein kinase cascade in plants. Proc. Natl. Acad. Sci. U. S. A. **97,** 2940-2945.

Kruger C., Berkowitz O., Stephan U.W., and Hell R. (2002). A metal-binding member of the late embryogenesis abundant protein family transports iron in the phloem of Ricinus communis L. J. Biol. Chem. **277,** 25062-25069.

Kudla J., Xu Q., Harter K., Gruissem W., and Luan S. (1999). Genes for calcineurin B-like proteins in Arabidopsis are differentially regulated by stress signals. Proc. Natl. Acad. Sci. U. S. A. **96,** 4718-4723.

Kugler A., Kohler B., Palme K., Wolff P., and Dietrich P. (2009). Salt-dependent regulation of a CNG channel subfamily in Arabidopsis. BMC Plant. Biol. **9,** 140.

Kuhn C., Franceschi V.R., Schulz A., Lemoine R., and Frommer W.B. (1997). Macromolecular trafficking indicated by localization and turnover of sucrose transporters in enucleate sieve elements. Science **275,** 1298-1300.

Kuhn C., Hajirezaei M.R., Fernie A.R., Roessner-Tunali U., Czechowski T., Hirner B., and Frommer W.B. (2003). The sucrose transporter StSUT1 localizes to sieve elements in potato tuber phloem and influences tuber physiology and development. Plant Physiol. **131,** 102-113.

Lacombe B., Pilot G., Michard E., Gaymard F., Sentenac H., and Thibaud J.B. (2000). A shaker-like K(+) channel with weak rectification is expressed in both source and sink phloem tissues of Arabidopsis. Plant Cell **12,** 837-851.

Lahner B., Gong J., Mahmoudian M., Smith E.L., Abid K.B., Rogers E.E., Guerinot M.L., Harper J.F., Ward J.M., McIntyre L., Schroeder J.I., and Salt D.E. (2003). Genomic scale profiling of nutrient and trace elements in Arabidopsis thaliana. Nat. Biotechnol. **21,** 1215-1221.

Lalonde S, Tegeder M, Throne-Holst M, Frommer WB, and Patrick JW. (2003). Phloem loading and unloading of sugars and amino acids. Plant Cell Environ. **26,** 37-56.

Lalonde S., Boles E., Hellmann H., Barker L., Patrick J.W., Frommer W.B., and Ward J.M. (1999). The dual function of sugar carriers. Transport and sugar sensing. Plant Cell **11,** 707-726.

Lang A (1983). Turgor- related translocation. Plant Cell Physiol. **6,** 683-689.

Layzell DB, Pate JS, Atkins CA, and Canvin DT. (1981). Partitioning of carbon and nitrogen and the nutrition of root and shoot apex in a nodulated legume. Plant Physiol. **67,** 30-36.

Lee DR (1990). A unidirectional water flux model of fruit growth. Can. J. Bot **68,** 1286-1290.

Lee J.Y., Yoo B.C., Rojas M.R., Gomez-Ospina N., Staehelin L.A., and Lucas W.J. (2003). Selective trafficking of non-cell-autonomous proteins mediated by NtNCAPP1. Science **299,** 392-396.

Leng Q., Mercier R.W., Hua B.G., Fromm H., and Berkowitz G.A. (2002). Electrophysiological analysis of cloned cyclic nucleotide-gated ion channels. Plant Physiol. **128,** 400-410.

Leshem Y., Melamed-Book N., Cagnac O., Ronen G., Nishri Y., Solomon M., Cohen G., and Levine A. (2006). Suppression of Arabidopsis vesicle-SNARE expression inhibited fusion of H2O2-containing vesicles with tonoplast and increased salt tolerance. Proc. Natl. Acad. Sci. U. S. A. **103,** 18008-18013.

Lin M.K., Belanger H., Lee Y.J., Varkonyi-Gasic E., Taoka K., Miura E., Xoconostle-Cazares B., Gendler K., Jorgensen R.A., Phinney B., Lough T.J., and Lucas W.J. (2007). FLOWERING LOCUS T protein may act as the long-distance florigenic signal in the cucurbits. Plant Cell **19,** 1488-1506.

Lin M.K., Lee Y.J., Lough T.J., Phinney B.S., and Lucas W.J. (2009). Analysis of the pumpkin phloem proteome provides insights into angiosperm sieve tube function. Mol. Cell. Proteomics **8,** 343-356.

Lin S.J. and Culotta V.C. (1995). The ATX1 gene of Saccharomyces cerevisiae encodes a small metal homeostasis factor that protects

cells against reactive oxygen toxicity. Proc. Natl. Acad. Sci. U. S. A. **92,** 3784-3788.

Lin S.J., Pufahl R.A., Dancis A., O'Halloran T.V., and Culotta V.C. (1997). A role for the Saccharomyces cerevisiae ATX1 gene in copper trafficking and iron transport. J. Biol. Chem. **272,** 9215-9220.

Lincoln C., Britton J.H., and Estelle M. (1990). Growth and development of the axr1 mutants of Arabidopsis. Plant Cell **2,** 1071-1080.

Lohaus G, Hussmann M, Pennewiss K, Schneider H, Zhu JJ, and Sattelmacher B (2000). Solute balance of a maize (Zea mays L.) source leaf as affected by salt treatment with special emphasis on phloem retranslocation and ion leaching. J. Exp. Bot. **51,** 1721-1732.

Lough T.J. and Lucas W.J. (2006). Integrative plant biology: role of phloem long-distance macromolecular trafficking. Annu. Rev. Plant. Biol. **57,** 203-232.

Lucas W.J., Bouche-Pillon S., Jackson D.P., Nguyen L., Baker L., Ding B., and Hake S. (1995). Selective trafficking of KNOTTED1 homeodomain protein and its mRNA through plasmodesmata. Science **270,** 1980-1983.

Lucas W.J. (2006). Plant viral movement proteins: agents for cell-to-cell trafficking of viral genomes. Virology **344,** 169-184.

Lucas W.J., Ham B.K., and Kim J.Y. (2009). Plasmodesmata - bridging the gap between neighboring plant cells. Trends Cell Biol. **19,** 495-503.

Ma Y., Slewinski T.L., Baker R.F., and Braun D.M. (2009). Tie-dyed1 encodes a novel, phloem-expressed transmembrane protein that functions in carbohydrate partitioning. Plant Physiol. **149,** 181-194.

Maathuis FJM and Amtmann A (1999). K(+) nutrition and Na(+) toxicity: the basis of cellular K(+)/Na(+) ratios. Ann. Botany **84,** 123-133.

Maathuis F.J. and Sanders D. (2001). Sodium uptake in Arabidopsis roots is regulated by cyclic nucleotides. Plant Physiol. **127,** 1617-1625.

Madey E., Nowack L.M., and Thompson J.E. (2002). Isolation and characterization of lipid in phloem sap of canola. Planta **214,** 625-634.

Maeshima M. (2000). Vacuolar H(+)-pyrophosphatase. Biochim. Biophys. Acta **1465,** 37-51.

Mahajan S., Pandey G.K., and Tuteja N. (2008). Calcium- and salt-stress signaling in plants: shedding light on SOS pathway. Arch. Biochem. Biophys. **471,** 146-158.

Marschner H, Kirkby EA, and Cakmak I (1996). Effect of mineral nutritional status on shoot- root partitioning of photoassimilates and cycling of mineral nutrients. J. Exp. Bot. **47,** 1255-1263.

Marten I., Hoth S., Deeken R., Ache P., Ketchum K.A., Hoshi T., and Hedrich R. (1999). AKT3, a phloem-localized K+ channel, is blocked by protons. Proc. Natl. Acad. Sci. U. S. A. **96,** 7581-7586.

Martin A., Adam H., Diaz-Mendoza M., Zurczak M., Gonzalez-Schain N.D., and Suarez-Lopez P. (2009). Graft-transmissible induction of potato tuberization by the microRNA miR172. Development **136,** 2873-2881.

Maser P., Eckelman B., Vaidyanathan R., Horie T., Fairbairn D.J., Kubo M., Yamagami M., Yamaguchi K., Nishimura M., Uozumi N., Robertson W., Sussman M.R., and Schroeder J.I. (2002). Altered shoot/root Na(+) distribution and bifurcating salt sensitivity in Arabidopsis by genetic disruption of the Na(+) transporter AtHKT1. FEBS Lett. **531,** 157-161.

Mathieu J., Warthmann N., Kuttner F., and Schmid M. (2007). Export of FT protein from phloem companion cells is sufficient for floral induction in Arabidopsis. Curr. Biol. **17,** 1055-1060.

Matsushita N and Matoh T (1991). Characterization of Na(+) exclusion mechanisms of salt-tolerant reed plants in comparison with salt sensitive rice plants. Physiol. Plant. **83,** 170-176.

Mazel A., Leshem Y., Tiwari B.S., and Levine A. (2004). Induction of salt and osmotic stress tolerance by overexpression of an intracellular vesicle trafficking protein AtRab7 (AtRabG3e). Plant Physiol. **134,** 118-128.

Mengel K and Haeder HE (1977). Effect of potassium supply on the rate of phloem sap exudation and the composition of phloem sap of Ricinus communis. Plant Physiol. **59,** 282-284.

Minchin PEH and Thorpe MR (1987). Measurement of unloading and reloading of photo- assimilate within the stem of bean. J. Exp. Bot. **38,** 211-220.

Mira H., Martinez-Garcia F., and Penarrubia L. (2001). Evidence for the plant-specific intercellular transport of the Arabidopsis copper chaperone CCH. Plant J. **25,** 521-528.

Mlotshwa S., Voinnet O., Mette M.F., Matzke M., Vaucheret H., Ding S.W., Pruss G., and Vance V.B. (2002). RNA silencing and the mobile silencing signal. Plant Cell **14 Suppl,** S289-301.

Mukherjee S., Kallay L., Brett C.L., and Rao R. (2006). Mutational analysis of the intramembranous H10 loop of yeast Nhx1 reveals a critical role in ion homoeostasis and vesicle trafficking. Biochem. J. **398,** 97-105.

Munch E (1930). Die Stoffbewegungen in der Pflanze. Gustav Fischer, Jena.

Munns R, Tonnet L, Shennan C, and Gardner PA (1988). Effect of high external NaCl concentration on ion transport within the shoot of Lupinus albus. II. Ions in phloem sap. Plant Cell Environ. **11,** 291-300.

Munns R and Cramer GR (1996). Is coordination of leaf and root growth mediated by abscisic acid? (Opinion). Plant and Soil **185,** 33-49.

Munns R. (2002). Comparative physiology of salt and water stress. Plant. Cell. Environ. **25,** 239-250.

Munns R. (2005). Genes and salt tolerance: bringing them together. New Phytol. **167,** 645-663.

Munns R. and Tester M. (2008). Mechanisms of salinity tolerance. Annu. Rev. Plant. Biol. **59,** 651-681.

Neff M.M., Neff J.D., Chory J., and Pepper A.E. (1998). dCAPS, a simple technique for the genetic analysis of single nucleotide polymorphisms: experimental applications in Arabidopsis thaliana genetics. Plant J. **14,** 387-392.

Nerd A. and Neumann P. (2004). Phloem water transport maintains stem growth in a drought- stressed crop cactus (Hylocereus undatus). J. Am. Soc. Hortic. Sci. **129,** 486-490.

Öertli JJ (1968). Extracellular salt accumulation, a possible mechanism of salt injury in plants. **12,** 461-469.

Olias R., Eljakaoui Z., Li J., De Morales P.A., Marin-Manzano M.C., Pardo J.M., and Belver A. (2009). The plasma membrane Na(+)/H(+) antiporter SOS1 is essential for salt tolerance in tomato and affects the partitioning of Na+ between plant organs. Plant. Cell. Environ. **32,** 904-916.

Olias R., Eljakaoui Z., Pardo J.M., and Belver A. (2009). The Na(+)/H(+) exchanger SOS1 controls extrusion and distribution of Na(+) in tomato plants under salinity conditions. Plant. Signal. Behav. **4,** 973-976.

Oparka K.J., Roberts A.G., Boevink P., Santa Cruz S., Roberts I., Pradel K.S., Imlau A., Kotlizky G., Sauer N., and Epel B. (1999). Simple, but not branched, plasmodesmata allow the nonspecific trafficking of proteins in developing tobacco leaves. Cell **97,** 743-754.

Oparka K.J. and Turgeon R. (1999). Sieve elements and companion cells-traffic control centers of the phloem. Plant Cell **11,** 739-750.

Palauqui J.C., Elmayan T., Pollien J.M., and Vaucheret H. (1997). Systemic acquired silencing: transgene-specific post-transcriptional silencing is transmitted by grafting from silenced stocks to non-silenced scions. EMBO J. **16,** 4738-4745,.

Pardo J.M., Reddy M.P., Yang S., Maggio A., Huh G.H., Matsumoto T., Coca M.A., Paino-D'Urzo M., Koiwa H., Yun D.J., Watad A.A., Bressan R.A., and Hasegawa P.M. (1998). Stress signaling through Ca2+/calmodulin-dependent protein phosphatase calcineurin mediates salt adaptation in plants. Proc. Natl. Acad. Sci. U. S. A. **95,** 9681-9686.

Patrick JW (1990). Sieve element unloading: cellular pathway, mechanism and control. Physiol. Plant **78,** 298-308.

Peel AJ and Rogers S (1982). Stimulation of sugar loading into sieve elements of willow by potassium and sodium salts. Planta **154,** 94-96.

Perez-Alfocea F, Balibrea ME, Alarcon JJ, and Bolarin MC. (2000). Composition of xylem and phloem exudates in relation to the salt-tolerance of domestic and wild tomato species. J. Plant Physiol. **156,** 367-374.

Peuke A.D. (2010). Correlations in concentrations, xylem and phloem flows, and partitioning of elements and ions in intact plants. A summary and statistical re-evaluation of modelling experiments in Ricinus communis. J. Exp. Bot. **61,** 635-655.

Piao H.L., Lim J.H., Kim S.J., Cheong G.W., and Hwang I. (2001). Constitutive over-expression of AtGSK1 induces NaCl stress responses in the absence of NaCl stress and results in enhanced NaCl tolerance in Arabidopsis. Plant J. **27,** 305-314.

Pufahl R.A., Singer C.P., Peariso K.L., Lin S.J., Schmidt P.J., Fahrni C.J., Culotta V.C., Penner-Hahn J.E., and O'Halloran T.V. (1997). Metal ion chaperone function of the soluble Cu(I) receptor Atx1. Science **278,** 853-856.

Puig S., Mira H., Dorcey E., Sancenon V., Andres-Colas N., Garcia-Molina A., Burkhead J.L., Gogolin K.A., Abdel-Ghany S.E., Thiele D.J., Ecker J.R., Pilon M., and Penarrubia L. (2007). Higher plants possess two different types of ATX1-like copper chaperones. Biochem. Biophys. Res. Commun. **354,** 385-390.

Qi Z. and Spalding E.P. (2004). Protection of plasma membrane K+ transport by the salt overly sensitive1 Na+-H+ antiporter during salinity stress. Plant Physiol. **136,** 2548-2555.

Quaedvlieg N.E., Schlaman H.R., Admiraal P.C., Wijting S.E., Stougaard J., and Spaink H.P. (1998). Fusions between green fluorescent protein and beta-glucuronidase as sensitive and vital bifunctional reporters in plants. Plant Mol. Biol. **38,** 861-873.

Quan R., Lin H., Mendoza I., Zhang Y., Cao W., Yang Y., Shang M., Chen S., Pardo J.M., and Guo Y. (2007). SCABP8/CBL10, a putative calcium sensor, interacts with the protein kinase SOS2 to protect Arabidopsis shoots from salt stress. Plant Cell **19,** 1415-1431.

Quintero F.J., Blatt M.R., and Pardo J.M. (2000). Functional conservation between yeast and plant endosomal Na(+)/H(+) antiporters. FEBS Lett. **471,** 224-228.

Quintero F.J., Ohta M., Shi H., Zhu J.K., and Pardo J.M. (2002). Reconstitution in yeast of the Arabidopsis SOS signaling pathway for Na+ homeostasis. Proc. Natl. Acad. Sci. U. S. A. **99,** 9061-9066.

Ray F. Evert (2006). Phloem: Cell Types and Developmental Aspects In: Esau's Plant Anatomy. Meristems, Cells, and Tissues of the Plant

Body- their Structure, Function, and Development, 3rd ed. Hoboken, New Jersey: John Wiley & Sons, Inc. pp. 357-398.

Ren Z.H., Gao J.P., Li L.G., Cai X.L., Huang W., Chao D.Y., Zhu M.Z., Wang Z.Y., Luan S., and Lin H.X. (2005). A rice quantitative trait locus for salt tolerance encodes a sodium transporter. Nat. Genet. **37,** 1141-1146.

Rennie E.A. and Turgeon R. (2009). A comprehensive picture of phloem loading strategies. Proc. Natl. Acad. Sci. U. S. A. **106,** 14162-14167.

Rhoades M.W., Reinhart B.J., Lim L.P., Burge C.B., Bartel B., and Bartel D.P. (2002). Prediction of plant microRNA targets. Cell **110,** 513-520.

Riesmeier J.W., Willmitzer L., and Frommer W.B. (1994). Evidence for an essential role of the sucrose transporter in phloem loading and assimilate partitioning. EMBO J. **13,** 1-7.

Rodriguez-Rosales M.P., Jiang X., Galvez F.J., Aranda M.N., Cubero B., and Venema K. (2008). Overexpression of the tomato K(+)/H(+) antiporter LeNHX2 confers salt tolerance by improving potassium compartmentalization. New Phytol. **179,** 366-377.

Rubio F., Gassmann W., and Schroeder J.I. (1995). Sodium-driven potassium uptake by the plant potassium transporter HKT1 and mutations conferring salt tolerance. Science **270,** 1660-1663.

Ruiz-Medrano R., Xoconostle-Cazares B., and Lucas W.J. (1999). Phloem long-distance transport of CmNACP mRNA: implications for supracellular regulation in plants. Development **126,** 4405-4419.

Rus A., Lee B.H., Munoz-Mayor A., Sharkhuu A., Miura K., Zhu J.K., Bressan R.A., and Hasegawa P.M. (2004). AtHKT1 facilitates Na(+) homeostasis and K(+) nutrition in planta. Plant Physiol. **136,** 2500-2511.

Rus A., Baxter I., Muthukumar B., Gustin J., Lahner B., Yakubova E., and Salt D.E. (2006). Natural variants of AtHKT1 enhance Na+ accumulation in two wild populations of Arabidopsis. PLoS Genet. **2,** e210.

Santa Cruz S. (1999). Perspective: phloem transport of viruses and macromolecules - what goes in must come out. Trends Microbiol. **7,** 237-241.

Sasaki T., Chino M., Hayashi H., and Fujiwara T. (1998). Detection of several mRNA species in rice phloem sap. Plant Cell Physiol. **39,** 895-897.

Sauer N. (2007). Molecular physiology of higher plant sucrose transporters. FEBS Lett. **581,** 2309-2317.

Schneider I.R. (1965). Introduction, translocation, and distribution of viruses in plants. Adv. Virus Res. **11,** 163-221.

Scholthof H.B. (2005). Plant virus transport: motions of functional equivalence. Trends Plant Sci. **10,** 376-382.

Shabala L., Cuin T.A., Newman I.A., and Shabala S. (2005). Salinity-induced ion flux patterns from the excised roots of Arabidopsis sos mutants. Planta **222,** 1041-1050.

Shi H., Ishitani M., Kim C., and Zhu J.K. (2000). The Arabidopsis thaliana salt tolerance gene SOS1 encodes a putative Na+/H+ antiporter. Proc. Natl. Acad. Sci. U. S. A. **97,** 6896-6901.

Shi H., Quintero F.J., Pardo J.M., and Zhu J.K. (2002). The putative plasma membrane Na(+)/H(+) antiporter SOS1 controls long-distance Na(+) transport in plants. Plant Cell **14,** 465-477.

Slewinski T.L., Meeley R., and Braun D.M. (2009). Sucrose transporter1 functions in phloem loading in maize leaves. J. Exp. Bot. **60,** 881-892.

Smith A.M. and Zeeman S.C. (2006). Quantification of starch in plant tissues. Nat. Protoc. **1,** 1342-1345.

Srivastava A.C., Ganesan S., Ismail I.O., and Ayre B.G. (2008). Functional characterization of the Arabidopsis AtSUC2 Sucrose/H(+) symporter by tissue-specific complementation reveals an essential role in phloem loading but not in long-distance transport. Plant Physiol. **148,** 200-211.

Stadler R and Sauer N (1996). The Arabidopsis thaliana AtSUC2 gene is specifically expressed in companion cells. Bot. Acta. **109,** 299-306.

Stadler R., Brandner J., Schulz A., Gahrtz M., and Sauer N. (1995). Phloem Loading by the PmSUC2 Sucrose Carrier from Plantago major Occurs into Companion Cells. Plant Cell **7,** 1545-1554.

Stadler R., Wright K.M., Lauterbach C., Amon G., Gahrtz M., Feuerstein A., Oparka K.J., and Sauer N. (2005). Expression of

GFP-fusions in Arabidopsis companion cells reveals non-specific protein trafficking into sieve elements and identifies a novel post-phloem domain in roots. Plant J. **41,** 319-331.

Sunarpi, Horie T., Motoda J., Kubo M., Yang H., Yoda K., Horie R., Chan W.Y., Leung H.Y., Hattori K., Konomi M., Osumi M., Yamagami M., Schroeder J.I., and Uozumi N. (2005). Enhanced salt tolerance mediated by AtHKT1 transporter-induced Na unloading from xylem vessels to xylem parenchyma cells. Plant J. **44,** 928-938.

Suzuki N., Yamaguchi Y., Koizumi N., and Sano H. (2002). Functional characterization of a heavy metal binding protein CdI19 from Arabidopsis. Plant J. **32,** 165-173.

Tamaki S., Matsuo S., Wong H.L., Yokoi S., and Shimamoto K. (2007). Hd3a protein is a mobile flowering signal in rice. Science **316,** 1033-1036.

Tena G., Asai T., Chiu W.L., and Sheen J. (2001). Plant mitogen-activated protein kinase signaling cascades. Curr. Opin. Plant Biol. **4,** 392-400.

Tester M. and Davenport R. (2003). Na(+) tolerance and Na(+) transport in higher plants. Ann. Bot. **91,** 503-527.

Turgeon R (1991). Symplastic phloem loading and the sink- source transition in leaves: A model. In: Recent Advances in Phloem Transport and Assimilate Compartmentation. In , Ouest ed. , Bonnemain JL, Delrot S, Lucas WJ and Dainty J, eds (Nantes, France) pp. 18-22.

Turgeon R, Beebe DU, and Gowan E (1993). The intermediary cell: Minor- vein anatomy and raffinose oligosaccharide synthesis in Scrophulariaceae. **191,** 446-456.

Turgeon R. and Medville R. (1998). The absence of phloem loading in willow leaves. Proc. Natl. Acad. Sci. U. S. A. **95,** 12055-12060.

Tyerman SD and Skerrett M (1999). Root ion channels and salinity. Sci. Hort. **78,** 175-235.

Ueki S. and Citovsky V. (2001). Inhibition of systemic onset of post-transcriptional gene silencing by non-toxic concentrations of cadmium. Plant J. **28,** 283-291.

Ueki S. and Citovsky V. (2002). The systemic movement of a tobamovirus is inhibited by a cadmium-ion-induced glycine-rich protein. Nat. Cell Biol. **4,** 478-486.

Urquhart A.A. and Joy K.W. (1981). Use of Phloem exudate technique in the study of amino Acid transport in pea plants. Plant Physiol. **68,** 750-754.

van Bel AJE (1993). The transport phloem. Specifics of its functioning. Prog. Bot. **54,** 134-150.

Van Bel AJE and Van Rijen HVM (1994). Microelectrode- recorded development of the symplasmic autonomy of the sieve element/ companion cell complex in the stem phloem of Lupinus lutenus L. Planta **192,** 165-175.

Venema K., Belver A., Marin-Manzano M.C., Rodriguez-Rosales M.P., and Donaire J.P. (2003). A novel intracellular K(+)/H(+) antiporter related to Na(+)/H(+) antiporters is important for K(+) ion homeostasis in plants. J. Biol. Chem. **278,** 22453-22459.

Viola R., Roberts A.G., Haupt S., Gazzani S., Hancock R.D., Marmiroli N., Machray G.C., and Oparka K.J. (2001). Tuberization in potato involves a switch from apoplastic to symplastic phloem unloading. Plant Cell **13,** 385-398.

Voinnet O. and Baulcombe D.C. (1997). Systemic signalling in gene silencing. Nature **389,** 553.

Vreugdenhil D (1985). Source-to-sink gradient of potassium in the phloem. Planta **163,** 238-240.

Vreugdenhil E., Geraerts W.P., Jackson J.F., and Joosse J. (1985). The molecular basis of the neuro-endocrine control of egg-laying behaviour in Lymnaea. Peptides **6 Suppl 3,** 465-470.

Walz C., Juenger M., Schad M., and Kehr J. (2002). Evidence for the presence and activity of a complete antioxidant defence system in mature sieve tubes. Plant J. **31,** 189-197.

Walz C., Giavalisco P., Schad M., Juenger M., Klose J., and Kehr J. (2004). Proteomics of curcurbit phloem exudate reveals a network of defence proteins. Phytochemistry **65,** 1795-1804.

Walz C., Giavalisco P., Schad M., Juenger M., Klose J., and Kehr J. (2004). Proteomics of curcurbit phloem exudate reveals a network of defence proteins. Phytochemistry **65,** 1795-1804.

Weigel D and Glazebrook J (2002). In Arabidopsis: A Laboratory manual. Cold Spring Harbor, NY: Cold Spring Harbor Laboratory Press. .

Wimmers L.E., Ewing N.N., and Bennett A.B. (1992). Higher plant Ca(2+)-ATPase: primary structure and regulation of mRNA abundance by salt. Proc. Natl. Acad. Sci. U. S. A. **89,** 9205-9209.

Wolf S., Deom C.M., Beachy R.N., and Lucas W.J. (1989). Movement protein of tobacco mosaic virus modifies plasmodesmatal size exclusion limit. Science **246,** 377-379.

Wu S.J., Ding L., and Zhu J.K. (1996). SOS1, a Genetic Locus Essential for Salt Tolerance and Potassium Acquisition. Plant Cell **8,** 617-627.

Xoconostle-Cazares B., Xiang Y., Ruiz-Medrano R., Wang H.L., Monzer J., Yoo B.C., McFarland K.C., Franceschi V.R., and Lucas W.J. (1999). Plant paralog to viral movement protein that potentiates transport of mRNA into the phloem. Science **283,** 94-98.

Xoconostle-Cazares B., Ruiz-Medrano R., and Lucas W.J. (2000). Proteolytic processing of CmPP36, a protein from the cytochrome b(5) reductase family, is required for entry into the phloem translocation pathway. Plant J. **24,** 735-747.

Yokoi S., Quintero F.J., Cubero B., Ruiz M.T., Bressan R.A., Hasegawa P.M., and Pardo J.M. (2002). Differential expression and function of Arabidopsis thaliana NHX Na(+)/H(+) antiporters in the salt stress response. Plant J. **30,** 529-539.

Yoo B.C., Kragler F., Varkonyi-Gasic E., Haywood V., Archer-Evans S., Lee Y.M., Lough T.J., and Lucas W.J. (2004). A systemic small RNA signaling system in plants. Plant Cell **16,** 1979-2000.

Young JH, Evert RF, and Eschrich W (1973). On the volume- flow mechanism of phloem transport. Planta **113,** 355-366.

Zhang C., Barthelson R.A., Lambert G.M., and Galbraith D.W. (2008). Global characterization of cell-specific gene expression through fluorescence-activated sorting of nuclei. Plant Physiol. **147,** 30-40.

Zhang G.H., Su Q., An L.J., and Wu S. (2008). Characterization and expression of a vacuolar Na(+)/H(+) antiporter gene from the monocot halophyte Aeluropus littoralis. Plant Physiol. Biochem. **46,** 117-126.

Zhang H.X. and Blumwald E. (2001). Transgenic salt-tolerant tomato plants accumulate salt in foliage but not in fruit. Nat. Biotechnol. **19,** 765-768.

Zhang H.X., Hodson J.N., Williams J.P., and Blumwald E. (2001). Engineering salt-tolerant Brassica plants: characterization of yield and seed oil quality in transgenic plants with increased vacuolar sodium accumulation. Proc. Natl. Acad. Sci. U. S. A. **98,** 12832-12836.

Zhang X.Y., Wang X.L., Wang X.F., Xia G.H., Pan Q.H., Fan R.C., Wu F.Q., Yu X.C., and Zhang D.P. (2006). A shift of Phloem unloading from symplasmic to apoplasmic pathway is involved in developmental onset of ripening in grape berry. Plant Physiol. **142,** 220-232.

Zhu J.K., Liu J., and Xiong L. (1998). Genetic analysis of salt tolerance in arabidopsis. Evidence for a critical role of potassium nutrition. Plant Cell **10,** 1181-1191.

Zhu Y., Green L., Woo Y.M., Owens R., and Ding B. (2001). Cellular basis of potato spindle tuber viroid systemic movement. Virology **279,** 69-77.

Zhu Y., Green L., Woo Y.M., Owens R., and Ding B. (2001). Cellular basis of potato spindle tuber viroid systemic movement. Virology **279,** 69-77.

Zhu Y., Qi Y., Xun Y., Owens R., and Ding B. (2002). Movement of potato spindle tuber viroid reveals regulatory points of phloem-mediated RNA traffic. Plant Physiol. **130,** 138-146.

Zhu Y., Qi Y., Xun Y., Owens R., and Ding B. (2002). Movement of potato spindle tuber viroid reveals regulatory points of phloem-mediated RNA traffic. Plant Physiol. **130,** 138-146.

Zörb C, Noll A, Karl S, Leib K, Yan F, and Schubert S (2004). Molecular characterization of Na+/H+ antiporters (ZmNHX) of maize (Zea mays L.) and their expression under salt stress. J Plant Physiol. **162,** 55-66.

5. APPENDICES

Appendix 1: Effect of *nakr1-1* mutation on carbohydrate and mineral nutrients accumulation in the major sinks- roots and seeds

Phloem is involved in the long- distance transport of carbohydrates and mineral elements from the source and sinks along the osmotic pressure gradient. A gene expressed specifically in the phloem tissue, *nakr1-1* mutation led to the accumulation of starch and K^+/Na^+ in the source leaves and a significant small root phenotype. Qualitative starch accumulation in the inflorescence and developing siliques together with mineral element concentration in roots and seeds were studied to investigate the impact of *nakr1-1* mutation in the development of the major sinks: the roots and seeds.

RESULTS

A survey of starch accumulation in various tissues of Arabidopsis plants has revealed the difference in starch metabolism between photosynthetic and nonphotosynthetic tissues, however similar starch degradation mechanism is used in both photosynthetic and nonphotosynthetic tissues (Caspar et al., 1991). Study of the *nakr1-1* mutant revealed starch overaccumulates in the source leaves, and *nakr1-1* leaves are less efficient in degrading all the leaf starch, even after 88h of continuous darkness. It was of interest to study the effect of the *nakr1-1* mutation on starch metabolism in the tissues other than leaves. Qualitative starch accumulation in the floral tissue and developing siliques were performed in Col-0 wild type and *nakr1-1* mutant. In Col-0 wild type plants, the starch accumulation is most abundant in the developing seeds, and staining was largely reduced in the inflorescence and the maternal tissue of siliques (Fig. Ap.1A-B). Different starch accumulation patterns were detected in *nakr1-1* mutant, with strong iodine staining in the maternal tissues including the inflorescence stem, the sepal and the silique epidermis (Fig. 1C-

D). Starch accumulation in immature seeds however was greatly reduced when compared to Col-0 seeds at similar developmental stages (Fig. Ap. 1D).

To study the effect of *nakr1-1* mutation on mineral nutrients allocation from the source to sinks, elemental analysis was performed in seeds and root samples from Col-0 and the *nakr1-1* mutant. For seed elemental analyses Col-0 and *nakr1-1* plants were grown the same short day conditions. The smallest difference in bolting time has been found under this growth conditions between Col-0 and *nakr1-1* plants. Significant difference has been detected between Col-0 and *nakr1-1* seeds in the accumulation of multiple elements (Fig. Ap. 2A). Compared with Col-0 seeds, *nakr1-1* seeds exhibit reduced levels of K, Mg, Mn and B, and increased accumulation of Fe, Zn, S, Rb, Mo, etc.. The concentrations of K, Mg and Ca in Col-0 and nakr1-1 seeds were indicated in Fig. Ap. 2B-D.

Plants were grown in hydroponic culture to facilitate the sampling of root tissues. Col-0 and *nakr1-1* plants and two individual complementation lines NO. 8 and NO.13 were grown under short day conditions for two months and leaf and root tissues were collected for ICP-MS analysis. As shown in Ap. Fig. 3, *nakr1-1* mutant leaves accumulate higher K^+, Rb^+ than Col-0 in the leaf tissues. This phenotype was recovered in the two complementation lines (Fig. Ap. 3B-C). Similar results were obtained for plants grown in both soil and the Turface, where higher $Na^+/K^+/Rb^+$ accumulation in *nakr1-1* leaves had been detected.

Figure Ap.4 shows K^+ (Fig. Ap. 4A) and Rb^+ (Fig. Ap.4B) concentrations of root samples from Col-0, *nakr1-1*, and complementation lines 8 and 13. Similar to the increased K^+/Rb^+ accumulation detected in *nakr1-1* leaf tissue, higher K^+/Rb^+ levels was detected in *nakr1-1* roots by ICP-MS analysis. These high K^+/Rb^+ phenotypes were also complemented by the *NaKR1* whole gene construct.

METHODS

Starch accumulation in inflorescence and developing siliques were tested using I_2/KI staining. For seed ionome analysis, plants were grown under short day conditions (8h/16h; 50-75 µmol m^{-2} s^{-1}) in BM-2 soil, plants were watered once every week from the bottom of the tray using DI- H_2O, and fertilizered (All Purpose Plant Food, Vigoro) twice during their growth period. Clean seeds were collected for ICP-MS analysis. The results of seeds elemental analysis are from 5 Col-0 and 5 *nakr1-1* plants. Leaf and root elemental analysis was performed from plants grown under hydroponic growth conditions. Hydroponic culture was set up using the method described by Norén et al., (2004) except the nutrient solution was prepared using 0.1x Hoagland supplemented with 4.15mg/L (4.5 µM) sodium ferric EDDHA. Plants were grown in hydroponic culture for 2 months before leaves and roots were harvested for ICP-MS analysis. Nutrient solution was replenished every two weeks. 50mM of NaCl were applied to the nutrient solution within the last two weeks of plant growth. Root and leaf samples were collected by rinsing in ice cold DI H_2O containing 0.1% Triton X-100 followed by 3 times of rinse in ice cold DI H_2O. The samples were put in 13ml plastic tubes (SARSTEDT) and dried at 120°C overnight before subjected to ICP-MS analysis.

DISCUSSION

As the major transitory storage form of carbon, starch has been detected in photosynthetic tissue including leaves, stem and immature seeds. In *Brassica napus*, it is found that starch initially accumulates in developing seeds and degraded at seeds maturation when lipids and proteins are synthesized (Norton and Harris, 1975). Mutation affecting starch degradation led to increased starch accumulation in leaves, roots, flowers and seeds, and the dynamic changes of starch content during photoperiod could not be detected ((Caspar et al., 1991). *nakr1-1* mutant still exhibits diurnal changes of starch content in rosette leaves. The reduced starch accumulation in developing seeds of *nakr1-1* mutant combined with increased starch accumulation in *nakr1-1* leaves, stems and the

sepals suggest the compromised ability of *nakr1-1* mutant in carbohydrate allocation from the source to the sinks, rather than the decreased ability of the mutant in starch degradation. The reduced carbon accumulation in the major sinks might be the result of reduced sucrose loading from the source leaves or the uncontrolled sucrose leakage along the transport phloem. Reduced sucrose loading/long- distance transport in *nakr1-1* mutant is supported by the result of ^{14}C- sucrose loading experiment. Both sucrose loading and recruitment along the transport phloem are mediated by phloem specific sucrose/ H^+ symporter (AtSUC2). Previous research on phloem specific K^+ channel AKT2/3 revealed AKT2/3 mediated K^+ transport along the SE plasma membrane is responsible for stabilize the negative membrane potential of the SE cells and thus helps to maintain the activity of sucrose transporter (Deeken et al., 2002). Whether the affect of *NaKR1* mutation on long- distance sucrose transport is through directly or indirectly affecting the plasma membrane potential still requires further research.

Another possible explanation for reduced carbon accumulation in the major sink tissue is the deficiency of *nakr1-1* in sucrose unloading. This is supported by reciprocal grafting experiment between Col-0 and *nakr1-1* plants. Col-0 roots grafted to *nakr1-1* shoot still grow normally however *nakr1-1* roots grafted to Col-0 shoot exhibit root growth defects. These results indicate unloading process plays important roles in root development. The exact mechanism of unloading process remains unknown. It's currently believed except for few species and development stages, the unloading is symplastic thus energy free process (Oparka, 1990). The post- phloem transport process however is against sucrose gradient and an energy dependent process. The fact that *nakr1-1* embryos exhibit normal cell pattern, and *nakr1-1* seeds germinate normally and grow normally at early seedling stages however suggests the seed development process and post-phloem transport of nutrients into developing seeds are largely unaffected by *nakr1-1* mutation.

Previous research on the long- distance movement of mineral elements within plants revealed the different mobility of K^+, Mg^{2+} and Ca^{2+} between organs (Karley and White, 2009). K^+ and Mg^{2+} are mobile through both the xylem sap and the phloem translocation stream. There is however very little movement of Ca^{2+} from leaves to the phloem- fed tissues. This provides explanation for the accumulation patterns of K^+, Mg^{2+} and Ca^{2+} ions in *nakr1-1* seeds. The reduced accumulation of K^+ and Mg^{2+} in *nakr1-1* seeds when compared with Col-0 seeds is possibly due to the compromised phloem translocation activity of *nakr1-1* mutants. Ca^{2+} accumulation remains unchanged in *nakr1-1* seeds, possibly due to the very limited Ca^{2+} transport via the phloem translocation stream. Compared with the long- distance transport of K^+ and Mg^{2+}, recirculation of heavy metals involves more complicated mechanisms. The ions of Fe, Mn and Zn are highly active species and their redox changes favor the generation of highly reactive oxygen species. Their transport within the phloem involves bound to organic ligands or proteins to mask their electric charges (Krüger et al., 2002). Nicotianamine (NA) is one of the Fe chelators in plants (Bashir et al., 2006). The metal- NA complexes are transported by *yellow stripe 1- like* (YSL) family transport proteins. OsYSL2 in rice is specifically responsible for the long- distance transport of Fe(II)- NA and Mn(II)- NA complex through the phloem into the grain. The RNAi lines of *OsYSL2* exhibit decreased Fe and Mn concentrations in both the shoot and the seeds. Interestingly the constitutive *OsYSL2* overexpression lines exhibited reduced Fe accumulation in both the shoot and seeds, however increased Mn accumulation in seeds (Ishimaru et al., 2010). The elemental analysis of *nakr1-1* seeds revealed reduced Mn accumulation however increased Cu, Fe Zn and Rb in the seeds compared to that of the Col-0 seeds. Whether the increased accumulation of heavy metals (Cu, Fe and Zn) reflects the result of phloem-independent transport processes that are upregulated due to the phloem transport defect remains to be elucidated.

As a highly mobile element, K accumulation in the root is the result of several distinct processes. Although variation has been detected among species, when grown under K^+-sufficient conditions around 120% of K^+ taken up from the external environment is transported through the xylem to the shoot and about half of K^+ transported in the xylem is recycled in the phloem. Accordingly about 40% K^+ taken up from the outside environment is incorporated into the roots (Peuke, 2010; Karley and White, 2009). In K^+ deficient plants less K^+ is returned to the root, and the compensatory K^+ uptake from external environment is increased, possibly due to the upregulation of high affinity K^+ transporters (White, 1997). A hypothesis that has existed for many years is the K^+ transport systems in root is regulated by the demand of shoot, possibly through the amount of K^+ recycling in the phloem that serves as a negative feedback signal (Drew and Saker, 1984). In *nakr1-1* mutant the increased K^+ accumulation in the source leaves and reduced K^+ accumulation in seeds suggests reduced K^+ transport through the phloem. This is also supported by the reduced long- distance sucrose transport, since both sucrose and K^+ translocation through the phloem are driven by the same osmotic pressure gradient. The reduced phloem- mediated K^+ recirculation further activates K^+ transport into *nakr1-1* roots. The increased accumulation of K^+/Rb^+ in *nakr1-1* roots therefore might be the result of the enhanced K^+/Rb^+ uptake that combined with the reduced xylem transport of K^+/Rb^+ from root to shoot outcompete the decreased K^+/Rb^+ unloading at the root stele because of phloem function defect.

Ap. Fig. 1. *nakr1-1* mutation led to starch accumulation in the maternal tissues. (A). I_2/KI staining of Col-0 floral tissues. (B). I_2/KI staining of Col-0 siliques. Starch was mainly accumulated in the developing seeds. (C). I_2/KI staining of the floral tissues of *nakr1-1* mutant. Strong starch staining was detected in the sepal and inflorescence stem. (**D**). I_2/KI staining of *nakr1-1* siliques. Starch was accumulated in the maternal tissues more than the developing seeds.

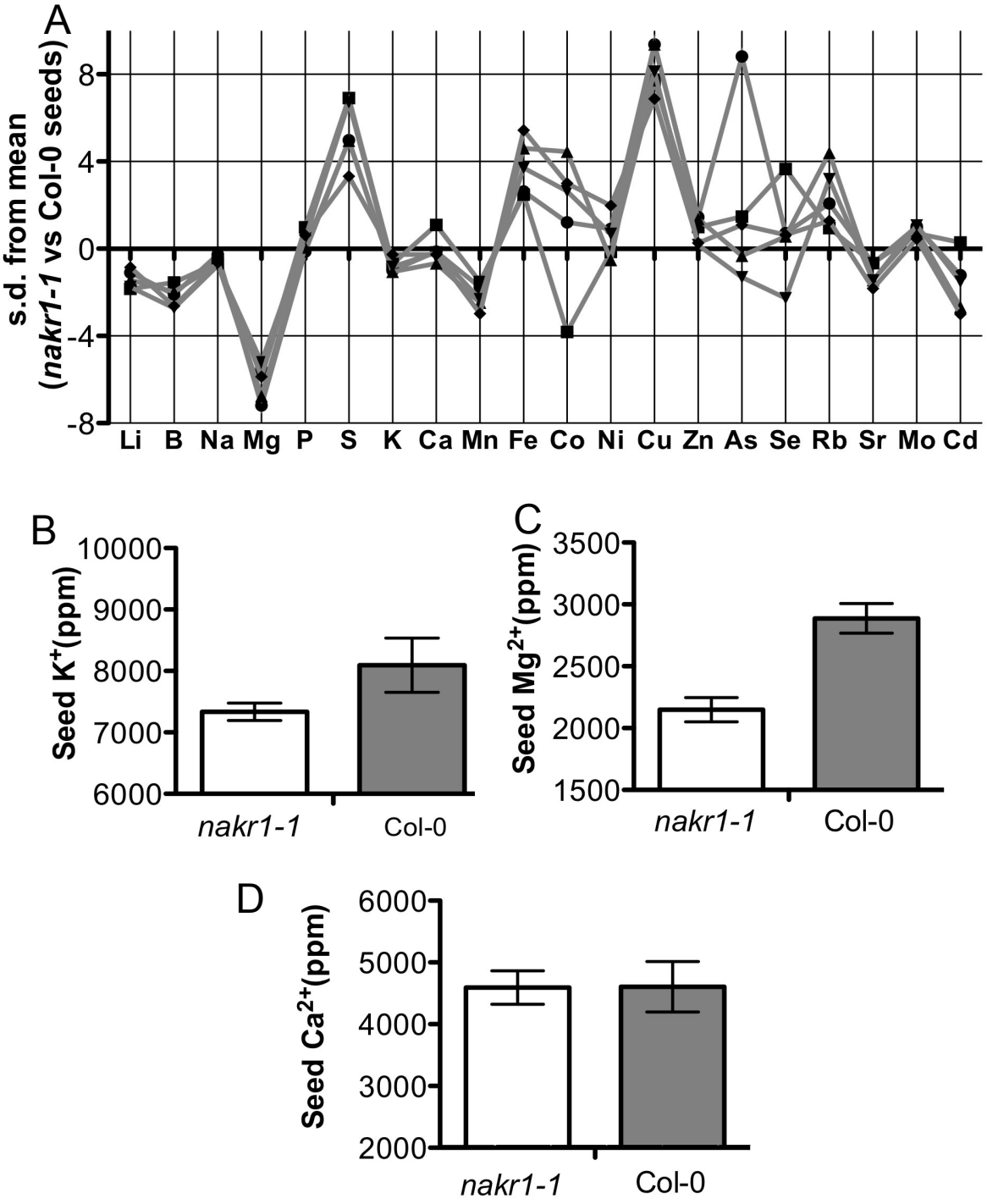

Ap. Fig. 2. *nakr1-1* mutation led to alteration in the accumulation of multiple mineral elements in arabidopsis seeds. A**.** Difference in the accumulation of mineral elements in *nakr1-1* seeds *vs.* Col-0 seeds is expressed as z- values (times of standard deviation), with each single line represent a single mutant plant, and the zero line represents the average for Col-0 seeds population. B. K^+ concentrations (ppm) of *nakr1-1* and Col-0 seeds. Error bars represent mean ± SE. C. Mg^{2+} concentrations (ppm) in *nakr1-1* and Col-0 seeds. Error bars represent mean ± SD. D. Ca^{2+} concentrations in *nakr1-1* and Col-0 seeds. Error bars represent

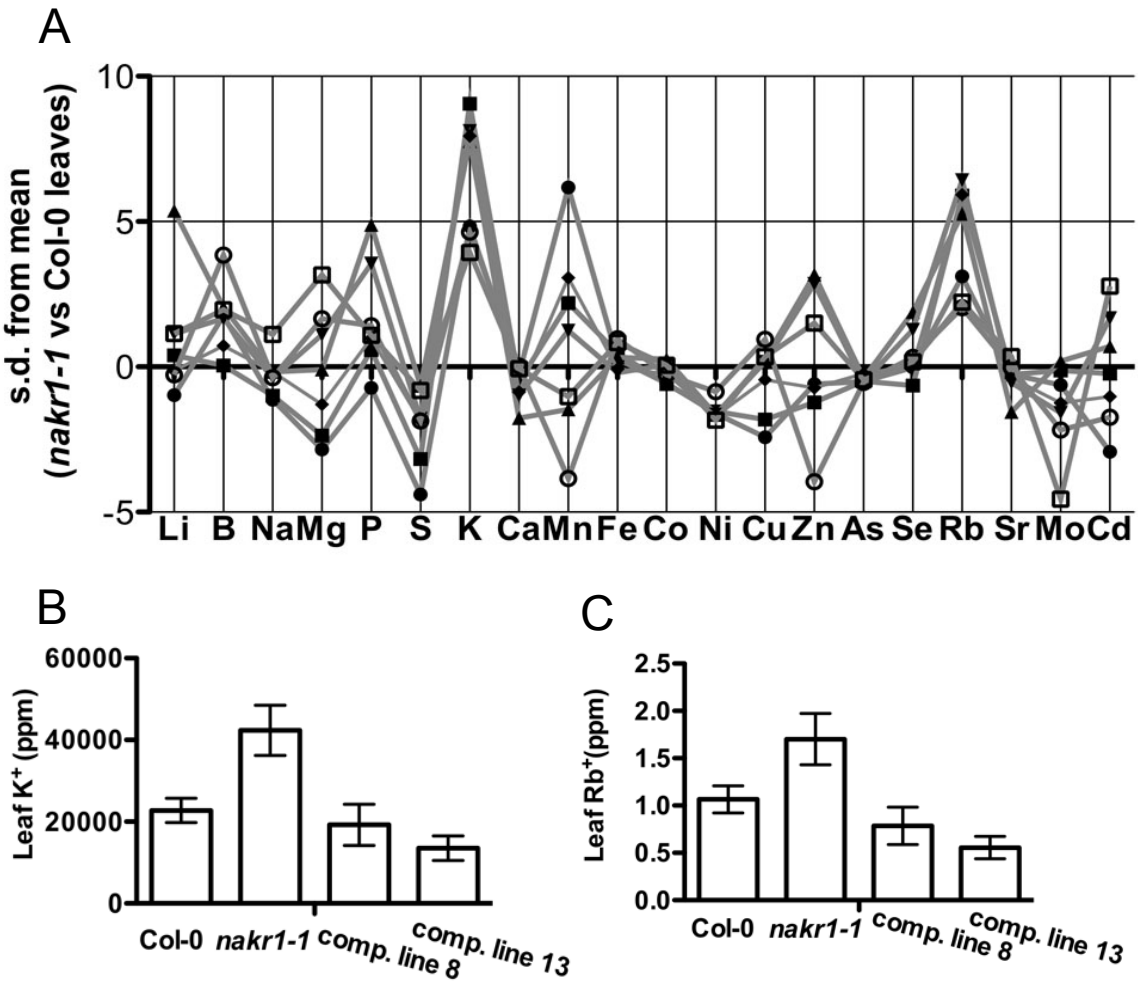

Ap. Fig. 3. Under hydroponic growth conditions *nakr1-1* plants accumulate higher K^+ and Rb^+ than Col-0 plants in the leaf tissue. This phenotype was complemented by introducing *NaKR1* whole gene construct into the mutant background. A**.** Difference between *nakr1-1* and Col-0 leaves in elemental contents was expressed as z- values (times of standard deviation). The zero line represents the average of Col-0 population. B**.** Leaf K^+ concentrations (ppm) in Col-0, *nakr1-1*, complementation line 8 and complementation line 13 plants. The error bars represent mean ± SD. C. Leaf Rb^+ concentrations (ppm) in Col-0, *nakr1-1*, complementation line 8 and complementation line 13 plants. The error bars represent mean ± SD. n= 7 for *nakr1-1*, n=6 for Col-0 and complementation line 13, and n=4 for complementation line 8.

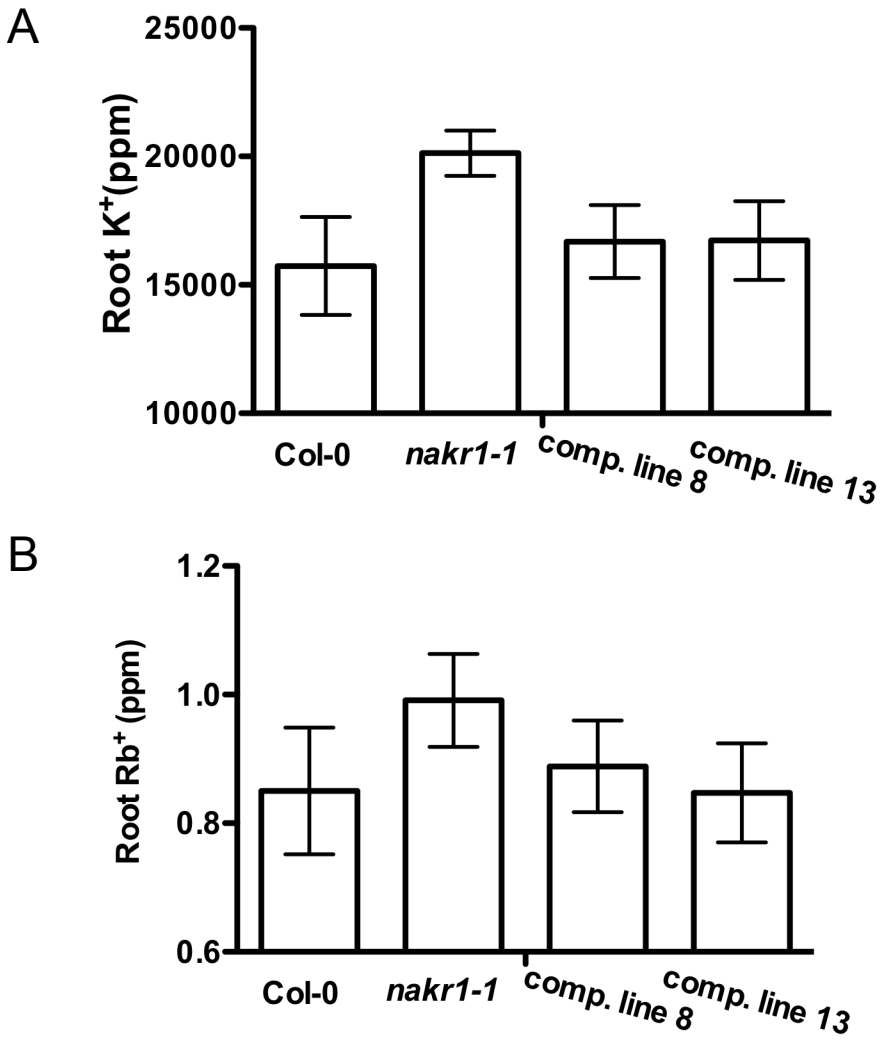

Ap. Fig. 4. *nakr1-1* plants accumulate higher K^+/Rb^+ in the root than Col-0 plants and complementation lines NO. 8 and NO. 13. A. Root K^+ concentrations (ppm) in Col-0, *nakr1-1*, and complementation line 8 and 13. The error bars represent mean ± SE. B**.** Root Rb^+ concentrations (ppm) in Col-0, *nakr1-1*, and complementation line 8 and 13. The error bars represent mean ± SE . n=6 for Col-0, *nakr1-1* and complementation line 13; n=4 for complementation line 8.

Appendix 2. Identifying a Na^+ accumulation mutant 103:06 by map based cloning.

103:06 is a fast neutron induced mutant originally isolated by Lahner et al., (2003) by using elemental profiling to screen the leaf tissue of an Arabidopsis population. Compared with Col-0 control plants, 103:06 exhibited the specific phenotype of elevated Na^+ accumulation in the shoot. 103:06 has been crossed to both Col-0 and Ler-0 and shoot Na^+ concentrations were measured in the F1 hybrid plants. In both cases the Na^+ concentrations in F1 plants were higher than the wild type control plants, suggesting the mutation that causes higher Na^+ accumulation is dominant. Interestingly, a continuous Na accumulation pattern was detected within the F2 population, with 75% of the plants showing increased Na^+ accumulation in the shoot (Ap. Fig. 5). Therefore it's concluded 103:06 is a semidominant mutant caused by a single gene mutation.

For 103:06 mutation mapping, a 103:06 x Ler F2 populaiton of around 900 plants was grown in the soil and elemental profiling was performed in rosette leaves of each plant. The elemental profiling data for the population can be obtained at the open access Purdue Ionomics Information Management System (PiiMs) at http://www.purdue.edu/dp/ionomics (tray NO. 1197- 1206). Result from the tray 1198 is shown in Figure Ap. Fig. 6. Two groups of plants were selected to create the mapping population. Plants with shoot Na^+ levels similar to Col-0 WT plants grown in the same tray were selected as the putative wild type segregation lines. The plants with the highest Na^+ levels in the F2 population were also selected as the putative homozygous mutant. With this method a mapping population of around 200 plants was created. Map based cloning revealed that the 103:06 mutant locus is within the region of 220kb-550kb at the top of chromosome 1. There are 128 genes within this region. Genetic markers that were used for 103:06 mutation mapping are shown in Ap. Table 1.

Several high Na^+ lines were selected to further test their genotype and shoot Na^+ accumulation. Seeds were collected from these lines and leaf elemental profiling performed on their selfed progeny. Results for the line 1198-15 are shown in Ap. Fig. 7. The homogenous high Na^+ accumulation pattern of the progeny indicated that 1198-15 is a homozygous mutant. Detailed genotyping of this line revealed the homozygous Col-0 genotype at the top of chromosome 1 (0- 3,600 kb).

Under normal growth conditions, 103:06 mutants grow similarly as wild type Col-0 plants. To test if elevated shoot Na accumulation render the plants more sensitive to NaCl stress, Col-0 and 103:06 homozygous line were germinated and grown in ATS medium with 50mM NaCl. The growth of control plants was relatively unaffected by this level of NaCl stress, however the 103:06 plants show significant growth phenotypes including shorter petiole, smaller and curled leaves and anthocyanin accumulation (Ap. Fig. 8). The F2 population of both 103:06 backcross and outcross to Col-0 exhibited a 1:3 segregation ratio the occurrence of the growth phenotypes, indicating 103:06 mutation is recessive in regarding to the mutant sensitivity to NaCl.

To test the possibility of using the NaCl sensitive phenotype for the 103:06 mutation mapping, line 1198-15 was crossed to Ler-0 and the F2 seeds were germinated on the medium containing 50 mM NaCl. A mapping population of 400 plants was created based on the NaCl sensitivity phenotypes. Map based cloning defined the mutation to the same region as have been described above by using the population created based on Na^+ levels in shoot.

My work on 103:06 mutant mapping led to two results. 103:06 is a semidominant mutant in causing accumulating Na^+ in the shoot tissue, with the heterozygous plants accumulating shoot Na^+ in between of the homozygous and the wild type plants. Previous work on selecting 103:06 mutant had hard time identifying homozygous 103:06 mutant, for the selected mutants were

always segregating in shoot Na^+ levels. By selecting plants with highest Na^+ accumulation in the shoot from the F2 population and by testing the shoot Na^+ accumulation pattern in their progeny the homozygous 103:06 mutants were isolated. The 103:06 homozygous mutant is sensitive to elevated NaCl as a result of Na^+ overaccumulation in the shoot. Interestingly, although heterozygous 103:06 plants also accumulate more Na^+ than the wild type control plants in the shoot they were not hypersensitive to NaCl stress. The result suggests 103:06 might be a recessive, loss of function mutation, and the wild type allele acts quantitatively to control Na accumulation in the shoot.

By using ICP-MS analysis to analyze rosette leaves of 106:06 x Ler-0 F2 population, a mapping population of 200 plants was created and the mutation mapped to a region of 230kb at the top of chromosome 1. To further identify the mutation a larger mapping population is required. The growth phenotypes of 103:06 mutant at elevated NaCl provides an efficient way of selecting homozygous mutants from the F2 population. When grown at 50mM NaCl the homozygous mutant could be easily discriminated from the heterozygous and wild type segregation lines. Moreover selecting mutants from the agar medium is inexpensive and less time- consuming than ICP-MS based elemental profiling of the F2 population; therefore creating a large mapping population becomes possible. In spite of the fact that 103:06 mutants are hypersensitive to NaCl stress, when transplanted to soil most plants recovered growth and set seeds normally. Therefore F3 progeny is available to confirm the genotype and growth phenotypes of the individual F2 plants.

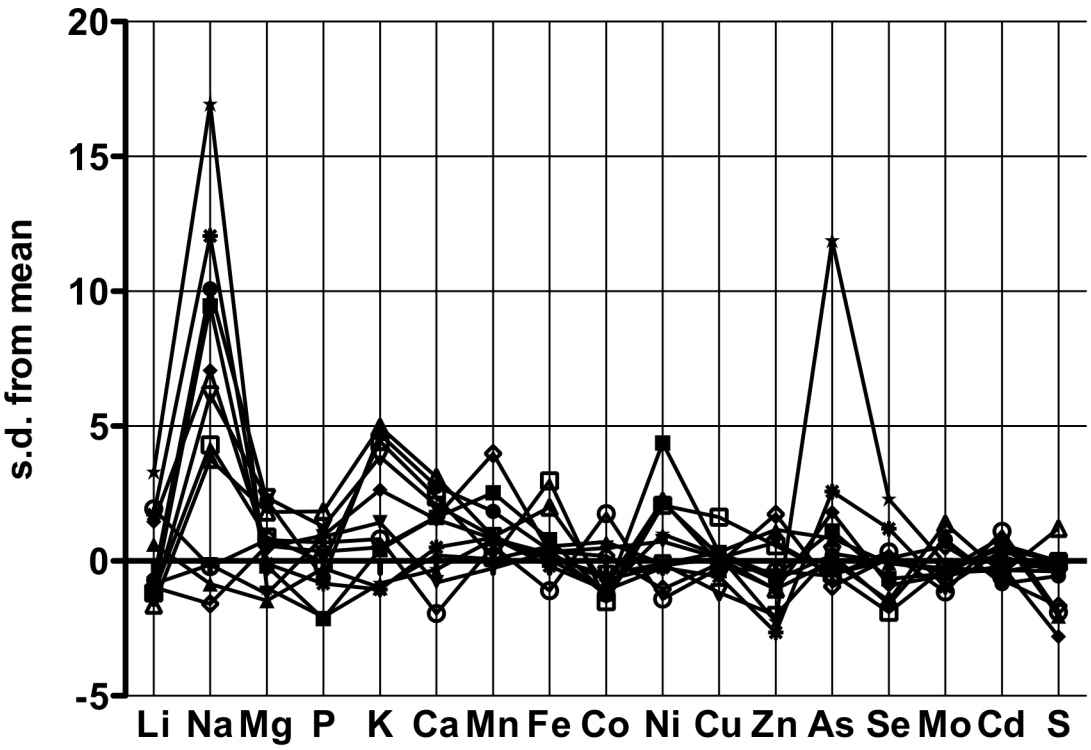

Ap. Fig.5. 103:06 is a semidominant mutant that overaccumulates Na^+ in the shoot tissue. Plants were grown under conditions described by Lahner et al., (2003). Difference between the 10306 heterozygous progeny (12 individual plants) and Col-0 plants in shoot Na^+ contents was plotted as z- values (standard deviations). The 103:06 segregating populaton exhibited a continuous pattern of Na^+ accumulation in leaves.

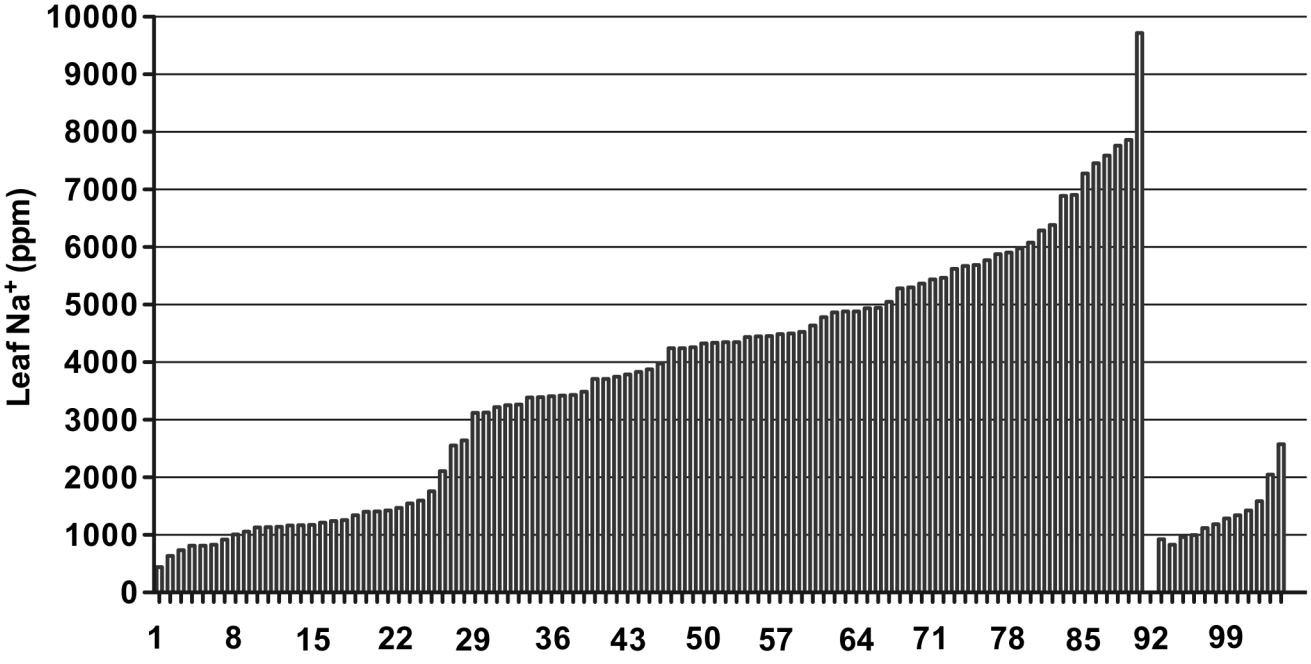

Ap. Fig. 6. Leaf Na^+ accumulation patterns of the F_2 population (line NO. 1-91) of 103:06 crossed to Ler-0, and Col-0 wild type plants (line NO. 92-103) grown on the same tray (tray NO. 1198. The original data is available on Piims website). Line 1-25 and 74-91 were selected from this segregation population for 103:06 mapping.

Appendix Table 1. Genetic markers used for 103:06 mutation mapping. Their primer sequences, relative positons in chromosome 1 and marker types were indicated.

Marker name	F Primer Sequence:	R Primer Sequence:	Position	Marker type
§HT/T25K16 F1/R1	tcgttcccggaaataatcaa	tgtggctgagattgcttctg	0 kb	Indel
HT/F22L4 F4/R4	tggtttacatgttcccgatg	ccgtcagttgctgctgattc	214 kb	For Sequencing
HT/T1N6 F2/R2	ccggaaacgaagaatccata	caagctcttcatcggtaggg	268 kb	For Sequencing
HT/Kea F2/R2	tctgaactgaccgaggtgtg	ctcgcttctggaacatgaca	290 kb	CAPs, AseI
HT/F22M8 F1/R1	ggcaattcaaagacccgata	cctacgtaatggagccaaatgtgtc	314 kb	dCAPs, EcoRV
HT/T7I23 F3/R3	gggagatttggaggagcttacc	agaggagtaaaagtgaaaatatt	450 kb	dCAPs, XmnI
HT/T6A9 F1/R1	gaggagtccctgacaatgga	atgcgtagggttgacacaca	483 kb	For Sequencing
HT/F22D16 F1/R1	tgcagcgaatcttctctttg	cataagagttatgttaagagaccatca	685 kb	Indel
§HT/F10O3 F1/R1	tttaatgaaaccaacccaaga	caggtgcgaagaaccactaa	705 kb	Indel
HT/F21B7 F1/R1	tgactacatggagattatggcc	cacgatatgatcaagctttaacg	850 kb	Indel
HT/F21M11 F1/R1	tcagtccctcttcgacgttt	aaagaatcagggacgggttc	972 kb	Indel
HT/F20D22 F1/R1	aacaaaatgagtttctctgcatg	cccaagtgacgtctggtttc	1,100 kb	Indel
HT/T1G11 F1/R1	gaagacaaagctctgcagtaatgt	ttgcataaggcacttgaaagtta	1,323 kb	Indel
HT/T7A14 F1/R1	gaccatgaagatctggtctcg	gcctttgcttccacacaaat	1,450 kb	Indel
HT/YUP8H12 F1/R1	ttgagacttacgaggatgaaacaa	catgggctttaggccattta	1,500 kb	Indel
HT/T25N20 F1/R1	ctgcagcacctctccctact	ttcgcgagtaccttcaggat	1,600 kb	Indel
HT/F3F20 F1/R1	tttgactgcgtcttccttgg	tggtggtgggagagagagag	1,600 kb	Indel
HT/F12K11 F1/R1	ccatatcttggagttggcaga	aatgtcttcaggaacacaacca	2,000 kb	Indel
HT/T23G18 F1/R1	tgagtggccaagtgttacga	tggaattatcggaaatgacga	2,573 kb	Indel
HT/F7G19 F1/R1	tttgtgtttcatcaattggtaagttt	tggatccccattgtacagtta	2,900 kb	Indel
HT/T28P6 F1/R1	tgaaaactccttttgtctctcca	ggaaaagcatatgggctacg	3,700 kb	Indel

§ markers that were used to screen the F_2 populaiton for recombinations that occurred at the top of chromosome 1 on both sides of the mutation region.

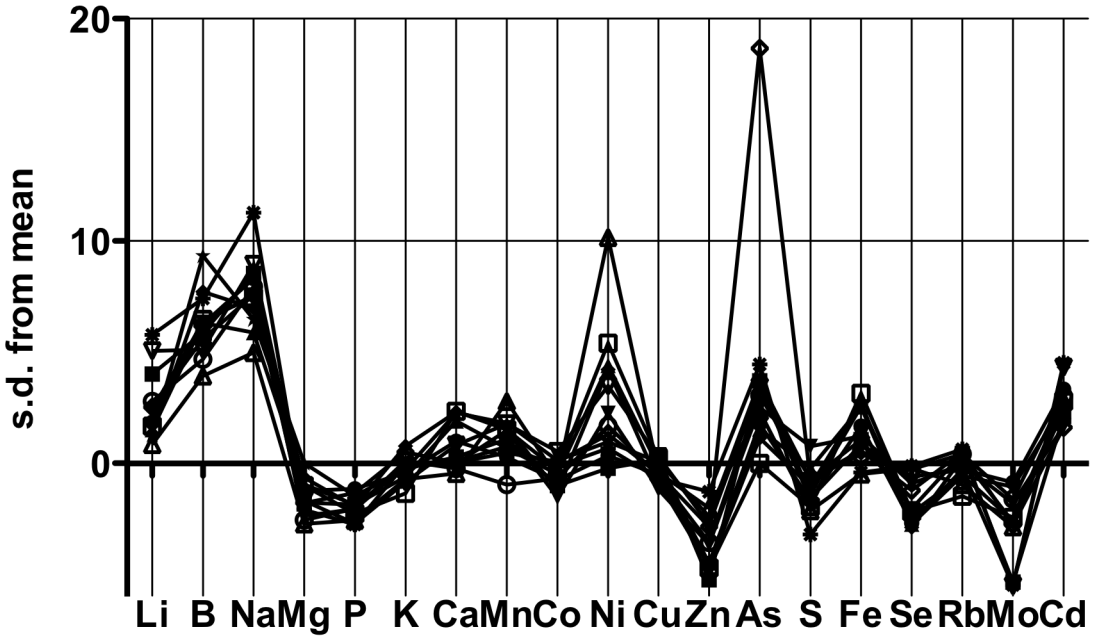

Ap. Fig. 7. Differences in leaf Na^+content between the 103:06 homozygous line 1198:15 plants and the average of Col-0 WT population were plotted as the z- values. Results from 12 individual plants were included and the zero line represents the average of the wild type population. 1198:15 was originally isolated based on the super high Na^+ accumulation in its leaf tissue from the F2 population of 10306 x Ler-0.

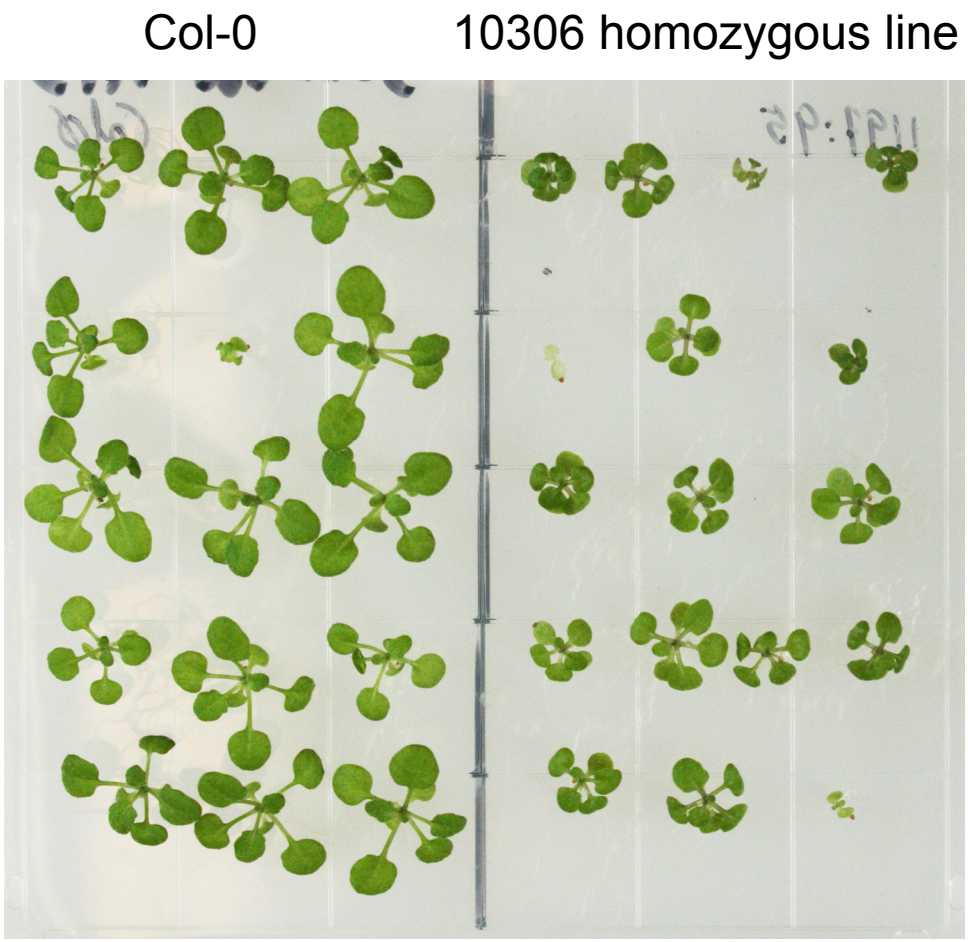

Ap. Fig. 8. 103:06 homozygous plants are hypersensitive to elevated NaCl. Col-0 (the left) and one 103:06 homozygous line 1197:95 (the right) were germinated on ATS medium supplemented with 50mM NaCl and grown under the long day growth conditions (16h/8h, 55umol m-2 s-1) for one month.

Appendix 3. Elemental analyses of seeds from Arabidopsis ecotypes, FN induced and T-DNA insertion mutants

Plant seeds are a major dietary source for humans of the essential mineral elements. Their accumulation in seeds is the result of selective transport processes mediating the short- and long- distance movement within plant. Identifying mutants and natural accessions with altered elemental accumulation in seeds therefore is important for our understanding of the molecular mechanisms regulating these processes, and with potential applications in improving seed quality, nutrition and plant based bioremediation. In previous research a high throughput ion-profiling strategy had been performed to analyze shoot tissue of Arabidopsis plant population using inductively coupled plasma spectroscopy (ICP-MS). From 6,000 fast neutron mutagenized M2 arabidopsis plants, 51 mutants with altered shoot elemental profiles were identified (Lahner et al., 2003). DNA microarray based genotyping of natural genetic variants in arabidopsis led to the identification of gene involved in controlling shoot Na accumulation (Rus et al., 2006). In this study a list of Arabidopsis accessions, FN induced mutants and T-DNA insertion lines were grown on both control and acidified soil. Seeds were harvested, dried, and the accumulation of 13 elements was assayed using inductively coupled plasma- atomic emission spectroscopy (ICP-AES). The shoot ionomes of these ecotypes, FN- induced and T-DNA insertion mutants have been tested previously using ICP-MS. An interesting hypothesis to be tested is whether these natural variation gene loci and

mutations that caused changes in shoot ion accumulation have similar effects on seed elemental accumulations. The results from these seed elemental analyses were summarized in Ap. Table 2. Significant changes in the seed elemental profile of ecotypes and mutants compared to Col-0 wild type were recorded as z-values (standard deviations).

Plants were grown as follows: The soil LB2 mixed basic (SUNGROW) was used to as control soil and the acidified soil. The original soil pH was around 6.3. To make acidified soil, the soil was mixed thoroughly with sulfuric acid (approximately 430ml of 1M H_2SO_4 was mixed with 1500g soil) and the soil pH was tested twice every week, continuously for one month. The final pH was stabilized to 5.0-5.2. Seeds of various ecotypes, FN and T- DNA mutants and Col-0 controls were sowed directly onto the soil. Two weeks after germination extra seedlings were removed from each tray, and for each genotype 6 individual plants were retained for growing and harvesting seeds. The trays were watered from the bottom every 3 days with 0.8L of 0.1x Hoagland (Sigma, H2395) and 5μM chelated iron supplement (Diethylenetriamine pentaacetate, Sprint 330). To maintain and mimic the acidified condition, 10μM $AlCl_3$ and 5mM NaH_2PO_4 were also added to the nutrient solution to water the acidified soil trays. All the trays were placed under long day conditions (16h/8h, 50-75 μmol. S^{-1}. m^{-2}).

Ap. Table 2 Statistically significant changes in the elemental profile of ecotypes/ mutants compared to Col-0

ig #	Ecotype/mutant	Growth conditions	Al	Ca	Fe	K	Li	Mg	Mn	Na	P	S	Si	Zn
1	Ler-0	Acidified Soil		-4					3	3		-2		2.5
1	Ler-0	Control Soil		-3					2.5					
5	cvi-0	Acidified Soil		-7		3						-6		
5	cvi-0	Control Soil		-5								-3		
3	ts-1	Acidified Soil		-3		2				10		-8		
3	ts-1	Control Soil								>2.7				
4	sha	Acidified Soil		-6	1.5				4			-6		
4	sha	Control Soil		-5					5			-4		
7	WS	Acidified Soil		-2.5	-2.5		2		8			-3		
7	WS	Control Soil		-2		4					-2	-2		
8	tsu-1	Acidified Soil		-4		5				16			-3	
8	tsu-1	Control Soil								0-10				
9	nd-1	Acidified Soil		-3.5		4.5				1.5	2	-2		
9	nd-1	Control Soil		-3								-2		
10	mrk-0	Acidified Soil		-4		5					2	-2	-3	
10	mrk-0	Control Soil							1.5					-2
2	Kas1-1	Acidified Soil		-20	2	5		2.6				-10		
2	Kas1-1	Control Soil		-5	2				2			-3	-2	2
12	134-19	Acidified Soil	>5				>5						>6	
12	134-19	Control Soil	0-10	-5		5	0.99-16							
13	131-61§	Acidified Soil		5					-3			4		
15	116-49	Acidified Soil				5				>10		-3		
15	116-49	Control Soil						3			2.5	-3		
17	124-05	Acidified Soil							4					
17	124-05	Control Soil		-2					5			-2		
18	82-70	Acidified Soil								2				
18	82-70	Control Soil		2	3									
19	145-01	Acidified Soil		-5		>7				8				
19	145-01	Control Soil							4					
20	126-45§	Acidified Soil		-2		-2								
21	cor 78-2 (At5g52310)§	Acidified Soil		-2		-2								
22	cor 78-3 (At5g52310)§	Acidified Soil		-2		4				4				

§ data not available for control soil